Research Report

LATERAL FLANGE BENDING IN HEAVILY SKEWED STEEL BRIDGES

Prepared by

Francisco Morera, Ph.D.
Research Assistant

Emmett A. Sumner, Ph.D., P.E.
Principle Investigator

Submitted to

North Carolina Department of Transportation
Research and Analysis Group
Raney Building
104 Fayetteville Street
Raleigh, North Carolina 27601

NCSU-CFL Report No. RD-09-03
NCDOT Report No. FHWA/NC/2007-09

December 2010

Constructed Facilities Laboratory (CFL)
Department of Civil, Construction and Enviromental Engineering
North Carolina State University

Technical Report Documentation Page

1. Report No. FHWA/NC/2007-09	2. Government Accession No.	3. Recipient's Catalog No.
4. Title and Subtitle Lateral Flange Bending in Heavily Skewed Steel Bridges		5. Report Date December 2010 6. Performing Organization Code
7. Author(s) Francisco Morera, Emmett A. Sumner		8. Performing Organization Report No.
9. Performing Organization Name and Address Department of Civil, Construction and Environmental Engineering North Carolina State University Raleigh, NC 27695		10. Work Unit No. (TRAIS) 11. Contract or Grant No.
12. Sponsoring Agency Name and Address North Carolina Department of Transportation Research and Analysis Group Raney Building 104 Fayetteville Street Raleigh, North Carolina 27601		13. Type of Report and Period Covered Final Report January 2007 – August 2009 14. Sponsoring Agency Code 2007-09
15. Supplementary Notes		

16. Abstract

Two different simple span steel I-girder skewed bridges were monitored during the non-composite phase of the construction process in order to study the effects of Lateral Flange Bending (LFB) on displacements and stresses. Using finite element analysis, numerical models of the bridges were developed in an effort to identify the key components that allow characterization of the out-of-plane (torsional) rotation displacements and the LFB stress profile. A parametric study was performed to single out the most sensitive parameters and to establish possible mitigation strategies. The study identified that increasing the torsional strength of the cross section is more beneficial effects than the traditional idea of increasing the number of cross-frames or diaphragms along the span. It was also found during the study that the worst case scenario produced a maximum LFB locked-in stress of eighteen percent of the yield stress.

17. Key Words Skew bridges, steel structures, torsion, torsional strength, stresses, finite element method	18. Distribution Statement		
19. Security Classif. (of this report) Unclassified	20. Security Classif. (of this page) Unclassified	21. No. of Pages 155	22. Price

Form DOT F 1700.7 (8-72) **Reproduction of completed page authorized**

DISCLAIMER

The contents of this report reflect the views of the author(s) and not necessarily the views of the University. The author(s) are responsible for the facts and the accuracy of the data presented herein. The contents do not necessarily reflect the official views or policies of the North Carolina Department of Transportation of the Federal Highway Administration at the time of publication. This report does not constitute a standard, specification, or regulation.

ACKNOWLEDGMENTS

The authors acknowledge the North Carolina Department of Transportation (NCDOT) for providing the funding, information, assistance, and support to successfully bring about this ambitious project. In particular, special thanks to Mr. Brian Hanks, on the NCDOT Structures Division, for his continuous willingness and readiness to solve the different problems we ran into throughout the investigation.

EXECUTIVE SUMMARY

The problem related to lateral flange bending of steel plate skewed girders during the non-composite phase of construction can be simply stated as a consequence of the significant support skew, typical staggered cross-frames along the span in between adjacent girders, differential deflections commonly present on skewed bridges, out-of-plumb condition associated with girder camber and imperfections, and the force transfer mechanism due to the overhang falsework.

Two different simple span steel I-girder skewed bridges were monitored during the non-composite phase of the construction process in order to study the effects of Lateral Flange Bending (LFB) on displacements and stresses. Using finite element analysis, numerical models of the bridges were developed in an effort to identify the key components that allow characterization of the out-of-plane (torsional) rotation displacements and the LFB stress profile. A parametric study was performed to single out the most sensitive parameters and to establish possible mitigation strategies. The study identified that increasing the torsional strength of the cross section is more beneficial effects than the traditional idea of increasing the number of cross-frames or diaphragms along the span. It was also found during the study that the worst case scenario produced a maximum LFB locked-in stress of eighteen percent of the yield stress.

TABLE OF CONTENTS

LIST OF FIGURES

LIST OF TABLES

1.0 INTRODUCTION

1.1 Overview

The need to use heavily skewed structural steel girder bridges is becoming more common in the bridge design industry. This has become necessary to deal with more complex site constraints and to accommodate the more demanding roadway geometries (see Figure 1-1). In consequence it has become necessary to gain a better understanding of the complex behavior of these types of structures.

Figure 1-1. Photograph of skewed bridge construction

The problem related to lateral flange bending of steel plate skewed girders during the non-composite phase of construction can be simply stated as a consequence of the significant support skew, typical staggered cross-frames along the span in between adjacent girders, differential deflections commonly present on skewed bridges, out-of-plumb condition associated with girder camber and imperfections, and the force transfer mechanism due to the overhang falsework. However, this phenomenon is the result of out-of-plane rotations due to torsional moments acting on the girders because of unsymmetrical distribution of forces and constraints throughout the whole structure. Figure 1-2 illustrates the deflection and rotation of the girders of a significantly skewed steel plate girder bridge during placement of the concrete bridge deck. The out-of-plane rotation of the girder at each support is apparent.

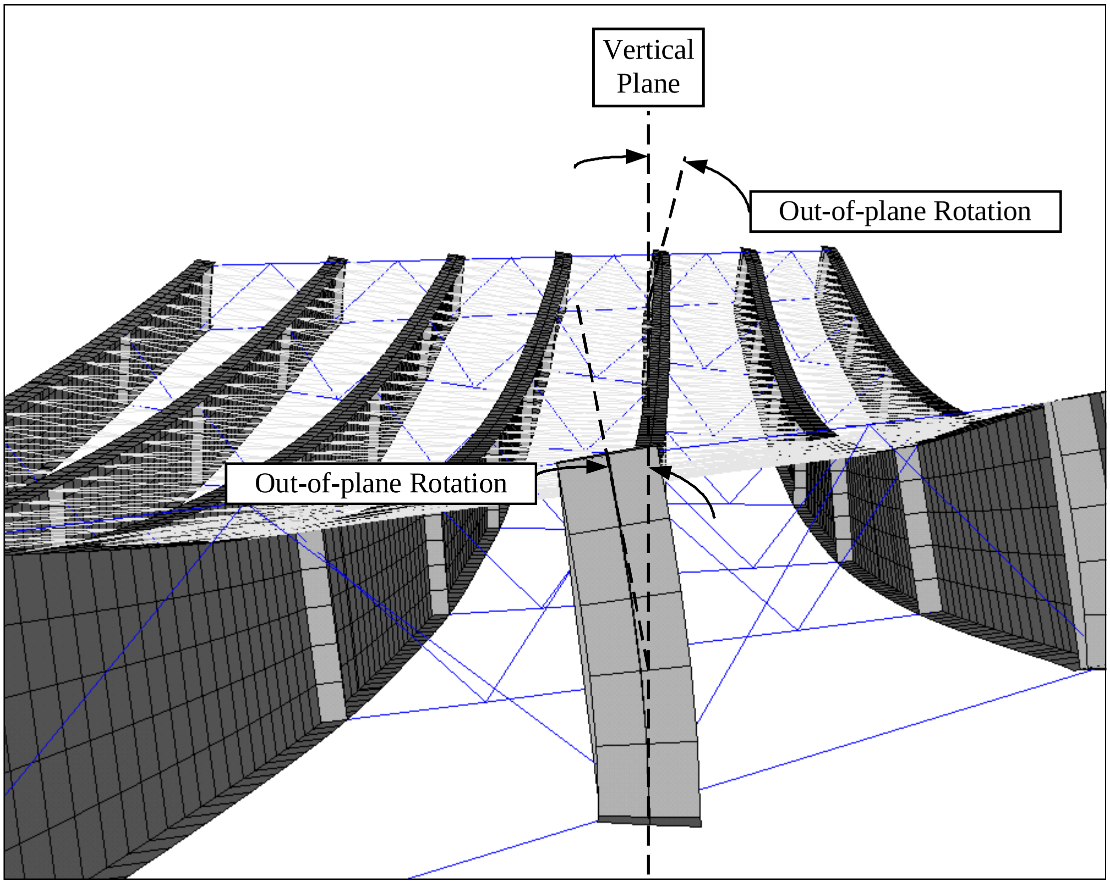

Figure 1-2. Displaced Shape of a Skewed Bridge Finite Element Model

Current AASHTO design specifications address this issue by considering the evident difficulties arising from this situation that can lead to costly construction delays and the potential need for further analysis to account for the additional stresses on girders, cross-frames and bearings as well as potential sources of undesirable problems such as fatigue and durability. Nonetheless, the available information related to this condition is scarce, hence an extensive investigation was carried out with the primary objective of understanding the out-of-plane torsional rotation phenomenon by means of a comprehensive parametric analysis, including quantifying the effects of each parameter, evaluating and predicting the response, and providing some insight of possible remedies to mitigate the eventual undesirable outcomes. In an effort to properly evaluate the out-of-plane rotation condition, two steel plate girder bridges were selected, in collaboration with the NCDOT, and monitored during placement of the concrete deck to observe the rotations of the girders at different locations along the span. The field recorded behavior of the girders was utilized to validate the finite element modeling technique used in the parametric study.

Based upon previous investigations conducted by Whisenhunt (2004) and Fisher (2005) at North Carolina State University, three-dimensional finite element modeling procedures were developed to capture the effects of stay-in-place forms along the entire girder span, cross-frame connection gusset plates, and elastomeric bearing pads on the overall behavior of the structure. The analysis was conducted using the commercially available ANSYS version 11 finite element code. Once the modeling procedure development was completed and validated, a computational pre-processing program was developed to facilitate the generation of the necessary input data to carry out the parametric analysis. More than 180 cases were studied to determine the sensitivity of the system to each parameter, and to develop a simplified model to predict the out-of-plane rotation profile of the structure and the overall magnitude of the possible locked-in stresses due to lateral flange bending.

With the information gathered from the analysis, it was possible to generate proposed mitigation schemes, on which it was demonstrated that some variations in certain parameters either enhanced the rotational response of the structure (favorable changes), did not produce a major effect whatsoever (neutral changes) or decreased the ability of the girders to withstand the external conditions (unfavorable changes).

With this information, Lateral Flange Bending (LFB) stresses were thoroughly studied to gain a detailed understanding of the factors influencing the response of the girder. From the total bending stresses acting on the flanges, the LFB component was singled out and compared to the corresponding yield stress. Additionally the LFB displacement and stress profile were compared to determine the overall influence of each component of displacement (lateral or rotational) on the bridge behavior. It was found that the LFB lateral displacement component was negligible and the torsional rotation component governed the phenomena.

1.2 Objectives and Scope

The primary objectives of this research are to quantify the lateral flange bending of steel plate girders in heavily skewed bridges, develop a methodology for predicting the magnitude of lateral translation of the girder flanges due to this effect, and establish recommended strategies for mitigating the effect of heavy skew.

To achieve the objectives and as part of the research methodology, a series of tasks were completed. These tasks are as follows:

1.2.1 Task 1: Literature Review.

An extensive literature review was conducted to survey the available literature on the lateral flange bending behavior of steel girder bridges. The review focused on past analytical and experimental studies that were used in the development of the very limited design and constructability recommendations included in the current AASHTO specifications.

1.2.2 Task 2: Field monitoring of steel girders during placement of the bridge deck.

This task was carried out on a moderate skew steel bridge located on Chicken Road over a construction segment of US 74 between Maxton and Lumberton, and a heavily skewed bridge located over Roaring Fork Creek in the mountain region of north western North Carolina. Rotations and strains were monitored on both of these bridges to determine the lateral translation of the girder flanges due to lateral flange bending. The girders were instrumented to measure the rotations on both the web and bottom flanges at quarter points along the span of the girders.

Measurements were recorded at various stages of the deck placement to capture the response of girders throughout the deck construction.

1.2.3 Task 3: Analytical investigation and quantification of lateral flange bending.

An analytical investigation was conducted to quantify the lateral flange bending of steel plate girders in heavily skewed bridges. More than 180 three-dimensional finite element models were developed for each of the bridges monitored in the field. The field measurements were used to validate the finite element models. Once the validation study was completed additional models were created with the help of a computational program specifically developed for this research to simulate the effects of numerical parameters like exterior-to-interior moment of inertia (strong axis) ratio, exterior-to-interior load ratio, number of girders, number of transverse stiffeners, number of cross-frames, cross-frames stiffness, stay-in-place forms stiffness, and spacing-to-span ratio. Additionally non numerical parameters like cross-frame type, cross-frame layout and pouring sequence were also considered. The finite element simulations were used to quantify the lateral flange bending effects due to the out-of-plane torsional rotations and the overall behavior of the possible locked-in stresses during the construction stage. Particular attention was given to the modeling of the bridge cross-frames, end-bent diaphragms, and support bearings.

1.2.4 Task 4: Development of mitigation strategies

From the extensive parametric analysis it was possible to classify the effects each parameter had on the entire structure. This allowed quantifying the potential benefits or harms each of them poised on the overall rotational behavior of the girders. The effects of the numerical parameters were classified as favorable, neutral, or unfavorable with respect to the original structure.

2.0 LITERATURE REVIEW

2.1 Overview

An extensive literature review is conducted herein. It will be clear that information directly related to quantifying lateral flange bending in steel plate skewed bridges is scarce. Nevertheless, related research to the topic has been done. Parameters like skew angle, type of bearing, stay-in-place (SIP) forms, cross-frames and/or diaphragms, overhang falsework, torsional, and lateral stiffness of steel girders are among the most important variables to be taken into account in the investigation. Additionally, influence of the non-composite and composite construction phases in the girder torsional behaviour as well as a finite element modelling to understand the skewed system are also presented.

To facilitate the understanding of the topics presented, this review was divided into the following sections: construction issues, parametric studies, steel bridge modelling, NCSU/NCDOT related studies, and a final discussion about the need for research.

2.2 Construction Issues

Back in the early 70's the problem related to skewed bridges was identified. Hilton (1972) observed that during deck pouring, there are various issues that the designer should account for such as non-uniform deck thickness along the span and the differential temperatures existing between the top and bottom flanges on the girders, which may differ from temperatures when forming elevations were established. Measurements were taken from various bridges, using instruments such as thermocouples, high precision levels, and special design rod and scale units. Gathered field data was compared to theoretical data obtained using an analysis of semi-rigidly connected girders, which turned out to be in good agreement with the field deflections. It was detected that the girder deflections would be considerably greater if differential thermal conditions did not exist. However, the most important finding was that resulting predictions tended to be larger than measured data in the field on account of the bridge superstructure deflecting as a unit, rather than individual girders.

The problem studied by Swett (1998) and Swett et al (2000), in response to WSDOT, was how to control the inherent constructability issues that arise while either widening an existing bridge or during a staged construction, particularly for straight bridges without significant skew. It is desirable that the new structure ends up having the same elevation and cross slope as the existing structure, after placing the concrete deck. This problem becomes more critical when the new structure is not symmetric, since torsional moments will cause the bridge to twist. To solve this, six different design and construction methodologies were presented with their corresponding pros and cons as well as applicable situations. Utilizing finite element analysis (FEA) comparisons of the actual deflections with those given by the model were made. These comparisons were used to evaluate the accuracy of the six methodologies. It turns out that there is no universal solution, though appropriate choices of construction sequences can lead to significant reductions in both unwanted deflections and locked-in stresses.

Another unique situation related to steel skewed bridges is the differential deflections. To address this condition AASHTO/NSBA (2003) stated that girder deflections under dead load for skewed bridges are not equal across the width of the bridge making it difficult to install cross-frames at locations with significant differential deflection. Therefore, once cross-frames are installed in these situations, they may restrain deflections causing girders to rotate out-of-plumb and lateral stresses to be induced in the flanges. Additionally, if the girders are required to be plumb under full dead load or steel dead load, engineers should address the expected rotations in advance.

On the other hand, for cross-frames at skewed piers or abutments the major source of problem is the rotation of the girders at those locations. In a square bridge, rotation of the girders at the bearings is in the same plane of the girder web whereas when supports are skewed, girder rotation due to non-composite loads will be normal to the piers or abutments. This rotation displaces the top flange transversely from the bottom flange and causes the web to be out-of-plumb. The type of bearing (elastomeric pad, pot bearing, spherical, etc.) used plays an important role. If the bearings can tolerate the rotation and no other problems are present, the situation may be acceptable. However, the designer should look at the size and capacity of end cross-frame members for the degree of skew and the out-of-plumb bearing. This bearing problem has been mentioned in the early 80's.

Burke (1983) focused his study mainly on describing different types of bearing systems that can accommodate typical displacements developed by girder ends of skewed bridges, such as rotations and lateral translations. Four different types of bearings were described in great detail: Pot, spherical, disk, and elastomeric bearings. It was also noted that, particularly for skewed and curved bridges, designers should account for rotations and translations at the supports as a result of live loads. This particular phenomenon is often ignored and designers only consider vertical deflections, so it is common to observe problems associated with the bearings, such as fatigue cracks, in those bridges with considerable skew.

Norton (2001) and Norton et al. (2003) used the information obtained from measurements on an actual skewed steel bridge during deck pouring to compare the theoretical deflections and rotations of the girders versus the actual displacements. Parameters like screed orientation, deck pouring sequence, dimension of the model (two-dimensional versus three-dimensional) were considered. It was noted that the structure had the particular characteristic that the webs were out-of-plumb prior to concrete pouring.

Of particular importance was that the three-dimensional model was more accurate than the two-dimensional model. The deck pouring sequence had no major effect on the forces developed at the cross-frames if the concrete is assumed to be plastic, though when pouring the concrete perpendicular to the center line of the bridge leads to higher support reactions and displacements during the intermediate stages of construction. Both rotations and lateral displacements were considered linear along the girder web, and while lateral displacements did not match what was predicted, measured vertical displacements did.

2.3 Parametric Studies

2.3.1 Stay-in-Place (SIP) Metal Forms

Helwig (1994) conducted an investigation to determine the bracing capacity of SIP metal forms, involving both experimental and analytical studies. The experimental studies, previously carried out by Currah (1993) and Soderberg (1994), consisted of a series of tests on isolated decks to determine their shear capacity, various deck to girder connections, and buckling of twin girders with SIP metal forms. The dissertation covered the analytical research done by using a FEA with the finite element program ANSYS to compute the bracing effect given by the SIP metal forms to the girders. Parameters such as shear rigidity of the deck, shape of girder cross-section, in plane boundary conditions, number of transverse stiffeners, type of loading, and load height were considered. It was determined that for simply supported or continuous girders, considering the effects of moment gradient, load height and cross-section distortion either from web bend or shear buckling, the design approach was reasonably accurate. From all these considerations it was possible to confirm that lateral torsional buckling at the supports is only critical after completion of the bridge, but by accounting the lateral stiffness given by the SIP forms it is possible to eliminate cross-frames, with the consequent benefits such as fewer weak points in terms of fatigue and a structure easier to erect.

Few years later, Jetann et al. (2002) and Egilmez et al. (2007) developed a practical and economical method to improve the strength and stiffness of the connection between SIP metal forms and the girders. This was done by measuring the bracing behavior of metal deck forms with both existing and new stiffer connections. The process included experimental and computational studies, including parameters such as metal gauge of deck forms, support angle connection details and panel aspect ratio. The outcome was that for systems with eccentric connections details, stiffening angles spaced roughly twice the span of the diaphragm would suffice both effectively and economically.

The diaphragm behavior the SIP forms was also studied. By conducting both experimental (lab tests) and analytical (FEA) research Egilmez et al. (2003) were able to determine that SIP forms add both shear and flexural stiffness. In this sense, it is worth mentioning that the experiments were conducted on a full scale 50 foot span twin girder with SIP fastened to the top flanges and the results were compared to a finite element analysis to develop a more accurate model of the bracing behavior. Results demonstrated that it is not good practice to model SIP forms as a shear diaphragm since it tends to significantly underestimate bracing behavior. On the other hand, it was demonstrated that incorporating additional “in deck plane” bracing elements, such as angles connected in a truss shape configuration, the FEA can account for the additional stiffness not present in the shear diaphragm model.

Egilmez and Helwig (2004) continued the work by Jetann et al. (2002) on shear tests and Egilmez et al. (2003) on full scale lateral displacements tests on a twin girder system with SIP forms for bracing. This time the research was focused on buckling tests as well as results from the FEA. The experiments were carried out with the same configuration used on the previous phases and including a gravity load simulator to apply transverse load to the system. Lateral displacements were recorded and three different sets of 20 gauge deck forms were placed on the beams.

To account for imperfections, the worst scenario was considered while setting up the system. This included placing the support angles at their maximum eccentricity and simulating the most critical shape imperfection for torsional bracing systems in beams that occurs when the top flange experiences a displacement equal to the unbraced length divided by 500, as shown by Wang and Helwig (2003). To account for this condition, a three phase test was carried out including no offset, loads offset by half an inch in one direction, and load offset to simulate the $L_b/500d$ initial twist imperfection, where d is the depth of the cross-section. The results from the FEA, which included the effect of imperfections, were in good agreement with the test results. Finally, test results revealed that a stiffened deck system provides better control of the deformations when compared to the unstiffened systems.

Egilmez et al. (2006) continued the investigation in both experimental and computational studies performed on permanent metal deck forms (PMDF), also known as stay-in-place forms (SIP), by Jetann et al. (2002) and Egilmez et al. (2003, 2004 and 2005). This paper presented results from the computational study on the stiffness requirements for SIP forms used for stability bracing of steel bridge girders. Research consisting of three testing phases was conducted. The first phase involved testing to determine shear properties of metal deck forms. The second phase focused on measuring the lateral stiffness of the SIP form panels when subjected to deformations similar to the actual deflected top flange profile of buckled girders. The final phase was related to buckling tests on twin girder systems with SIP forms for bracing.

A computational study was conducted using a three-dimensional finite element modeling to perform parametric analysis on the behavior of steel I-girders braced with SIP forms. The SIP forms were modeled as shear diaphragms by means of truss panels, considering a distance of 16 feet between stiffening angles. Parameters like girder span to depth ratio, girder cross-section, and shear rigidity of the deck system were also taken into account. An elastic eigenvalue buckling condition was analyzed to determine the critical buckling load of the system. To account for the effects of imperfections in the system geometry, a large displacement finite element analysis was performed to determine that as the depth and length of the girders increase, so does the stiffness requirements to control deformations, and therefore a limit on the unbraced length for girders braced with SIP forms should be established.

2.3.2 Skew Angle

Gupta and Kumar (1983) tested five small scale models with skew angles within 0 to 40 degrees. They found during their research, that there were two main issues to be considered: skew angle and contribution of the slab to the girders. The study included both experimental and analytical research. The analytical portion consisted of a FEA of the slab – girder interaction. It was concluded that for a skew angle less than 30 degrees, skew has little effect and for angles higher than that, the moments, rotations, and deflections increase with the increase in the skew angle, but the reactions in the loaded girder decrease. They also pointed out that deflections and moments are greatly reduced by restraining the girder ends.

Bakht (1988), proposed an alternate parameter instead of the traditional skew angle. This parameter was defined by means of three variables: the girder spacing S, the bridge span L, and the angle of skew ϕ ($S \tan \phi / L$). For values of this parameter less than 0.05, it is safe to analyze the bridge as non-skewed.

An investigation by Bishara and Elmir (1990) was conducted to develop a three-dimensional finite element algorithm to determine internal forces in end and intermediate cross-frames on composite steel bridges. Four steel bridges were analyzed, three of them skewed, and it was found, among other things, that for skewed bridges most members of intermediate cross-frames develop the maximum compressive forces on those attached to the ends of exterior girders close to the obtuse angles and maximum tensile forces occur on the chord members at midspan. If the skew angle is increased, forces on the cross-frames also increase. A similar situation occurs if the sizes of the cross-frames are increased as well, but for cross-frame members on the girder ends whose size was not changed, the internal forces were not affected if intermediate cross-frames were changed. The maximum differential deflections occurred between the exterior girders and those adjacent to them close to the obtuse angle and the torsional moments developed on the girders never exceeded 2 percent of the maximum bending moment.

Berglund and Schultz (2006) focused their investigation on three things: the development of a Finite Element Model (FEM) model to accurately predict the vertical differential deflections between adjacent girders, a parametric study to determine the key components on relative deflection on skewed bridges, and a technique to determine both the vertical differential deflections and their inherent distortional stresses. The FEM was implemented using SAP2000 Nonlinear as the software package. The three-dimensional model included shell elements for the deck and girder webs and frame elements to model girder flanges and concrete railing. The composite behavior was modeled by using rigid frame elements as a connection component. The parametric study included three primary parameters: span length, angle of skew, and girder spacing. The secondary parameters were deck thickness, girder spacing, adjacent span length, and diaphragm depth. As a result of the investigation a formula to represent the variation of the differential deflection was determined. $\Delta/S = (aL^2 + bL + c) / L$, where L is the span length, S the girder spacing, Δ the differential deflection, and a, b and c are coefficients depending upon the angle of skew.

Other findings indicate that the higher the skew angle the higher the differential deflections, the maximum diaphragm deflections occur on the obtuse corner of each loaded lane, longer bridges do not undergo high differential deflections and the relationship between differential deflections and girder spacing is linear.

2.3.3 Cross-frames / Diaphragms

Shi (1997) addressed the fact that an adequate bracing system for lateral torsional buckling must satisfy both stiffness and strength requirements, therefore special attention must be given to the design of these components of a steel girder bridge. He mentioned that the critical stage for buckling of steel girders takes place during deck pouring, therefore providing intermediate cross-frames or diaphragms not only solves this problem, but helps the negative moment region to resist wind load on the girder bottom flange. Usually, cross-frames and diaphragms are built stiffer than needed (using the 2 percent method), leading to a development of larger forces which induce fatigue problems at their locations. The research included the evaluation of the buckling behavior of a simply supported twin girder system with discrete torsional braces by using a FEA. Parameters like skew angle, load type, load height, cross-section shape, and brace orientation relative to skew angle were also considered. Finally, Shi (1997) modified previous formulas developed for normal girders to determine both the capacity and the stiffness of the cross-frames.

According to Helwig and Wang (2003), AASHTO provisions are not clear enough when referring to the design of bracing systems. This leads to possible greater sections in cross-frames and diaphragms than actually needed and subsequently to fatigue prone locations along the girder. The main purpose of the investigation was to clarify the bracing requirements for bridge girders so that properly sized braces can be employed, as well as to provide details to minimize fatigue damage. To do this, a FEA was developed based upon previous laboratory testing and then compared results with proposed equations for the design requirements of cross-frames and diaphragms. Helwig and Wang (2003) compared the results for bridges with normal supports-stiffness and strength requirement, bridges with skewed supports-parallel braces-stiffness and strength requirement, and bridges with skewed supports-normal braces-stiffness and strength requirement. To finally enhance the buckling capacity of the girders, slight modifications are needed on the strength requirements. For girders with skewed supports and bracing perpendicular to the center line, the FEA was in good agreement with the equations for non-skewed supports. However, simple modifications are required for bridges with skewed supports and bracing parallel to the skew angle.

Regarding AASHTO LRFD Bridge Design Specifications (2004), it is worth mentioning that the requirement for diaphragms spaced at no more than 25 feet is no longer valid. Instead it was replaced by a requirement for rational analysis that could eventually lead to the elimination of fatigue prone details. Additionally, flange lateral bending may be caused by "*wind, by torsion from eccentric concrete deck overhang loads acting on cantilever forming brackets placed along exterior girders, and by the use of staggered cross-frames in conjunction with skews exceeding 20 degrees*". In these cases, it is up to the design engineer to consider the flange lateral bending, usually addressed by the use of refined analysis methods, though it is not strictly required. Some of these effects have not been previously mentioned.

Herman et al. (2005) provided a thorough discussion of the lean-on bracing concepts and an overview of one of the implementation bridges on which the bracing is being utilized (TxDOT Study 0-1772).

The research study included examinations of intermediate bracing systems framed both parallel to the skew and perpendicular to the longitudinal axis of the girders. By simply modifying the bracing strength and stiffness expressions developed by Yura (2001) for bridges with normal supports, it was possible to account for the impact of brace or support skew angles as discussed by Helwig and Wang (2003). In addition to modifying the bracing design expressions to account for the impact of support skew, details were also recommended in TxDOT Study 0-1772 (2003) to both reduce the number of intermediate braces required and to lessen the forces induced in these braces due to truck traffic.

The lean-on concept gives the engineer the flexibility of selecting positions for the cross-frames within a given bracing line to minimize the cross-frame forces induced by truck traffic in the completed bridge. To minimize the forces induced in the cross-frames by truck traffic, the transverse position of the cross-frames should be selected such that they are as far away from the support as possible, because for cross-frames positioned near support locations the relative deflection across the cross-frame induces large cross-frame forces. By positioning the cross-frames away from the supports at locations with smaller relative vertical girder deflection the brace forces induced from live loading can be reduced.

The lean-on layout also produces a reduction in the total number of cross-frames required on the bridge, and subsequently less fatigue prone points The implementation scheme was conducted on three skewed bridges, all of which are two-span continuous systems with severe support skews of 50 to 60 degrees. The outcome was that using a conventional layout for the cross-frames, with cross-frames across the width of the bridge at every intermediate cross-frame line, one of the bridges with nine girders would have required 128 intermediate cross-frames, however 35 intermediate cross-frames would be required using the lean-on system. It is imperative that every single girder would be braced. As long as intermediate cross-frames are placed between each girder, a smooth transverse profile, analogous to that seen with conventional cross-frame layouts, can be obtained.

2.3.4 Lateral and Torsional Strength / Stiffness

A comprehensive review of the beam bracing stability was conducted by Yura (1993). Beam bracing systems such as lateral and torsional bracings were evaluated in great detail. It is noteworthy the fact that both strength and stiffness of the brace system must be checked for design purposes. Current published bracing requirements for beams do not account for out-of-straightness, and should not be used in design. Similarly, design of those systems based on the 2 percent rule could eventually lead to inadequate brace systems (usually over designed).

Using BASP (Akay, 1977; Choo, 1987), an elastic FE software that considers local and lateral-torsional buckling including cross-section distortion, it was possible to solve different loading and support cases for beams braced at different locations. For the case of lateral bracing of beams the results indicated that because of cross-section distortion and top flange loading effects, lateral braces at the centroid are not recommended. Instead, lateral braces must be placed near the top flange for many support conditions, and although loading through the deck can provide a beneficial tipping effect that increases the buckling capacity, it is not recommended to be considered in design. On the other hand, when a beam is expected to be subjected to both positive and negative moment along its span, not only it is incorrect to assume that the inflection point is the most suitable brace point but also that bracing requirements for beams with double curvature are greater than those with single curvature.

Additional analysis was conducted evaluating parameters like the number of bracing points along the span of the beam. This analysis led to the conclusion that moment gradient, brace location, load location, brace stiffness, and number of braces affect the buckling capacity of laterally braced beams. The analysis ultimately made it possible to develop design recommendations that account for all the previous conclusions. Torsional bracing of beams was also considered, conducting the same tests used for laterally braced beams. It was shown that torsional bracing is less sensitive than lateral bracing to conditions like top flange loading, brace location, and number of braces, but more affected by cross-section distortion.

Additional studies by Yura (1999) covered four different types of bracing: relative, discrete, continuous, and lean-on. Relative bracing is considered to control the relative movement of points along the beam or to prevent relative displacement of the top and bottom flanges. Discrete bracing controls the movement at a particular point (cross-frames/diaphragms). Continuous bracing is attached to the beam along its length (SIP forms), and lean-on systems are those on which the element relies on adjacent structural members for support. In these particular systems structural members are linked to one another so the buckling of one of them will require adjacent members to buckle with the same lateral displacement. In any case, both stiffness and strength properties must be satisfied, considering that out-of-straightness condition of the element plays an important role.

As far as beam bracing is concerned, only relative and discrete lateral bracing requirements were considered. Both lateral and torsional bracing were discussed and particular considerations were given to define what a brace point is, since in many cases the inflection point of the buckling deformed shape is not located at those points. Hence, as long as the two flanges move laterally the same amount, twist will not be present, and in such a case the beam can be considered braced. Additionally, expressions included in LRFD for determining strength and stiffness on systems with lateral bracing were presented along with design examples.

For torsional bracing only cross-frames / diaphragms and metal decks or slabs are considered as discrete or continuous torsional bracing systems respectively. However, it was found that factors that had a significant effect on lateral bracing, such as number of bracings, top flange loading, and brace location did not produce similar effects for torsional bracing. A torsional brace is equally effective if it is attached to either the tension or compression flange. Nevertheless, the effectiveness of a torsional brace is greatly affected by the cross-section distortion at the brace point, so web stiffeners are highly recommended.

2.4 Steel Bridge Modeling

During the early nineteen eighties, an extensive FEA study was performed by Schilling (1982) in order to develop lateral distribution factors suitable for use in fatigue calculations. The study consisted of modeling 500 combinations of bridge configuration and load position with the help of the general purpose finite element program ANSYS. Parameters such as number of beams, beam position, truck (loading) position, and relative stiffness were considered. The slab was modeled as rectangular and triangular isoperimetric plate elements to account for bending and no membrane stresses. The girders were discretized as beam elements to solely include bending in a vertical plane. For verification purposes the mesh was refined using elements half of the size of the originals, but the results varied within 1 percent, so it was concluded the original mesh was small enough. Finally, a convenient and conservative chart was developed to give lateral distributions factors for fatigue.

Brockenbrough (1986) used a parametric study using FEA to determine rational factors for lateral distribution of live loads on composite curved I steel girder bridges. The models consisted of QUAD4 shell elements, which included membrane and bending effects for the concrete slab. For the girder web, BAR elements including axial and bending strains in two directions as well as torsional effects were selected for the discretization the flanges of the steel girders and the cross-frames. In addition, effects of the end offsets and pinned joints were included in the modeling of the cross-frames. The interface between the top girder and the concrete deck was modeled with rigid link (RBAR) elements to simulate the no slipping condition typically developed at that location. For the boundary conditions, zero vertical displacement was used at all the supports and zero horizontal displacements were used at the center supports. The noteworthy aspect about this research is that the numerical model was in very close agreement with the existing AASHTO formulation.

Bishara and Elmir (1990) used ADINA as the FEA software and considered three components of the analysis: concrete deck, girders, and cross-frames. The concrete deck was discretized with triangular plate elements. The girders were divided in two parts: top and bottom, each part being discretized with beam elements joined to the other half by steel link elements. The top part was connected to the deck by constraint equations or rigid link elements. The cross-frames were also discretized as beam elements, but the stiffeners were not included. The three simply supported multi-girder skewed bridges of 20, 40 and 60 degrees and the right angle bridge were subjected to a load scheme consisting of dead load due to weight of slab, sidewalks and parapets, girders cross-frames, and asphalt, and to live load according to AASHTO(1) HS 20-44, which included truck load and lane load. Results showed that while in a non-skewed bridge forces in the cross-frames due to dead load are tension for intermediate chords and compression for diagonals; on a skewed bridge these transverse elements develop either compression or tension depending on the loading condition. Furthermore, not only the higher the cross-sections of the cross-frames and the skew angle the higher the forces developed on the cross-frames but also the forces developed on the end bent cross-frames were insensitive to intermediate cross-frame size changes.

Bishara (1993) carried out a parametric investigation whose main objective was to develop a procedure for evaluating internal forces in intermediate cross-frame members of simply supported multi-girder steel bridges taking into account factors like skew angle, span length, deck with, and spacing of cross-frames. By means of a three-dimensional finite element discretization scheme of the system to simulate the interaction between all the elements and a validation procedure using five multi girder bridges, it was possible to analyze 36 bridges with the already mentioned geometrical configuration.

Using ADINA as the FEM software, and with some modifications to the scheme used by Bishara and Elmir (1990) it was possible to model the system. Thin triangular plate elements with six degrees of freedom per node were used to simulate the concrete slab. The girder flanges were discretized as beam elements, the girder webs as shell elements, and web stiffeners as truss elements. Rigid elements simulated the connection between the top flange and the slab while cross-frames were discretized using beam elements and bearings by means of constraining degrees of freedom. Results obtained were very similar to those obtained by Bishara and Elmir (1990).

Tarhini and Frederick (1992) conducted a parametric study to investigate the wheel load distribution on steel bridges using ICES STRUDL II three-dimensional finite element analysis models subjected to static wheel loading. The parameters involved were the size and spacing of the steel girders, presence of cross bracing, concrete deck thickness, span length, single and continuous span, and composite or non-composite behavior. The model consisted of isotropic eight node brick element IPLSCSH, with three degrees of freedom at each node, to model the concrete slab. The girder flanges and the web were discretized using three-dimensional quadrilateral four node plate element SBCR (shell element) to account for both membrane and bending deformation properties.

Regarding the composite bridge action at the deck-flange interface, no releases were imposed to those nodes at that location, therefore no slip was allowed. However, to simulate slip typical of the non-composite phase three linear springs were inserted at the interface nodes, one on each three-dimensional direction, whose stiffness was selected to allow the slab to move with respect to the top flange. In the end, a new formula was developed to predict the wheel load distribution as a function of the girder spacing and the span length that works for both composite and non-composite bridges.

Ebeido and Kennedy (1995) studied the influence of several parameters on the shear distribution in skew composite steel – concrete bridges. The parameters were the angle of skew, girder spacing, bridge aspect ratio, number of lanes, number of girders, end diaphragms, and number of intermediate cross-frames. The experimental studies involved six simply supported skew composite steel bridge models. Each model was subjected to load at various locations simulating truck loads. Deflections of steel beams, strains of beams and slab, and reactions at the supports were measured. Three-dimensional finite element modeling of skew composite bridges was conducted, using ABAQUS as the computing software. The reinforced concrete deck slab was modeled using a four node shell element with six degrees of freedom at each node. The girders, end diaphragms, and intermediate cross-frames were discretized using three-dimensional two node beam elements with six degrees of freedom at each node.

While the two end supports were simulated using a boundary constraint option that restricted the vertical displacements along the nodes at those locations, the multi point constraint option was used between the shell nodes of the reinforced concrete slab and the beam elements nodes on the girders. This was done to ensure full composite interaction, which is usually done by means of the shear stud connectors. It was concluded, among other things, that the results from the theoretical analysis were very close to those obtained on the lab tests.

Later on, Ebeido and Kennedy (1996) conducted an extensive parametric study of three continuous composite skewed steel bridges. They were able to deduce empirical formulas to determine span and support moment distribution factors for both interior and exterior girders when subjected to full and partial dead and live (truck) loads. The results from lab tests combined with a FEA were used to validate the models. Parameters like girder spacing, angle of skew, bridge aspect ratio, spans ratio, number of lanes, number of girders, and intermediate transverse diaphragms were considered.

The modeling process incorporated four node shell elements with six degrees of freedom at each node to discretize the slab using ABAQUS as the software package. The longitudinal girders and the transverse cross-frames were modeled using a three-dimensional two node beam element with six degrees of freedom at each node. Intermediate supports and abutment supports were modeled using specific boundary constraints, and with multipoint constraint options (MPC) between the slab and the beam nodes on the longitudinal steel beams to simulate full composite interaction. It was found that the exterior girder controls the design of skewed bridges, as far as the span and support moments are concerned. One of the most important findings is that the higher the skew angle, the smaller the span and support moments of the girder, particularly when the angle is greater than 30°. It was also found that transverse diaphragms moment connected to the girder improves load distribution on the bridge.

In an effort to determine live load distribution on bridges with irregular plan geometries, Tabsh et al. (1997) developed a methodology on which an isolated deck strip is loaded and then analyzed as a continuous beam on elastic supports. The displacements and rotational stiffness of the supports are computed based upon several parameters such as the girders geometric properties, position of the truck wheels, etc. Finally the reactions from all strips are transferred to the top flange of the girder in question to compute the girder distribution factor as the ratio of the beam moment (or shear) due to the effect of the truck load divided by two. The parameters considered were span length, continuity, number and spacing of girders, bridge width, girder stiffness, and number of loaded lanes.

To verify the exactness of the aforementioned methodology a three-dimensional finite element analysis was implemented using the computer program ANSYS. It involved the use of three different elements to model the entire system. To discretize the top and bottom flanges two node three-dimensional beam elements with six degrees of freedom at each node were selected. The steel web and the concrete deck were idealized with four node rectangular shell elements with six degrees of freedom at each node in order for plane membrane and out-of-plane bending effects to be computed. For the cross-frames and diaphragms, three-dimensional beam elements were considered and rigid three-dimensional beam elements were used to connect the centroid of the top flange steel beam elements to the centroid of the slab elements. The verification of the model was part of the work by Sahajwani (1995).

SAP 90 and ICES-STRUDL II were the computer software Mabsout et al. (1997a, 1997b,1998) used when they carried out an investigation to assess the degree of accuracy and the performance of four different finite element modeling techniques of common use in evaluating the wheel load distribution factors of steel girder bridges. The first model consisted of quadrilateral shell elements with five degrees of freedom per node for the concrete slab and space frame elements with six degrees of freedom per node for the girders. The centroid of the concrete deck coincided with the centroid of the girder cross-section. For the concrete deck, the second finite element model considered the use of quadrilateral shell elements and eccentrically connected space frame members representing the girders, while rigid links were imposed to account for the eccentricity of the girders with respect to the slab. The third model included the idealization of the concrete slab as well as the steel girder webs by means of quadrilateral shell elements, while girder flanges were discretized as space frame elements and flange to deck eccentricity was modeled by imposing rigid links. Isotropic eight node brick elements with three degrees of freedom at each node were used on the fourth model to idealize the concrete slab and quadrilateral shell elements for discretizing the steel girder flanges and webs. Results indicate that when dealing with non-skewed bridges the use of quadrilateral shell elements for modeling the concrete deck and concentric space frame elements for modeling the girders is encouraged.

Samaan et al. (2002) carried out a parametric study to evaluate the load distribution of sixty continuous two span composite concrete slab-steel spread box girder bridges using ABAQUS as the FEA software. Several parameters were considered such as span length, number of spread boxes, number of lanes, and number of cross bracings. All the models were subjected to eleven loading conditions. The models used, previously verified by Sennah and Kennedy (1998, 1999), were analyzed with four node shell element S4R with six degrees of freedom at each node for the concrete slab, steel girder webs, bottom flanges, and end diaphragms. This element could account for membrane, bending, and torsional effects. A three-dimensional two node beam element B31H was adopted to model top flanges, cross bracings, and top chords. The composite behavior between the slab and the top flange, due to the shear studs, was modeled by using multi point constraints MPC on the interface nodes. The bridge supports were modeled by constraining both vertical and lateral displacements at the lower end nodes of each web located at the end supports, whereas all displacements were restrained at the support on the mid span. The outcome revealed that current practices were either too conservative or too under predicting.

In an effort to determine the accuracy of the numerical methods for predicting the response of skewed bridges during construction, Norton et al (2003) developed two different models. The first model was a 2-D grillage on STAAD/Pro, in which the girders were modeled as non-composite frame elements and wet concrete was considered as uniform loads acting along each girder, and applied in four stages to account for the pouring sequence and to simulate all the components of the system, such as self weight of the girders, weight of wet concrete, and point loads from the screed supports. The second model was a 3-D finite element model constructed and analyzed on SAP2000. The modeling process included shell elements for the girder webs while space frame elements were used to model girder flanges, stiffeners, and cross-frames. Boundary conditions included restrictions on the translations in the three directions of the bottom node of the girder webs at the supports and restrictions on the vertical and lateral translation only. The cross-frames were rigidly connected to the girders while accounting for non-composite behavior of the concrete deck by assigning a modulus of elasticity of 68.9 MPa to the shell elements of the deck.

The Finite Element procedure has always been a rational way to deal with cumbersome and complicated systems. This is the case of Fu and Lu (2003) in the development of a finite element model to simulate the composite deck girder interaction. The girders were discretized with traditional eight-node isoperimetric quadrilateral elements; though the flanges of the girder were modeled using plate elements and the web with plane stress elements. As for the shear studs, bar elements were used to provide a dimensionless link between the deck and the top flange of the girders. With the help of the computer program RESIDU and with the results from previous experimental studies (Yam and Chapman 1972) the numerical model was evaluated. The results were compared to those obtained using classical transformed area method. The numerical results yielded values that were very close to the experimental but considerably far from those obtained with the transformed area method.

Huang et al. (2004) conducted research to develop a better understanding of the transverse load distribution for highly skewed steel girder bridges by means of both numerical and experimental analysis. The field test was conducted to measure strains at different points along a 60 degrees skewed bridge when two fully loaded trucks pass over it, following a particular load scheme. The analytical model consisted on a three-dimensional finite element model using ANSYS as the software package. Four node three-dimensional elastic shell elements with six degrees of freedom per node were used to model the concrete slab and the girders while the cross-frames were modeled with two node three-dimensional elastic beam elements with six degrees of freedom per node. For both the end supports boundary constraints were imposed in which the translational displacements were restricted except for the longitudinal direction. However, for the intermediate pier support all the displacements were restrained. No rotational constraint was considered. The overhangs and parapets were ignored. The end results showed that AASHTO LRFD formulation for live load distribution tends to be safely conservative for positive bending and for negative bending they are accurate but not conservative.

The research by Chung and Sotelino (2005) was focused on evaluating the behavior of composite steel girder bridges using FEA, including non-linear behavior with the ABAQUS software. Flexible shell elements were used to model the deck. The four node Mindlin layered shell elements (S8R) were selected due to its improved ability to model the non-linear behavior that occurs on the failure mechanism of concrete, including crack propagation through the slab thickness and dowel effect. The girders were modeled using Timoshenko beam elements (B32) to eliminate potential incompatibility on the boundaries, and for modeling the bearings spring elements with displacement constraints were selected. To model composite action between the girders and the deck rigid multi point constrained elements (MPC) were used to connect the centroid of the girder cross-section and the mid surface of the slab. The models were verified by means of two experimental studies done by Jofriet and McNiece (1971) and Kathol et al. (1995). The predicted and actual results were in close agreement, with a 10 percent difference.

Choo et al. (2005) studied the effects of variables such as environmental and material and concrete placement on the response of a skewed High Performance Steel (HPS) girder bridge during the construction stage. Temperature changes during the pour and forces developed during the setting of concrete are among the most important parameters considered in the study, along with the comparisons between stresses on the exterior girders in terms of the two possible concrete pouring schemes. A numerical investigation was also conducted to carry out the parametric study, and SAP2000 was selected as the computer program for the finite element analysis. The girders were modeled with four node shell elements and the wet concrete was idealized by a combination of three and four node shell elements in order to accurately distribute the loads to the girders. They were modeled in this manner because deck stresses were not in the scope of the investigation. The connection between the deck and the girders was guaranteed by using rigid links, and the cross-frames were modeled with three-dimensional frame elements. To validate the model stresses from the FEA were compared to those obtained from instrumentation in the field (strain gauges). Boundary conditions, temperature effects, and concrete stiffness were studied in detail. They concluded that time dependant concrete modulus effect was negligible when determining the stresses on the structure but temperature changes were of paramount importance. It was also found that the best concrete pouring sequence for simply supported skewed bridges was that with the screed parallel to the supports.

Beckmann and Medlock (2005) used a scale model with girders made out of poster board to make them flexible enough to be able to measure both rotations and translations at the girder ends. Various AASHTO/NSBA issues were addressed such as the fact that ends of girders do not develop in plane rotations for different bearing alignment conditions. They also developed expressions to determine transverse movements and account for possible ways to deal with design problems like those mentioned in the AASHTO/NSBA G 12.1-2003 *Guidelines for Design for Constructability*. It was found that the ends of the girders will rotate about an axis that runs through the centerlines of rotation at the bearings, and do not rotate in a vertical plane parallel to the girder web, as it was assumed initially. The transverse movement of the top flange relative to the bottom flange results in the ends of the girders being out-of-plumb. This condition has a direct effect on the position (deflection, twist, etc.) of the girder webs at intermediate cross-frames where there is differential deflection between adjacent girders due to their relative locations in the span.

2.5 NCSU / NCDOT Related Studies

Whisenhunt (2004) measured deflections on five different skewed steel girder bridges during the construction phase in order to determine the real non-composite deflection behavior of the bridge and compare it to the behavior predicted by the current design methodology. The current design procedure involves computing deflections in each girder as though they worked independently or as single units. It was found that quantifying deflections by such a procedure turned out to not only be inaccurate by an average of 38 percent on interior girders or around 6 percent on exterior girders, but also it does not incorporate transverse distribution of loads along the cross-frames and diaphragms that interconnect the girders.

To make up for these discrepancies, a three-dimensional finite element analysis was conducted using ANSYS as the computing platform including parameters such as bridge skew, cross-frame stiffness, stay-in-place (SIP) metal deck forms, and partial composite action. The results from these studies were then compared to those obtained from the field and from the current design formulation. It was found that they significantly improved the accuracy of the predicted deflections (within 6 to 14 percent) and even accounted for the considerable effects of the SIP metal deck forms on the torsional stiffness and the overall behavior of the structure.

The objective of the research conducted by Paoinchantara (2005) was to develop a simplified modeling method to predict the non-composite dead load deflections of the steel plate bridge girder. The study was conducted in order to create a simplified modeling method for both single span and two-span continuous bridges including parameters such as bridge skew, cross-frame stiffness, and stay-in-place metal deck forms using SAP2000 as the primary finite element software. By measuring the deflections in the field during the construction the actual non-composite deflection behavior of the bridge was determined and compared to the results from modeling. Four simplified models were included in the research, which included a two-dimensional grillage model, a three-dimensional analytical model which included frame elements as the cross-frames, another three-dimensional model including the SIP forms as frame elements, and a three-dimensional model where the SIP forms were discretized as shell elements. As a result, the predicted deflection of the simplified models agreed well with the measured deflections and results from finite element models results for the single span bridges, whereas the predicted deflections from the simplified models did not agree with the measured results for the two-span continuous bridge. It was also concluded from both field measurements and modeling results that, on one hand stay-in-place metal deck forms have a significant effect on the non-composite dead load deflection behavior, and on the other hand that composite action has a slight effect on the vertical deflection behavior for skewed steel plate girder bridges.

Fisher (2005) carried out research to develop a simplified procedure to predict dead load deflections of skewed and non-skewed steel plate girder bridges. This was done by studying five bridges following Whisenhunt's (2004) approach of discussing bridge descriptions, field measurement techniques, and measurement results while increasing the variance in both bridge type and geometry to provide additional data for the validation of the finite element models. Using ANSYS as the FEM platform and MATLAB as the preprocessor program software, it was possible to carry out the numerical analysis including an extensive parametric study that was conducted to investigate the effect of skew angle, girder spacing, span length, cross-frame stiffness, number of girders within the span, and exterior-to-interior girder load ratio on the girder deflection behavior.

With the results from the parametric study it was concluded that the simplified procedure may be utilized to predict dead load deflections for simple span steel plate girder bridges. An alternate prediction method was proposed to predict deflections in continuous span steel plate girder bridges with equal exterior girder loads. Additional comparisons were made to validate this method.

2.6 Need for Research

AASHTO (2003) identifies the fact that there is a limited amount of literature available that documents in detail construction issues of steel plate girder bridges such as differential deflections between adjacent girders, out-of-plane girder rotations, and problems that occur during staged bridge construction. Our review of the literature confirms that there is very limited published research on the lateral flange bending (out-of-plane girder rotations) of steel plate girder bridges. Researchers have documented discrepancies related to predicting structural behaviour during bridge deck construction throughout the available literature. What is more, only a few investigators have dealt with the problem of how to control the lateral and transverse deformations a skewed bridge undergoes during the non-composite stage during the erection and construction phase. Documented parametric studies have included issues related to the skew angle, cross-frame stiffness, girder spacing, span length, influence of SIP metal deck forms, and torsional and lateral stiffness / strength. These variables have been identified as some of the factors to have the greatest influence on the skewed bridge behavior.

Based upon the literature review presented herein, the need for additional research on the topic of lateral flange bending of skewed steel girder bridges is apparent. Specifically, need for quantification and a prediction method of the out-of-plane girder rotations is paramount.

3.0 FIELD MEASUREMENTS

3.1 General

As part of the investigations related to characterization of lateral flange bending on skewed steel girder bridges it was necessary to obtain real time information generated during the construction process. The lack of available literature related to cross-section rotations on skewed bridges made the investigation even more challenging.

The field measurement process started by establishing the range of required geometrical conditions of the bridges that were considered ideal for the purpose of the investigation. Whisenhunt (2004) and Fisher (2005) suggested that the best results are obtained for skew angles greater than 20 degrees. Then from the available alternatives two bridges were selected that met the established criteria. Finally, out-of-plane rotations and deflections at quarter points and supports were selected as the primary measurement variables to be used on the field. Temperatures during the construction process were also considered.

3.2 Bridge Selection

As it was mentioned before, the first step was to select the bridges to be monitored during the construction process. To carry out such a task it was required to single out bridges that comply with certain geometrical constraints in order to ensure the adequate and reliable nature of data generated. These selection criteria included skew angles less than or equal to 45 degrees, simple spans, four or more girders, and girder spacing between six and ten feet.

3.3 Bridges Studied

3.3.1 General Information

There are some characteristics shared by the two bridges included in the analysis, such as:

- Steel plate girders were connected either by K-type cross-frames or by Diaphragms
- Elastomeric bearing pads: deformations at these locations were considered as part of the investigation
- All bridges were fabricated with AASHTO M270 steel. One of them was grade 50 and the other was grade 345W.
- Design phase included the differential deflection procedure to determine the required camber of the girders.

3.3.2 Bridges Monitored

presents part of the geometric parameters included for each bridge. The reason they were selected was not only because the met the selection criteria but their construction date was found to be within a period of six months, which met the time constraints for the investigation

Table 3-1 Summary of bridges

Bridge	Span (ft.)	Number of Girders	Skew angle (deg)	Spacing (ft.)	Cross-frame type
Chicken Rd	133	4	137	10	K-type
Roaring Fork	73.5	5	23	6.5	Diaphragm

Following is a brief description of the bridges selected for this study.

3.3.3 Bridge on SR 1003 (Chicken Road) over US 74 between SR 1155 & SR 1161 in Robeson County. Project # R-513BB

Chicken Road Bridge is a two single span, four girder bridge. It is located over a construction segment of US 74 between Maxton and Lumberton. Both spans are almost identical with the only difference of a few inches and a few fractions of a degree in skew because the bridge was located on a slight curve along the road (the maximum superstructure arc offset is 7 inches). For this reason both spans produced similar results and therefore only those from one of the spans will be presented. Deflections and rotations on both flanges and the web were monitored at quarter points along the girders as well as at the end bents to measure support settlements. At the end bents rotations were only monitored on the bottom flanges and web. The presence of formwork made the top flange unreachable. The pouring phase started close to midnight on one end bent and finished close to 9:00 a.m. on the other bent. A general view of the bridge is presented on Figure 3-1. All the geometrical properties of the bridge as well as material information are presented on Appendix B.

Figure 3-1. Chicken Road Bridge

3.3.4 Bridge No 338 over Roaring Fork Creek on SR 1320 (Roaring Fork Road) in Ashe County. Project # B-4013

Roaring Fork Bridge was located in the mountain region of north western North Carolina. It is a five girder simple span bridge and the most outstanding feature is that it has a severe skew angle of 23 degrees (See Figure 3-2). The bridge spans across a creek so the typical quarter point locations for monitoring were compromised. Therefore deflections and rotations were only monitored at end bents and mid points.

Similar to what occurred on Chicken Road Bridge, rotation measurements were limited to bottom flange and web at the end bents due to constraints associated to the formwork. The concrete was cast during a five hour period of time. Appendix C presents the most important geometrical and material information for this bridge.

Figure 3-2. Roaring Fork Road, in Ashe County

3.4 Field Measurements

3.4.1 Overview

The primary purpose of the investigation was to monitor girder cross-section rotations at a given location. Nevertheless, to have sufficient data to validate the analytical modeling procedure it was necessary to measure deflections along the span. All the information regarding how those deflections were determined using string potentiometers, dial gauges, or the alternate procedure can be found in the Whisenhunt (2004) and Fisher (2005) investigations.

3.4.2 Girder Cross-section Rotations.

A digital level with a precision of 0.1 degrees combined with a carpenters level were the main instruments used to monitor rotations along the span.

First the carpenter's level was placed against the element (i.e.: the bottom flange or web) to be measured. The digital level was then placed against the carpenters to determine the corresponding rotation in degrees, as shown on Figure 3-3

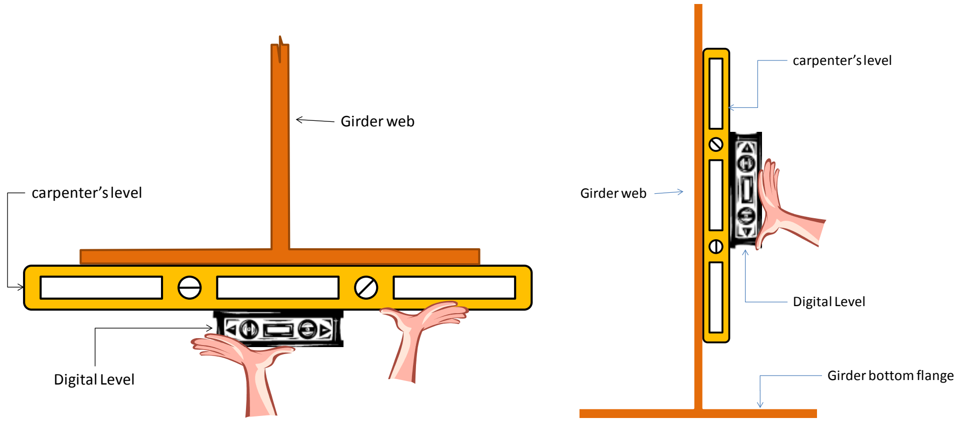

Figure 3-3. Procedure to measure rotations on the Bottom Flange (left) and Web (right)

Due to the existence of different constraints such as the stay-in-place forms, reinforcing steel, etc. the top flange rotations were measured from the lower side at those locations where it was possible to access the top flange area and using the level directly on the steel element (See Figure 3-4).

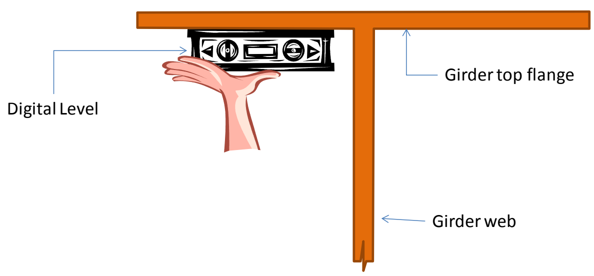

Figure 3-4. Procedure to measure rotations on Top Flanges

3.4.3 Temperature

Besides the typical deflections and rotation readings it was important to keep track of the temperature changes during the placement of the concrete. An infrared thermometer was used to measure temperature changes on the structure. For a typical bridge, large temperature changes are possible in a period of 24 hours and these changes may produce significant stresses and deformations that must be accounted. However, it was found that during the construction process of both bridges the largest recorded change in girder temperature was 10° F, which could be considered negligible with respect to the structural behavior being monitored.

3.4.4 Sign Convention

The sign convention used for all the field measured rotations was as follows: following the direction of the span, this is from end bent 1 towards end bent 2, positive rotations are clockwise. Figure 3-5 presents a schematic of this condition.

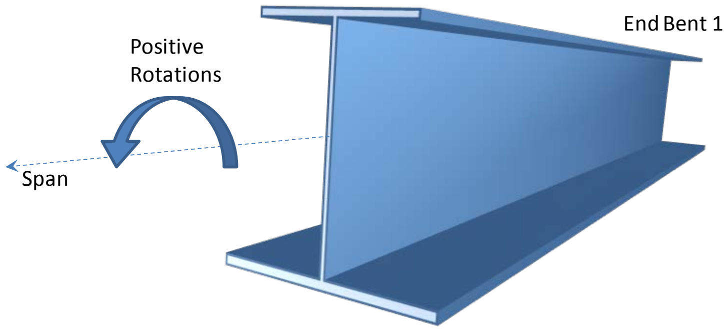

Figure 3-5. Directions of positive rotations

3.4.5 Sources of Error

It is worth mentioning that the reason to use the carpenters' level is that flanges and webs are not 100 percent flat. In an effort to capture the real behavior it was necessary to "average out" the rotation measurements. The carpenter's level covers almost all the web height and all the bottom flange width for both of the bridges studied; hence the values reported were the average rotations of the section (see Figure 3-6).

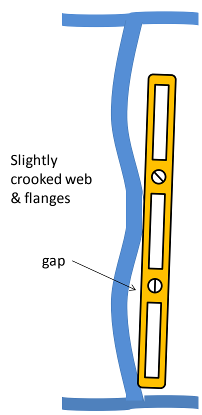

Figure 3-6. Imperfections of the straightness

3.4.6 Limitations

On most of the top flange locations access was severely compromised due to the different construction components located along the span. On Chicken Road Bridge there were several wood studs along the span used to control rotations during the construction process. On Roaring Fork Road Bridge the stream flow was particularly strong which made top flanges along the span impossible to reach. For this same reason on Roaring Fork only values at the end bents and mid span could be monitored.

3.5 Summary of Acquired Field Data

On Table 3-2 the different rotation can be found in degrees recorded for the two bridges included on this research. It is worth mentioning that these values represent the total rotations measured when all the concrete was poured. Figure 3-7 and Figure 3-8 present the field rotation values obtained for an exterior girder on Chicken Road Bridge and Roaring Fork Bridge, respectively Additional information with regards to deflections can be found on Appendices B and C.

Table 3-2. Summary of girder rotations, in degrees, recorded for both bridges

Bridge	Loc	Section	Girder				
			G1	G2	G3	G4	G5
Chicken Road (Span A)	First End Bent	Top Flange	-	-	-	-	-
		Web	-0.6	-0.6	-0.7	-0.7	-
		Bottom Flange	-0.6	-0.3	-1.1	-0.5	-
	First Quarter	Top Flange	-	-	-	-	-
		Web	-0.3	-1.2	-0.7	1.2	-
		Bottom Flange	0.1	0.3	0.5	0.7	-
	Mid Span	Top Flange	-	-	-	-	-
		Web	0.5	0.2	0	-0.2	-
		Bottom Flange	-1.4	-0.3	0.1	-1	-
	Third Quarter	Top Flange	-	-	-	-	-
		Web	0.9	0.4	0.5	0.2	-
		Bottom Flange	-1.6	-0.6	-0.8	-0.6	-
	Second End Bent	Top Flange	-	-	-	-	-
		Web	0.6	0.7	-0.7	0.5	-
		Bottom Flange	-0.4	-0.4	0.2	-0.2	-
Roaring Fork	First End Bent	Top Flange	-	-	-	-	-
		Web	-0.1	-0.2	-0.3	-0.4	0
		Bottom Flange	0.6	0.1	0	0.1	-0.7
	First Quarter	Top Flange	-	-	-	-	-
		Web	-	-	-	-	-
		Bottom Flange	-	-	-	-	-
	Mid Span	Top Flange	0.8	-2.7	-1.7	0.6	0
		Web	-0.3	-0.4	-0.2	-0.2	-0.2
		Bottom Flange	-5.3	0.4	0.3	0.1	-1.3
	Third Quarter	Top Flange	-	-	-	-	-
		Web	-	-	-	-	-
		Bottom Flange	-	-	-	-	-
	Second End Bent	Top Flange	-	-	-	-	-
		Web	0.7	1	0.4	2.3	0.1
		Bottom Flange	-0.9	-0.9	-0.8	-0.3	-0.1

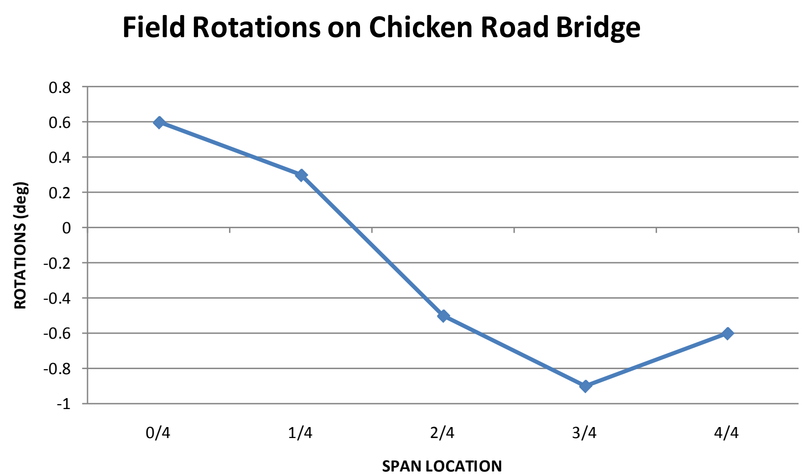

Figure 3-7. Field Measurements on an Exterior Girder (G1) for Chicken Road Bridge

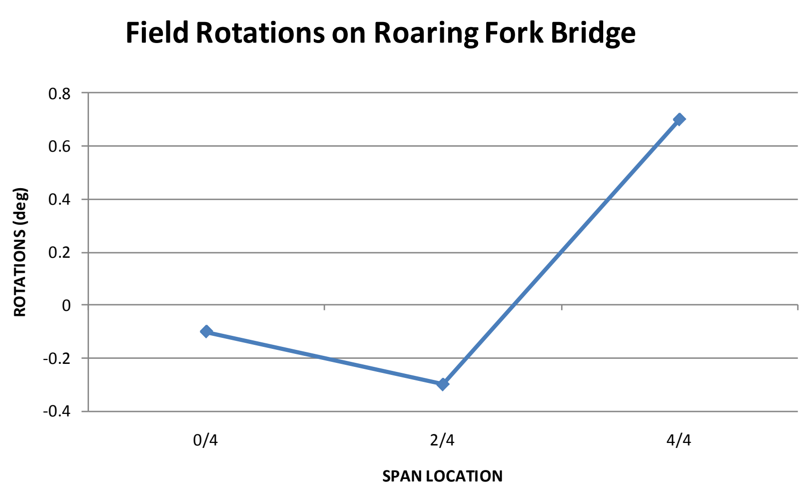

Figure 3-8. Field Measurements on an Exterior Girder (G1) for Roaring Fork Bridge

4.0 FINITE ELEMENT MODELING

4.1 Overview

Previous research conducted by Whisenhunt (2004) and Fisher (2005) has demonstrated the powerful abilities of three-dimensional finite element analysis (FEA) to accurately model the behavior of skewed steel girder bridge structures. Finite element modeling was utilized in this research program to conduct the parametric analysis to discover the influential parameters that affect the lateral flange bending behavior. The modeling techniques employed in this research program are similar to those used by Whisenhunt (2004) and Fisher (2005). However, the modeling of the cross-frames and the girder end bearings was greatly enhanced. The field measured data was utilized to validate the improved modeling techniques. To reduce the model generation time and effort, a preprocessor program was developed in Visual Basic 6.0 to automate the procedure of creating the models varying the corresponding parameters.

This research is focused on the behavior of steel plate girder bridges during the non-composite phase of construction. During this phase of construction the loading is primarily static and the corresponding response of the structure is typically well within the elastic range. As a result, static, linear elastic solution of the finite element models was employed. Descriptions of the techniques and procedures utilized to conduct the FEA are provided herein.

4.2 Bridge Components

Most of this investigation was based on findings and theories used in previous research by Whisenhunt (2004) and Fisher (2005). In an effort to be as concise as possible many of the bridge component descriptions were not included in this report and can be found in the aforementioned investigations. However, special attention will be given to those bridge components that were required to be modified to accommodate the rotations studied herein.

4.2.1 Cross-frames

Two types of end bent cross-frames and three different types of intermediate cross-frames were included in the analysis. Each was modeled with sufficient detail to capture the observed behavior of the components.

4.2.1.1 End Bent Cross-frames and Diaphragms

End bent cross-frames were used on Chicken Road Bridge whereas diaphragms were used for Roaring Fork Bridge. Figure 4-1 illustrates both the end bent cross-frames and diaphragms. The top channel of the cross frames and the diaphragms were modeled using SHELL93 elements. The SHELL93 elements are eight node isoperimetric shell elements that are an accurate and reliable type of element for modeling steel sections. This is due to not only their inherent ability to transfer shear forces within its plane, but to the possibility of accommodating flexural deformations along their span. A four node element can be too stiff and not represent the behavior appropriately. The WT sections of the cross-frame were modeled with BEAM 4 and LINK8 elements. The BEAM4 elements are capable of transferring forces and moments across its span and are defined with two or three nodes with six degrees of freedom each. The LINK8 elements are typically used to model those components that only transfer axial force, such as diagonals of a truss, etc. They are defined with two nodes with three degrees of freedom.

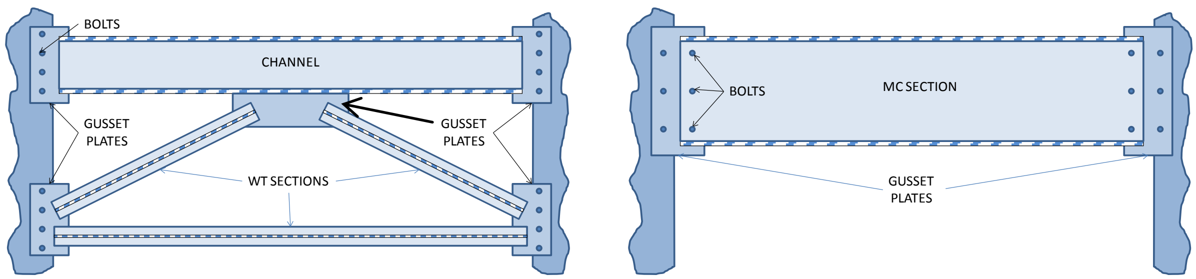

End Bent Cross-frame (Chicken Road Bridge)   End Bent Diaphragm (Roaring Fork Bridge)

Figure 4-1. Both types of end bent cross-frames considered

In addition to the struts and diagonals of the cross-frame, the gusset plates were also included in the modeling to enhance the response of the model. SHELL93 elements were used to model the gusset plates. The bolted connection was modeled by coupling the bolt locations on the gusset plates with those on the stiffeners (or connection plates) and the channel. Figure 4-2 depicts such a condition.

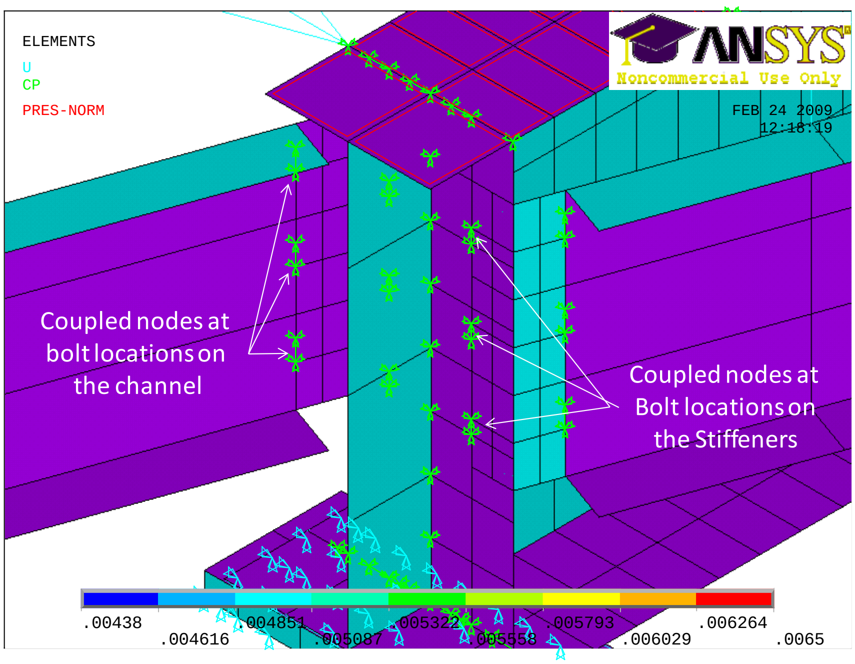

Figure 4-2. Coupling of nodes at bolt locations to simulate real interaction

4.2.1.2 *Intermediate Cross-frames*

Three types of intermediate cross-frames were considered within this study. The K-type and X-type cross-frames were modeled using the same techniques as Whisenhunt (2004) and Fisher (2005). However, the diaphragms were modeled the same as the previously described end bent diaphragms, using SHELL93 elements and coupling the nodes at the bolts locations with the intermediate stiffeners (or connectors). Figure 4-3 illustrates the three types of cross-frames.

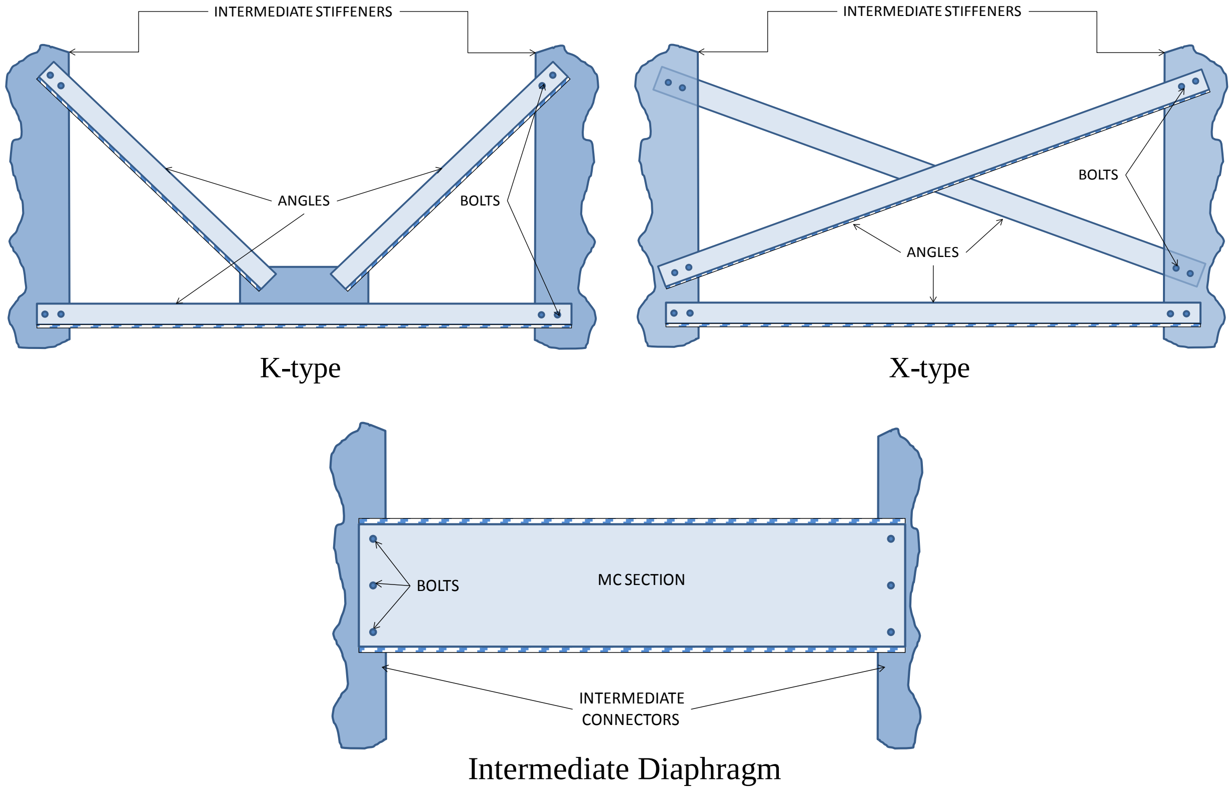

Figure 4-3. Three types of intermediate diaphragms or cross-frames

4.2.2 *Elastomeric Pads*

One of the model improvements included in this investigation was the incorporation of elastomeric pads at the girder end bearing locations. SOLID186 elements were selected to model the elastomeric pad. This higher order 20 node isoperimetric solid element has the particular property of exhibiting a quadratic displacement behavior, which allows it to depict deformations of the pad with a high degree of accuracy. The material properties, which include shear modulus and Poisson's ratio, were studied by Muscarella and Yura (1995). Although the type of connection between the elastomer and the concrete was constrained by “pins” or “rollers”, depending on the end bent, this study did not take into account variations of the pad material properties nor the friction between concrete and the elastomer and between the steel and the elastomer. Rigid links were used to connect the sole plate with the bottom flange of the girder. This was done to simulate the eccentricity due to the thicknesses of both the plate and the bottom flange, which can be up to 3 inches. This was possible with the MPC184 rigid element. This element only requires two nodes to be defined. A picture with the boundary conditions is shown on Figure 4-4.

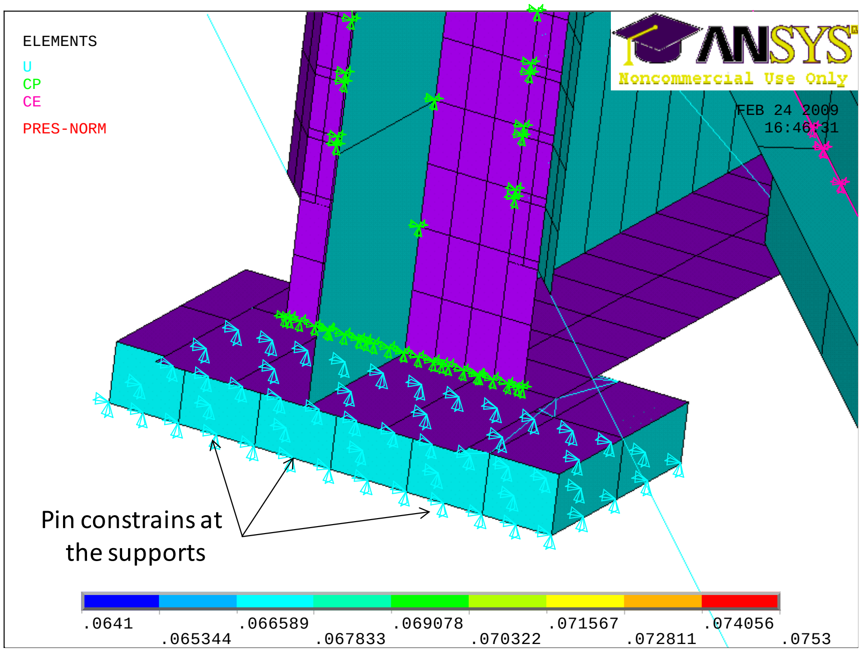

Figure 4-4. Constraints at the supports

4.3 Modeling Procedure

4.3.1 Initial Model (Model 1)

The first approach to the problem was to consider the original models developed by Whisenhunt (2004) and Fisher (2005). These particular models had the ability to accurately predict deflections along the span for steel skewed bridges. However, there were two conditions that needed to be re-evaluated.

One condition was the possible sources of error induced in measuring rotations due to the lack of part of the components, such as the stay-in-place (SIP) forms on the region between the end of one girder and the same end of the adjacent girder. The other condition was the fact that none of the original models account for diaphragm type of frames and the mechanism by which these diaphragms transfer forces which is different than those on the cross-frames. Figure 4-5 shows how the SIPs are not included on the end regions.

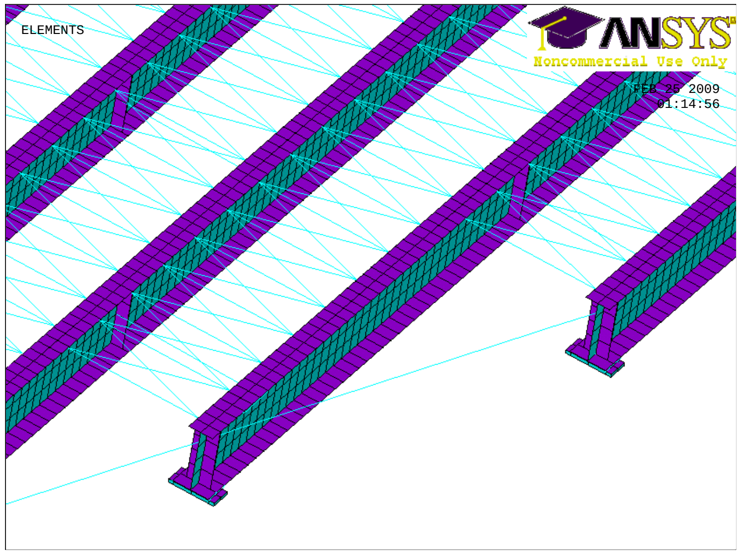

Figure 4-5. Girders end regions on Model 1

To capture the effect of the empty SIP region on the overall behavior of the bridge trial loading cases were carried out such that forces along the SIPs were recorded on one of the bridges. Figure 4-6 shows an example of those forces between an exterior girder (G1) and its adjacent girder (G2). It is clear that at no locations along the span, SIP forces reach the value of 1 kip, and most of the force is carried by the diagonal elements. The dotted lines represent an outline of the plan view of the bridge between the exterior girder 1 (G1) and its adjacent girder 2 (G2). It can be seen that no forces are developed in the initial region of G1 and the final region of G2. To determine the reliability of the model, the next step was to incorporate the SIP forms along those initial and final regions and measure the affect of such a modification.

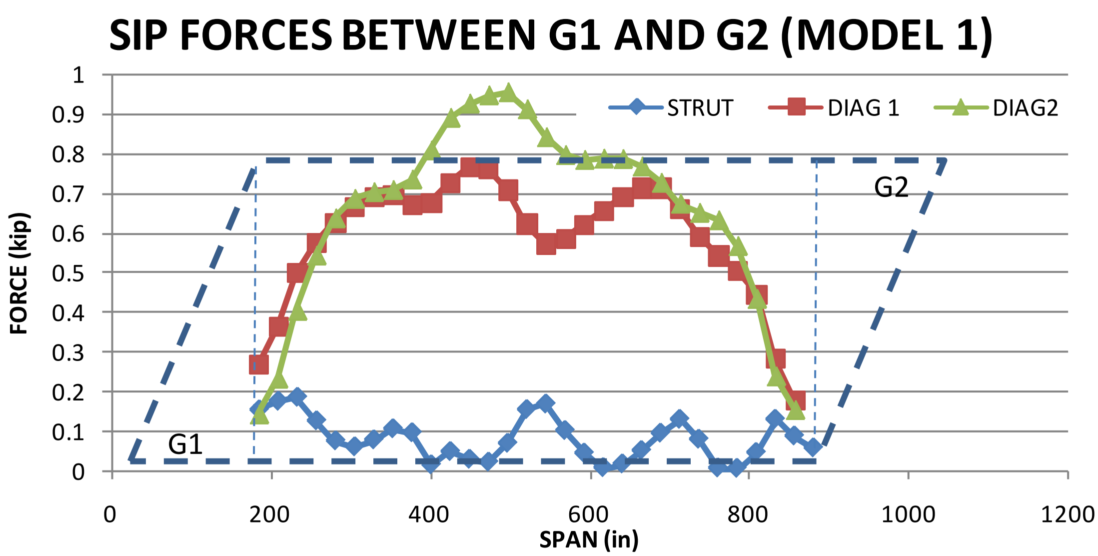

Figure 4-6. SIP force distribution along the span

4.3.2 Next Model (Model 2)

One of the challenges related to the incorporation of the stay-in-place elements in the final regions was the gap created between the end of the SIPs and the end bent diaphragms. To solve this situation it was necessary to link the SIP forms to the diaphragms with rigid element connectors. These elements allow the diaphragms to lock the ends of the SIP forms into themselves creating a particular connection in which no deformations occur along the connectors while the eccentricity between the end nodes of these elements accounted for the torsional component transferred into the end bents.

Although the lengths of the SIPs in this region are shorter, no adjustments were made to the cross-sectional area for either the struts or the diagonals. Figure 4-7 shows the new model incorporating the new SIP elements at the girder ends. Similarly to the original model, the forces developed on these SIP elements were monitored and the results presented in Figure 4-8.

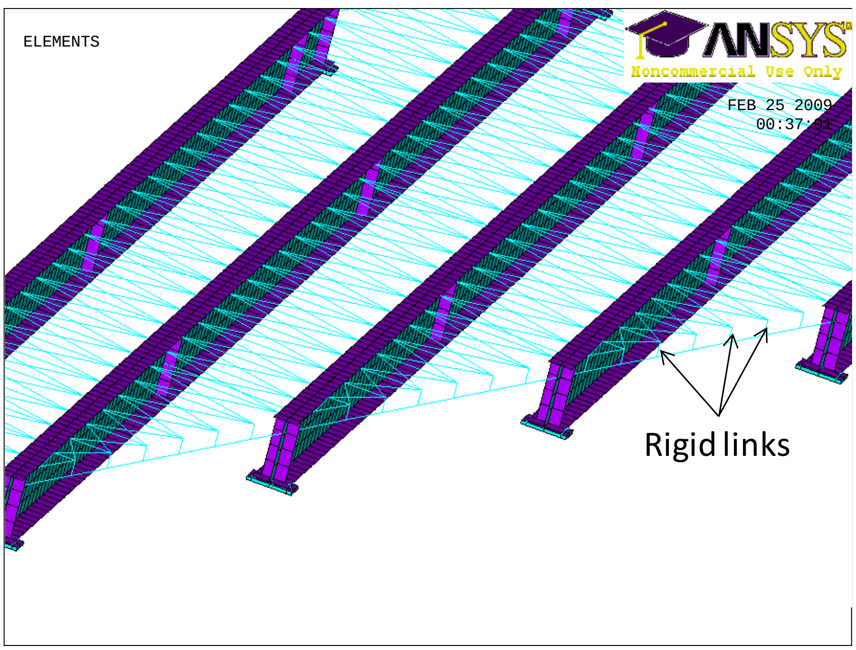

Figure 4-7. Second model detail, incorporating SIP forms on the end regions

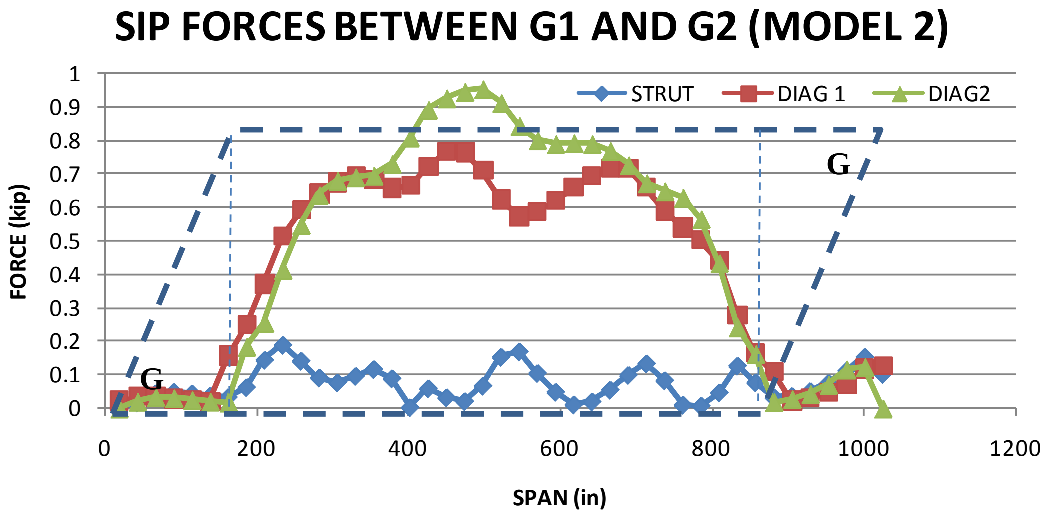

Figure 4-8. Force distribution along the SIP forms in Model 2

The SIP forces in the end regions are particularly smaller than the rest of the structure. Although the results may not agree with the higher stiffness values for the SIP forms in the end regions, they should have led to higher forces. The end bent diaphragm stiffness is even higher than the SIPs and therefore most of the forces developed in that region should be carried by these diaphragms. Figure 4-9 shows how the lateral forces are distributed between the SIP forms and the cross-frames or diaphragms. It can be seen that he relative value of lateral forces between these two components can be in the order of 8 to 1.

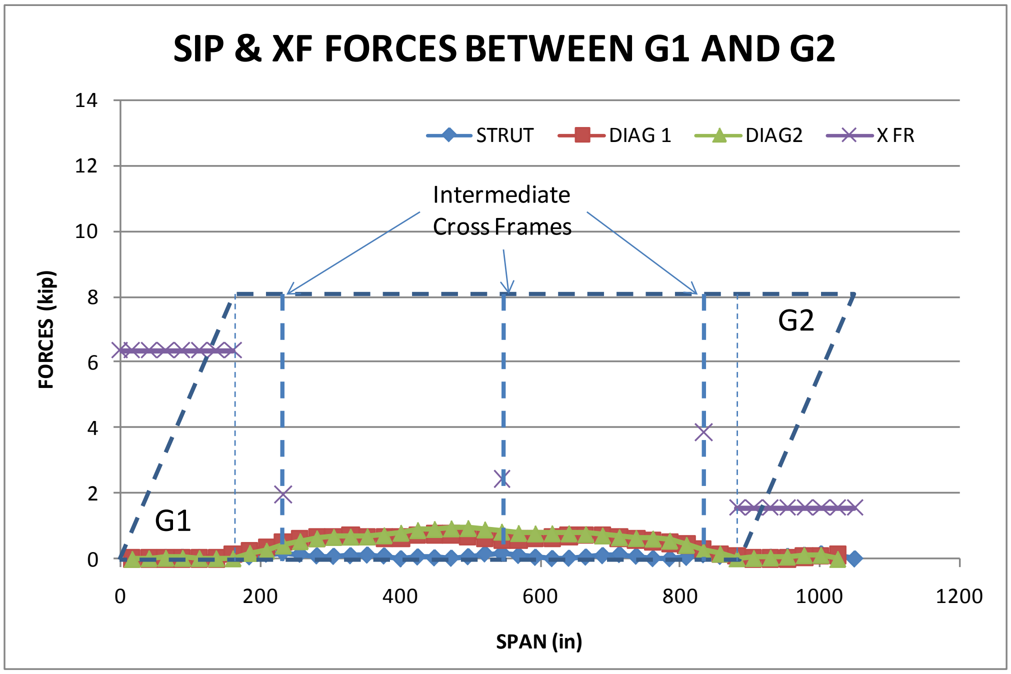

Figure 4-9. Force distribution between SIPs and Cross-frames

Figure 4-10 shows that the out-of-plane girder rotation for models 1 and 3 are essentially the same. To investigate the affect of the cross-frame and diaphragm connection flexibility on the girder rotations, the model was enhanced once again. The new model accounts for the rotational constraints imposed at the connections between the end bent stiffeners and the diaphragms.

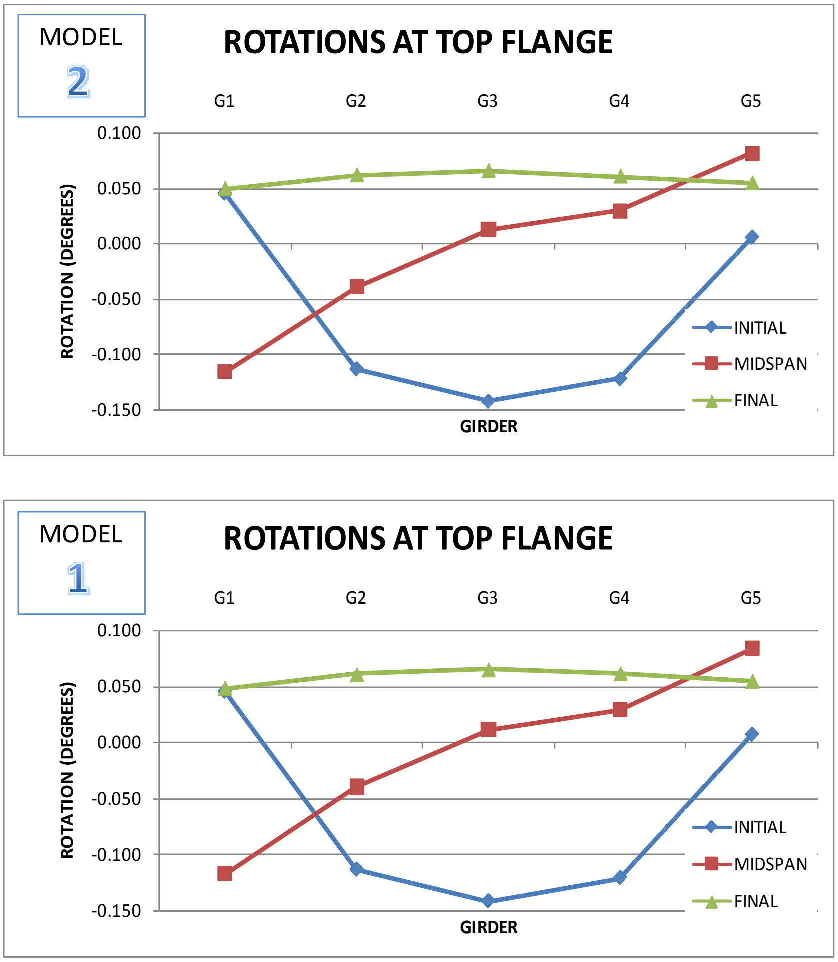

Figure 4-10. Rotations comparison between Models 1 and 2 at Top Flange

4.3.3 Model 3 - An improved discretization

A higher order approach was considered to assemble the new model of the bridge. For this case the end bent diaphragms and the intermediate diaphragms were modeled using SHELL93 elements and connected to the stiffeners at the bolt locations (Figure 4-11). This was possible by coupling the nodes on the diaphragms to the corresponding nodes on the stiffeners as previously depicted on Figure 4-2.

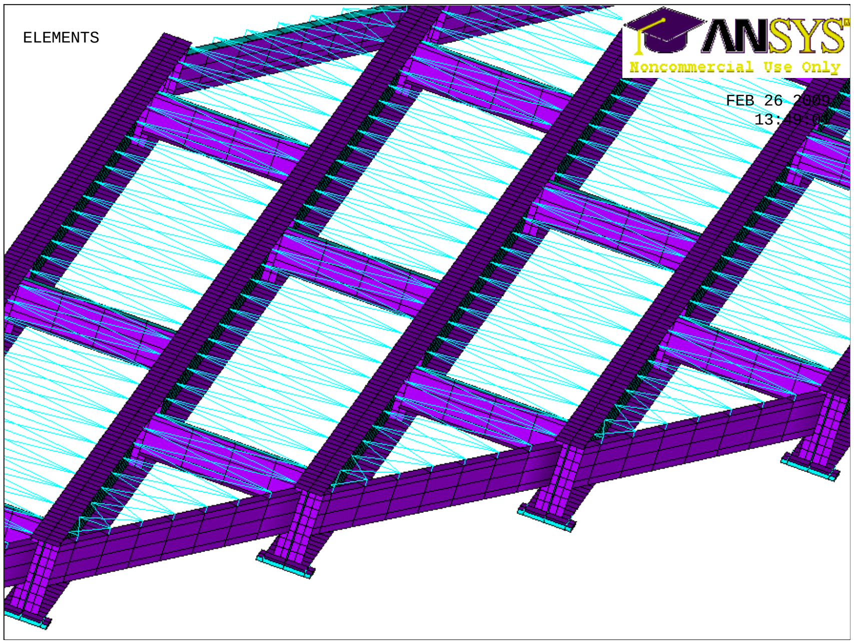

Figure 4-11. Model 3 including diaphragms discretized with shell elements.

With this improved model of the bridge structure, it was possible to carry out a preliminary study to determine whether there was any correlation between the skew angle and the maximum deformations of the bridge. Several different skew angles were considered ranging from 15 degrees to 90 degrees. The results are plotted in Figure 4-12. The good correlation between the skew angle and deflections leads to think that there is some type of systematic behavior on skewed bridges and the skew angle seems to play a major role on the behavior of these structures. This confirms the behavior reported by Whisenhunt (2004) and Fisher (2005).

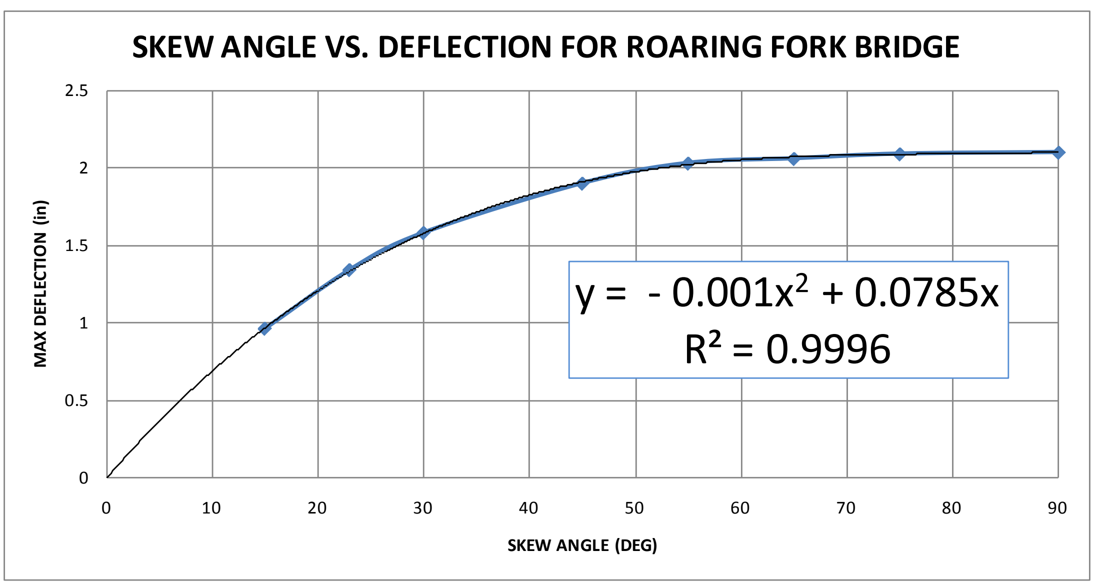

Figure 4-12. Relationship between skew angle and maximum deflections

4.3.4 Model 4 - Final Model

The most important objective throughout the investigation was to accurately predict the out-of-plane (torsional) rotations of the girders. To obtain the most accurate results, it was necessary to include all of the structural components in the finite element model. Figure 4-13 is an illustration of the final finite element model considered in these investigations. In this model the SIP forms are included along the entire length of the girders, the beam bearing and elastomeric pad is explicitly modeled, the cross-frames and cross-frame connections details are modeled. This final model was validated using the available experimental data and was utilized for the parametric study.

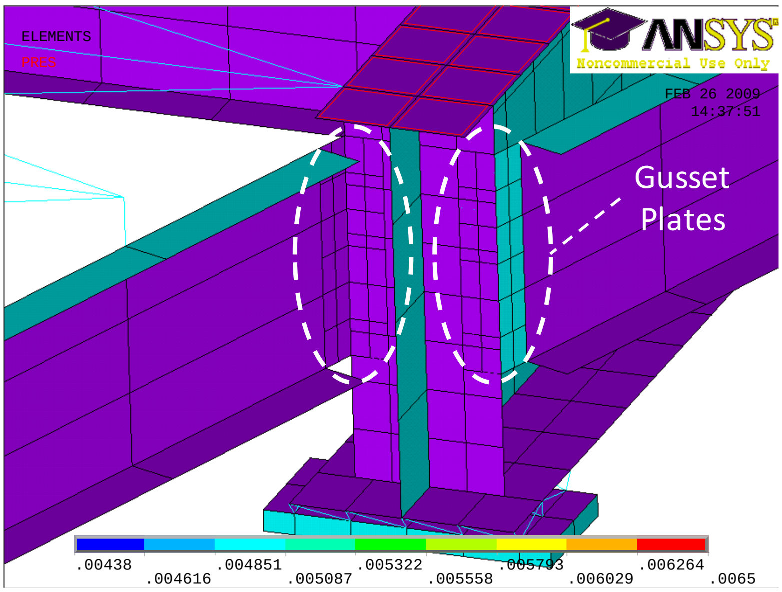

Figure 4-13. Detail of the end bent connection in the final model (Model 4)

4.3.5 Validation of Results.

In this section results from all four models are presented and compared in an effort to validate their accuracy and reliability. Both deflections and out-of-plane rotations were used as evaluation criteria. Figure 4-14 presents the results for the four models and the field measurements for both deflections and out-of-plane rotations in one of the bridges. It can be noticed the evident difference between rotations on model 4 and the rest of the models. In the case of deflections, it is noteworthy that in models 1 and 2, used by Whisenhunt (2004) and Fisher (2005), the beam elements used to model intermediate diaphragms did not accurately represent the flexural capabilities of these bridge components considering the lack of load transferring evidenced on the deflected shape of these two models, that resemble the deflected shape of a non-skewed bridge, where there is little interaction between the girders and the cross-frames. Once these cross-frames are modeled with two-dimensional elements a more suitable representation of the behavior is obtained. When comparing rotations on models 3 and 4 to those obtained in the field, it can be seen that the use of gusset plates to model the behavior of the end bent cross-frames (model 4) enhanced the rotational response of the bridge dramatically, creating a more flexible structure that that on model 3. As far as the deflections are concerned, both model 3 and 4 produced similar results to those obtained from the field.

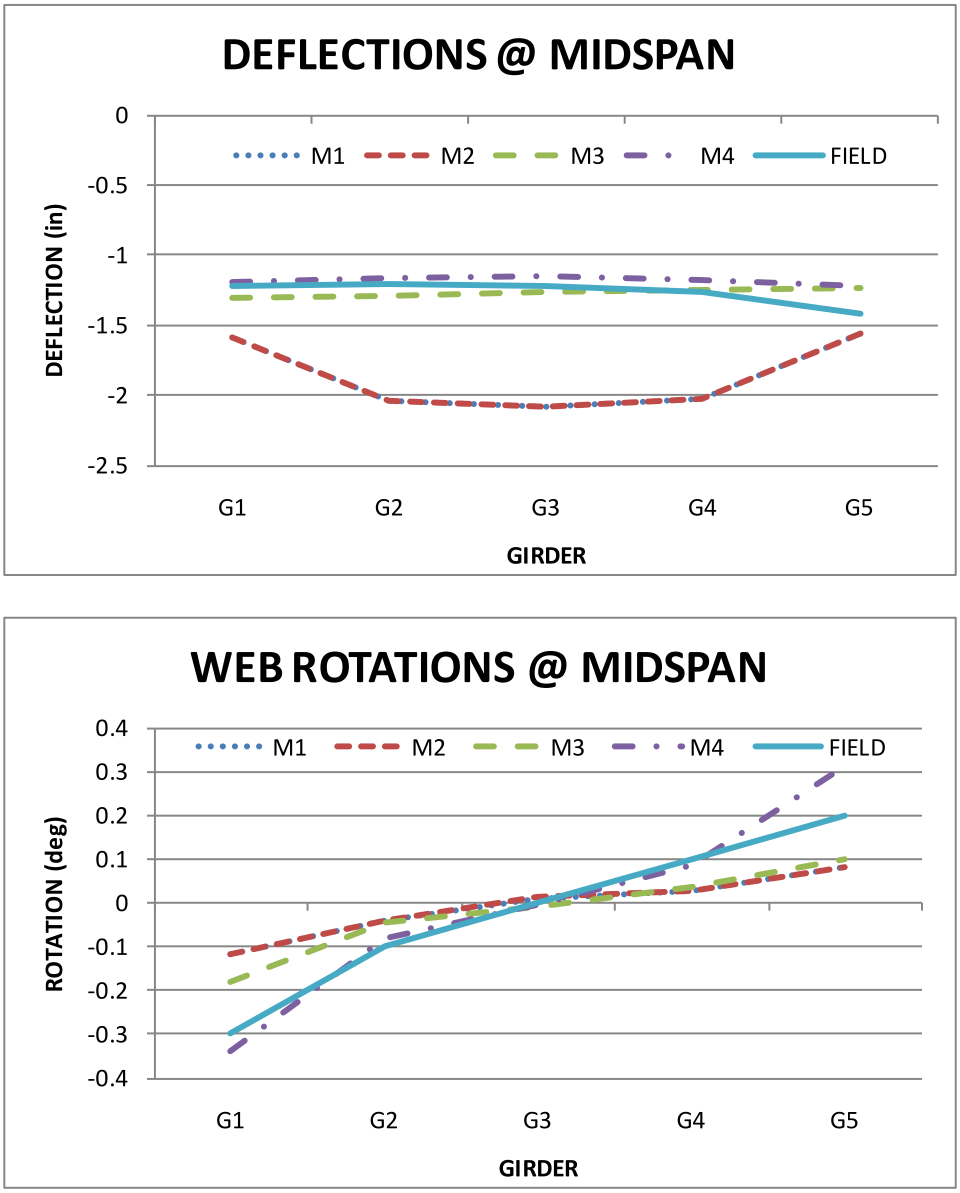

Figure 4-14. Deflections (top) and Out-of-plane Rotations (bottom) for Roaring Fork Bridge

4.4 TIPS FOR MODELING

4.4.1 General

The following are a series of general modeling rules that were found to be helpful during the Finite Element modeling stage of the investigation. The idea is to present a series of "useful tips" to be accounted during the modeling process and to be considered only as guidelines for future investigations. By no means should these tips be considered as mandatory.

4.4.2 Modeling Components

4.4.2.1 Girders and sole plates

It was observed from previous studies (Whisenhunt 2004 and Fisher 2005) that 8 node isoperimetric shell elements are adequate to model steel girders and sole plates due to their inherent ability to transfer shear forces as well as their membrane and bending capabilities. Table 4-1 presents the values for the geometrical dimensions of the girders and cross-sections of the bridges studied.

Table 4-1 Geometrical properties of the girders

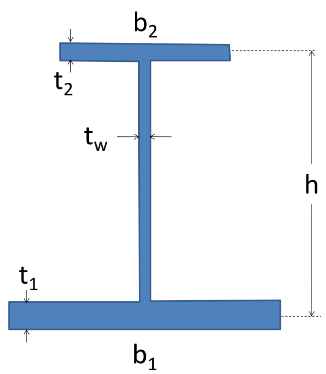

Chicken Road

b_1 (in)	t_1 (in)	h (in)	t_w (in)	b_2 (in)	t_2 (in)
18.1	0.9	57.1	0.6	14.2	0.9
18.1	1.6	57.1	0.6	14.2	0.9

Roaring Fork

b_1 (in)	t_1 (in)	h (in)	t_w (in)	b_2 (in)	t_2 (in)
18	1	32	0.5	12	0.75

It was found that an appropriate mesh size for the flanges was to divide the transverse dimension (width) into units of at least one quarter of the bottom flange width, one half of the top flange width and to divide the vertical dimension of the web into elements at least one quarter of its height. Finally the span can be divided into units that can create an aspect ratio of one or close to one. For the case of the two bridges studied this longitudinal dimension was 3 inches for Roaring Fork Bridge and 100 mm (3.9 in) because this bridge was originally detailed in metric units. Figure 4-15 presents an example of this situation.

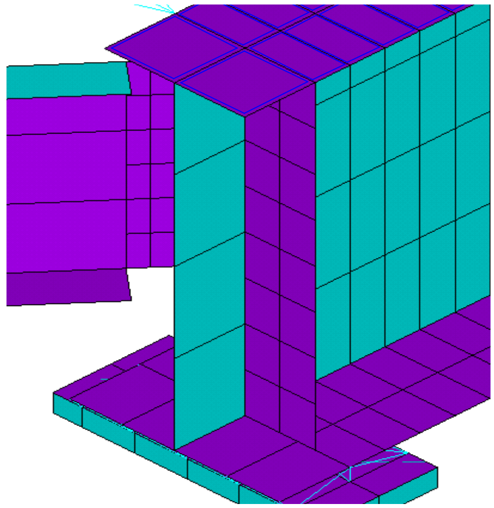

Figure 4-15. Detail of the mesh on one of the girders of Roaring Fork Bridge

This procedure not only ensures an adequate mesh density and keeps the element aspect ratio as close to one as possible without severely affecting the computational time, but also facilitates the SIP coupling procedure by minimizing the eccentricity between the top flange nodes and the SIP nodes.

The sole plates, on the other hand, were meshed using a criterion such that the nodes on the part of the plate that was below the bottom flange would coincide as much as possible with the nodes on the bottom flange above them. This means that the nodes on the plate would be on the same vertical of the nodes on the bottom flange. By doing this, the process of creating the rigid elements between them would be much easier.

4.4.2.2 Connectors and stiffeners

These particular components were modeled by creating a mesh of one half the top flange element transverse dimension and the vertical size was adjusted to ease the coupling process on the gusset plates on the end bent connectors as well as for the intermediate connectors, depending on the type of cross-frame used. However, the general idea was to locate the end nodes of the cross-frames / diaphragms coinciding as much as possible with the nodes on the connectors to avoid unnecessary eccentricities between the coupled nodes. Figure 4-15 shows the end bent stiffener meshed one half of the top flange element in the transverse dimension of the girder and one half of the vertical dimension of the element.

4.4.2.3 Diaphragms

The end bent diaphragms were divided into as many elements on the diagonal direction as the number of SIP end nodes converging into them. This number would depend upon the geometry of the bridge, in particular upon the skew angle. The vertical size depended upon the number of bolts connecting the gusset plates into the connectors. In this sense the criteria use was to define as many vertical elements as bolts used. In that way the bolt location would coincide with the mid nodes of the end elements, and the coupling process would be facilitated. For the intermediate diaphragms the procedure was similar, but the size of the elements along the axis of the diaphragm was one quarter of its total distance.

4.4.2.4 Stay-in-place (SIP)Forms, K-type and X-type intermediate cross-frames.

The K and X type cross-frames relative stiffness is considerably small compared to the much larger girder. In consequence, it seems reasonable to model these structural components using axially loaded truss elements that mimic a truss behavior, which basically means that these elements are free to rotate at the connection on the stiffeners and their bending capabilities will not be accounted for.

As for the case of the SIP forms, previous investigations from Helwig and Yura (2003) and Whisenhunt (2004) demonstrated that the use of an X-brace truss system with two diagonals produces a better representation of the shear stiffness of the SIP forms and also accounts for the direction of in-plane shear transfer much more accurately. The procedures to determine the SIP mechanical properties as well as the geometrical dimensions are described by Whisenhunt (2004).

Another interesting situation takes place at the end region of the SIP forms. At these locations it was required to use multi-point constraint elements to link the ends of the SIPs with the top strut or diaphragm of the end bent system. This was done to ensure proper behavior at these regions although no SIP property adjustment was required. A preliminary parametric analysis proved that by refining the values of the mechanical properties of the SIP forms to account for the change in length of the elements does not affect the behavior of the structure more than 1 percent, suggesting it is not worth the effort.

4.4.2.5 Bearing Supports.

As it was mentioned previously, the elastomeric bearing pads should be modeled with 20 node isoperimetric solid elements since this higher order element can more easily account for the typical shear behavior of these components. Additionally it was found that to avoid unnecessary and unreal stress concentrations at the end bents, it is required to model the support by means of contact elements. Initial approaches only considered pinned nodes to constrain the interface between the sole plate and the pad. However this condition induced large number of “artificial” stresses, which do not accurately represent the true behavior of that region. The difference between the two approaches ranges around 15 to 20 percent. To account for the eccentricity between the sole plate and the bottom flange, a grid of rigid elements was assembled at the interface between the sole plate at the bearing and the bottom flange.

4.4.2.6 End Bent Cross-frames / Diaphragms

At the end bent locations, the gusset plate that connect the cross-frame and diaphragms to the girders and the connection bolts were explicitly included in the model. In general, this intermediate plate is divided into eight elements arranged in a four by two configuration. Preliminary analysis suggests that the size of this plate is not very influential to the rotational behavior of the structure, and hence it can be inferred that it could be omitted. If omitted, the diagonal elements could be directly attached to the intersection of the bottom flange and the web of the channel at its mid-span. Of course, further analysis must verify this assumption. Figure 4-16 shows a detail of the end bent cross-frames.

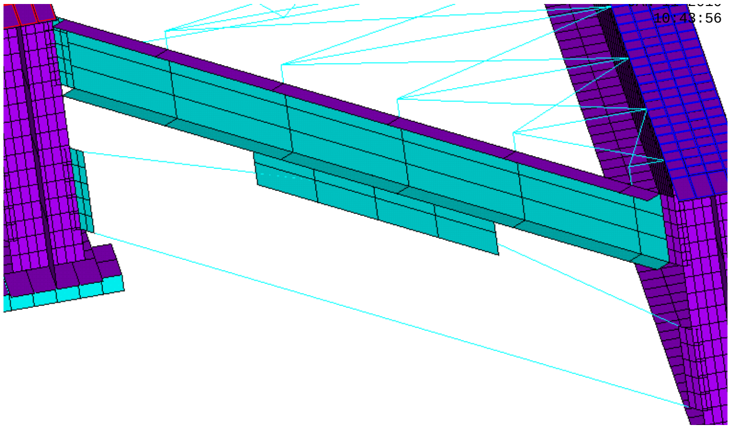

Figure 4-16. End Bent Detail of Chicken Road Bridge

5.0 A SIMPLIFIED MODEL PROCEDURE

5.1 Introduction

An extensive investigation was conducted herein to understand the lateral flange bending phenomena that occurs skewed steel girder bridges. Detailed analysis was conducted using three different skew angles for the two bridge structures studied. The resulting data was statistically analyzed to identify trends that could lead to identification of the key components required to propose a simplified model. As a result of the analysis, a particular and peculiar behavior was identified. The results were used to develop a simplified model to predict the out-of-plane girder rotations. Details of the simplified model and details of the development process are presented within this section of the report.

5.2 Cross-section Rotations

As part of the investigation process to understand the out-of-plane rotation behavior as well as to determine the sensitivity of the system to the different parameters, rotations along the span axis were selected to be the primary source of information. Although vertical deflections were also considered, their effects have already been thoroughly studied by Whisenhunt (2004) and Fisher (2005). The variables used to describe the rotations as well as sign convention used is presented in Figure 5-1. The corresponding equations to determine top flange, web, and bottom flange rotations are shown in Equations 5.1, 5.2 and 5.3.

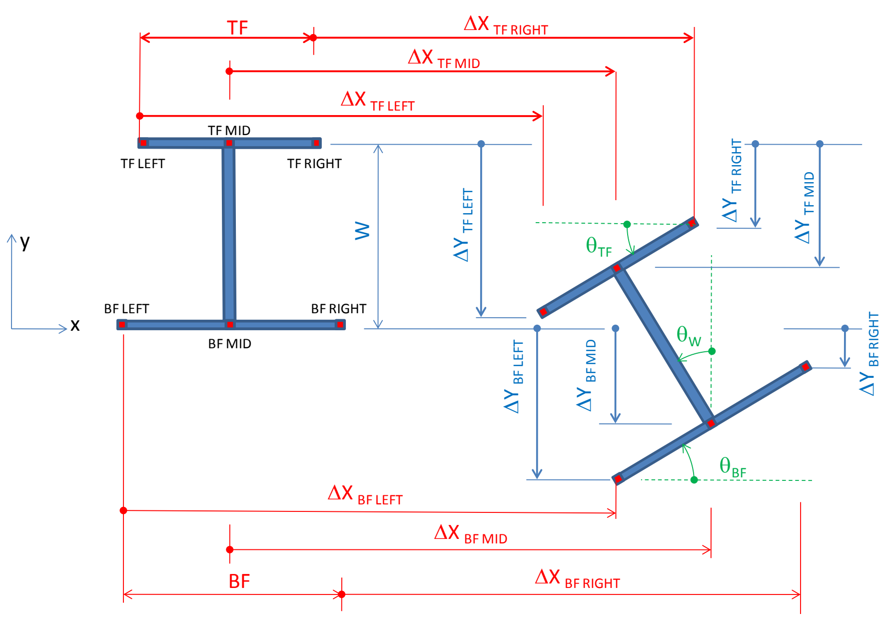

Figure 5-1. Rotations on the girder cross-section

$$TAN(\theta_{TF}) = \frac{\Delta Y_{TF\ RIGHT} - \Delta Y_{TF\ LEFT}}{\Delta X_{TF\ RIGHT} - \Delta X_{TF\ LEFT} + TF} \quad \textbf{[Eq. 5-1]}$$

$$TAN(\theta_W) = \frac{\Delta X_{BF\ MID} - \Delta X_{TF\ MID}}{\Delta Y_{TF\ MID} - \Delta Y_{BF\ MID} + W} \qquad \textbf{[Eq. 5-2]}$$

$$TAN(\theta_{BF}) = \frac{\Delta Y_{BF\ RIGHT} - \Delta Y_{BF\ LEFT}}{\Delta X_{BF\ RIGHT} - \Delta X_{BF\ LEFT} + BF} \qquad \textbf{[Eq. 5-3]}$$

5.3 Rigid Body Rotations

With the data obtained from the results of the finite element analysis it was possible to determine that the variation between the top flange (*TF*) and bottom flange (*BF*) rotations compared to the web (*W*) rotations were negligible. Even though the variations in the rotational values were insignificant, the web rotations were always the highest among them and therefore any conclusions derived from the use of web rotations will be conservative. Knowing this fact, web rotations were selected as the representation of the overall cross-section. Figure 5-2 shows the rotations for one of the bridges at five different locations along the span.

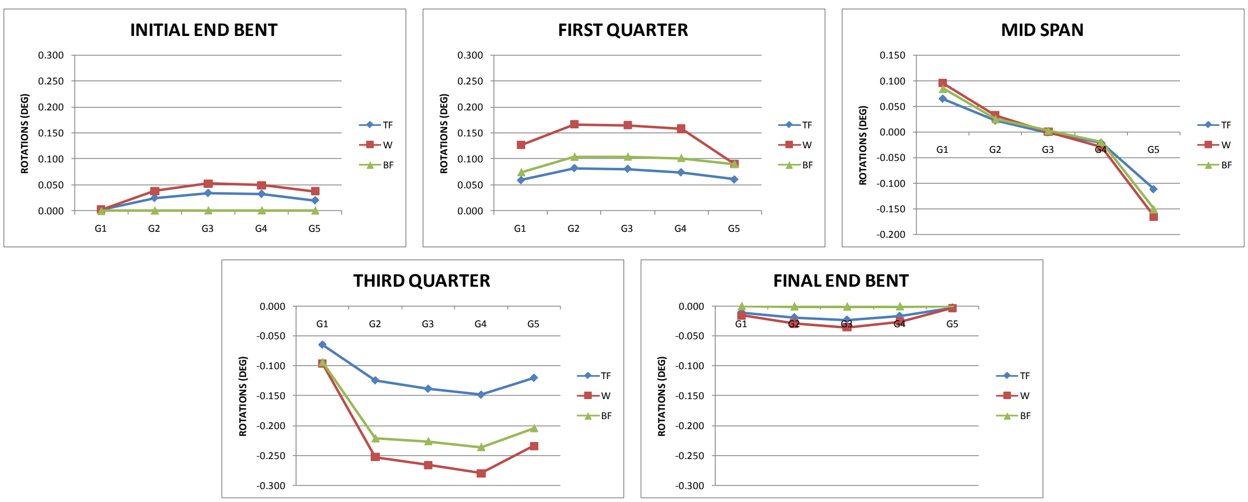

Figure 5-2. Rotations at five different locations for Roaring Fork Bridge

5.4 The Rotations Profile

Throughout the investigation it was possible to single out several properties that were inherent to the behavior of the steel skewed bridges. The out-of-plane rotations profile was one of them. Typically girders in non-skewed bridges experience rotations along their longitudinal axis only in one direction (clockwise or counterclockwise). However, it was found that girders in steel skewed bridges show a torsional rotation profile in which one part of the girder rotates in one direction and the rest of the girder rotates in the opposite direction.

Figure 5-3 and Figure 5-4 show a typical rotation profile for an intermediate girder. When comparing the average rotations profiles normalized with respect to the maximum absolute value for both bridges it is possible to identify the similarities between them. Figure 5-5 shows this comparison. The evident similarities in shape support the idea of a systematic behavior as far as out-of-plane rotations are concerned. Additionally, the rotations profile proved to be in good agreement with the field measurements obtained. From this profile several key points were identified in order to develop the simplified model to predict maximum and minimum rotations. This issue is discussed in the next section.

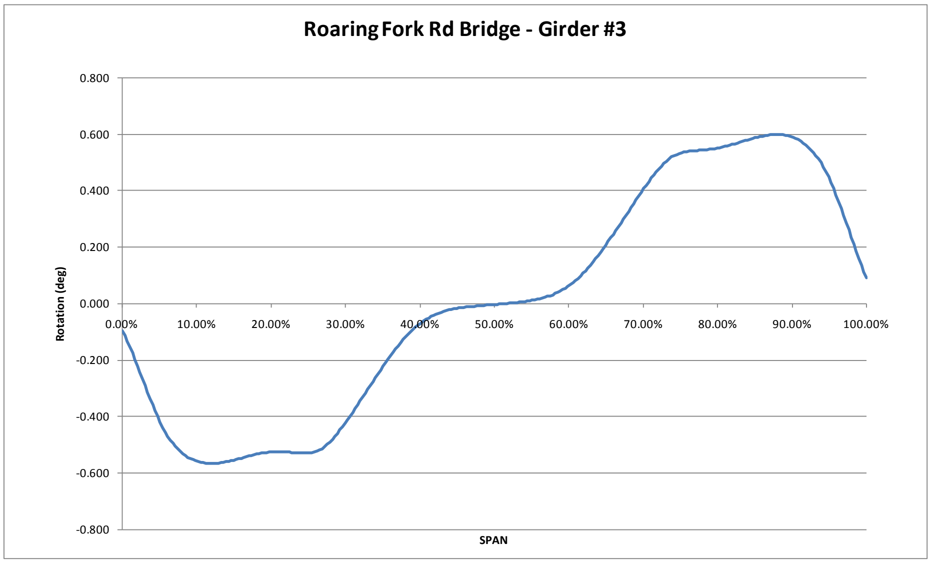

Figure 5-3. Rotations profile of an intermediate girder on Roaring Fork Bridge

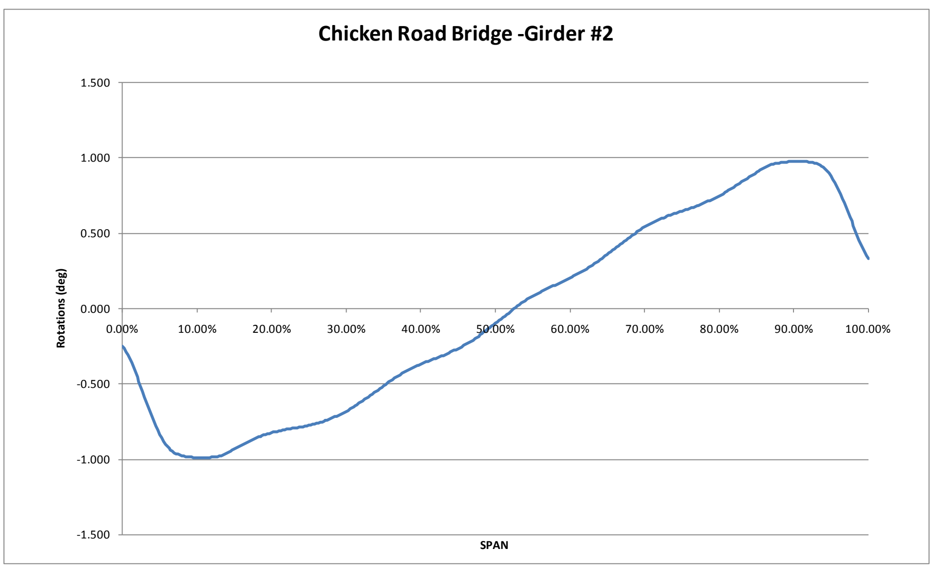

Figure 5-4. Rotations profile of an intermediate girder on Chicken Road Bridge

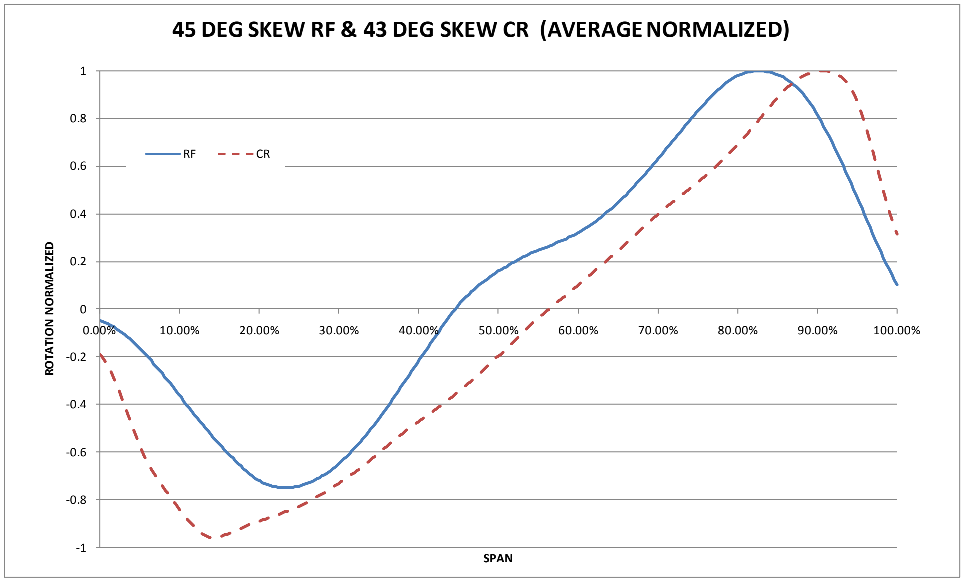

Figure 5-5. Comparison between normalized rotations in both bridges

5.4.1 Inflection point Location (X_0)

Inflection points represent the location along the span of the girder where out-of-plane rotations are equal to zero. Throughout the investigation it was determined this value varies depending upon the skew angle, as shown in Figure 5-6. After analyzing both the Chicken Road Bridge and Roaring Fork Road Bridge data, it was possible to develop a general equation for the X_0 value. X_0 can be obtained using Eq. 5-4.

$$X_0 = 66 - 0.35 \; x \; SKEW \; (deg) \qquad \textbf{[Eq. 5-4]}$$

This equation is valid for the mean value of X_0 and for skew angles between 30 and 75 degrees. However, to establish a reasonable range, for Chicken Road Bridge a 15 percent variation was found to be appropriate, whereas for Roaring Fork Road Bridge, a 10 percent variation led to values within two standard deviations. Therefore,

Chicken Road: X_0 -15% < Inflection Point Location < X_0 +15%

Roaring Fork Road: X_0 -10% < Inflection Point Location < X_0 +10%

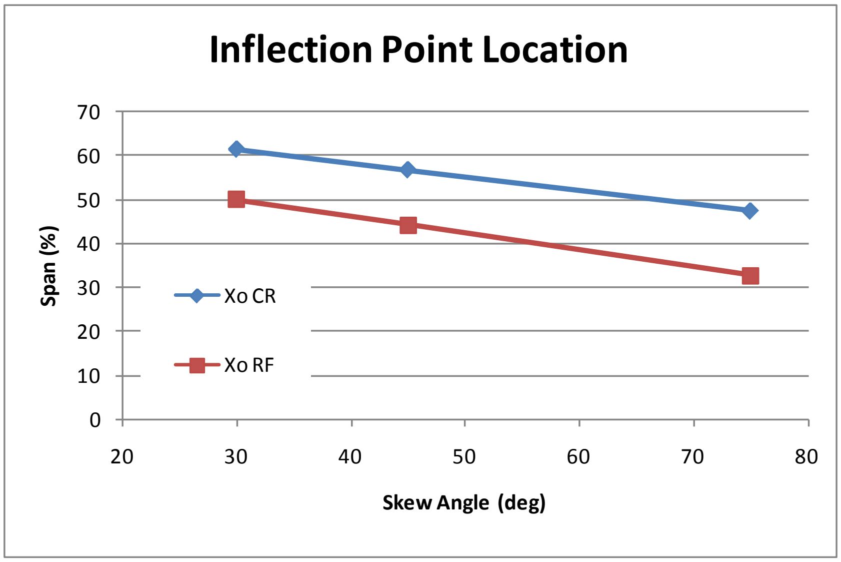

Figure 5-6. Variation of the inflection point location vs. skew angle for both bridges

5.4.2 The initial End rotations (θ_i)

Although the ends of the bridge are laterally restrained by the end bent cross-frames it was found that rotations are developed at those locations. These rotations also vary depending upon the skew angle of the bridge and the girder location (exterior or interior). Figure 5-7 depicts the values for the initial rotations of the first two girders of the two bridges. It can be seen that the higher the skew the larger the difference between the rotations. For Roaring Fork these differences were smaller than Chicken Road Bridge. In addition, interior girders (G2) experienced higher rotations than the exteriors (G1).

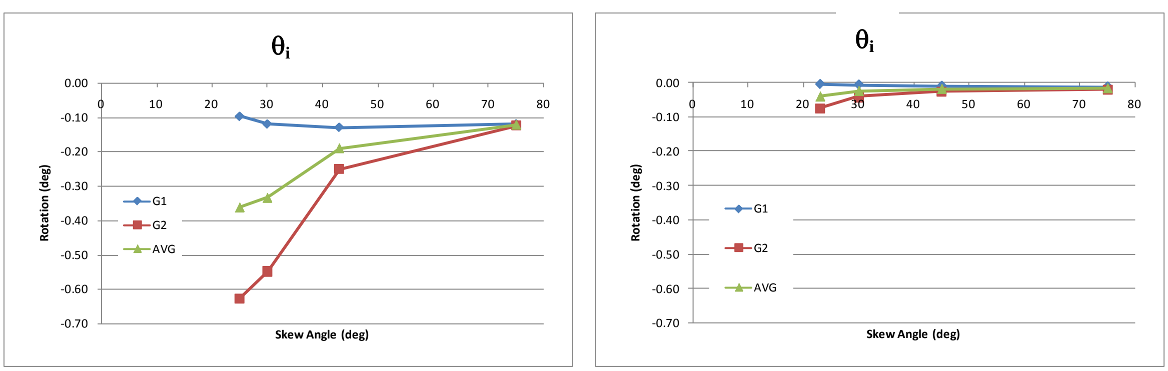

Figure 5-7. Initial rotations of Chicken Road Bridge (left) and Roaring Fork Bridge (right)

5.4.3 The Final End rotations (θ_f)

In the same fashion as the initial end rotations, the final end rotations also increase when the bridge is more skewed. However, for this case the differences between exterior and interior girders were negligible. Figure 5-8 depicts this situation.

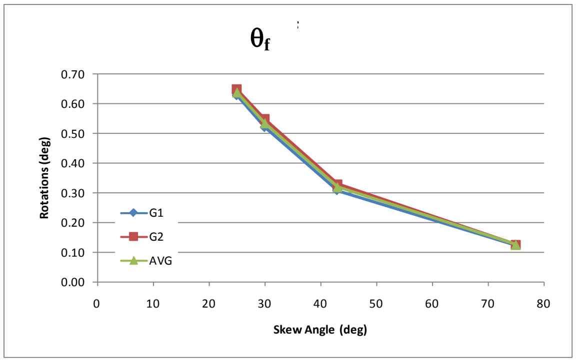

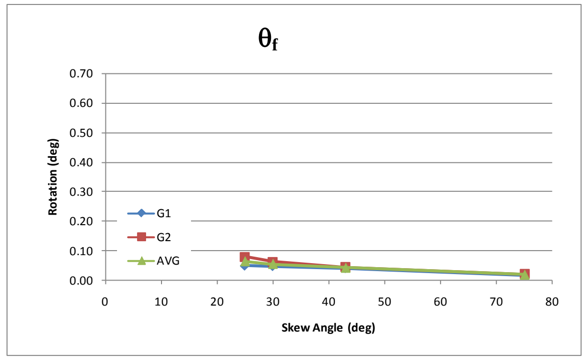

Figure 5-8. Final rotations of Chicken Road Bridge (left) and Roaring Fork Bridge (right)

5.4.4 Slopes- Overview

As part of the modeling process it was found that some of the possible parameters that allow simplifying the analysis of the out-of-plane rotation profile are the slopes of the straight portions of the simplified model, which will be discussed later. However, for illustration purposes it is worth mentioning that the model consists of three straight segments. The first segment begins at the initial end rotation and finishes at the minimum rotation value. The middle segment goes from the minimum rotation value, passes through the inflection point, and ends on the maximum rotation location. The final segment starts at the maximum rotation location and extends to the final end rotation. In any case, the slopes are valid for skew angles varying from 30 degrees to 75 degrees. Following is a description of each slope considered on the model.

5.4.4.1 Initial Segment Slope (m_i)

Initial segment slope represents the slope of the straight line from the initial end rotation to the minimum rotation along the span. Figure 5-9 shows how this value changes as the skew angle is changed for both Chicken Road Bridge (CR) and Roaring Fork Bridge (RF). As it was the case for the initial end rotations, the slope values increase as we decrease the skew angle. However, for this parameter the variation is almost linear. It was determined that the data associated with this parameter yielded extremely high scatter, and for that reason it will not be considered, at least initially, as a reliable source of information for the model configuration.

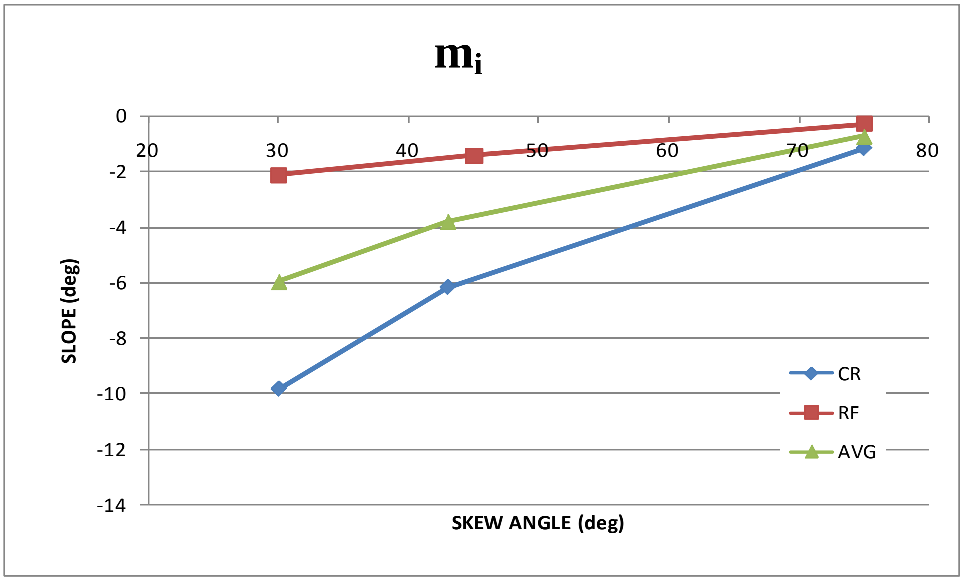

Figure 5-9. Initial segment slope variation for both bridges

5.4.4.2 Middle Segment Slope (m_0)

For the case of the middle slope the situation was clearly different. For this case the maximum variation within the skew angles considered was about 15 percent for Chicken Road Bridge and 10 percent for Roaring Fork Road Bridge, leading to upper and lower bound values of:

Chicken Road: $m_{0\ low} = 0.85\ m_0$ and $m_{0\ up} = 1.15\ m_0$

Roaring Fork Road: $m_{0\ low} = 0.90\ m_0$ and $m_{0\ up} = 1.10\ m_0$

It was proposed that for the general case, the middle segment slope m_o can be estimated by:

$$m_0 = 4.05 - 0.047 \times SKEW\ (deg) \qquad \textbf{[Eq. 5-5]}$$

Figure 5-10 presents how the middle segment slope changes with skew angle.

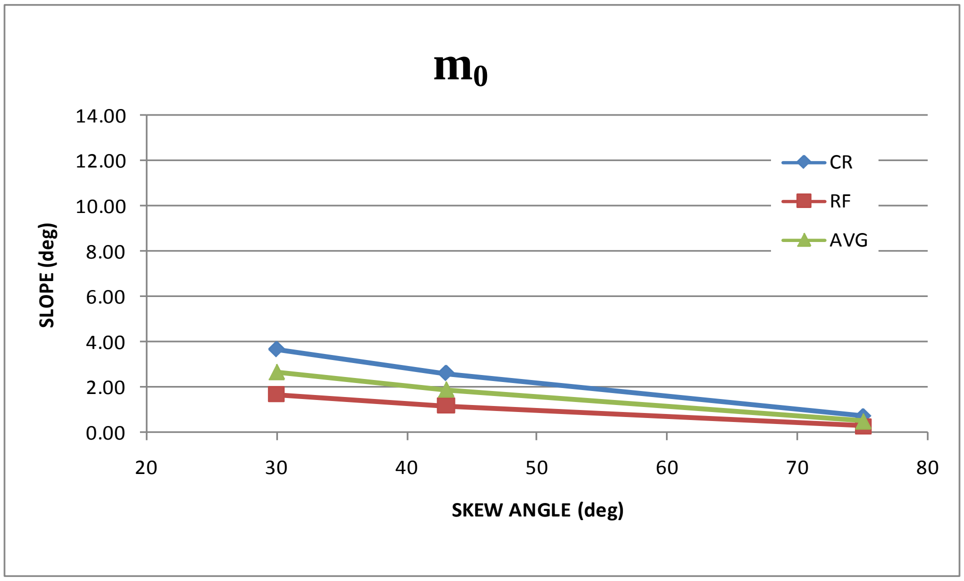

Figure 5-10. Variation of the middle segment slope

5.4.4.3 Final Segment Slope (m_f)

As it was found for the initial segment slope, the values for the final segment slope were almost identical to the initial ones, as shown in Figure 5-11. Therefore, as it will be seen on the next section, when it comes to develop the simplified model, they will be considered to have the same value. That is:

$$m_i = m_f \qquad \textbf{[Eq. 5-6]}$$

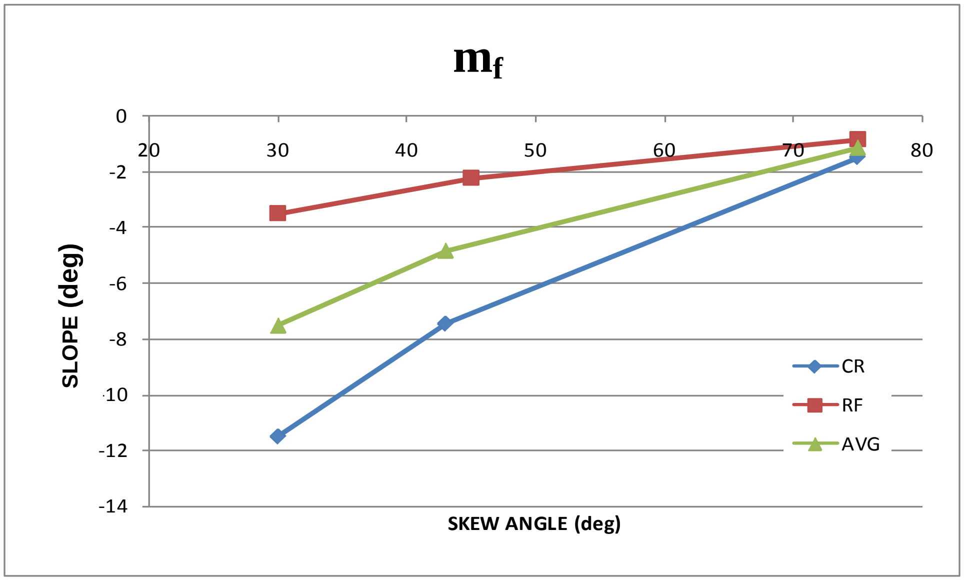

Figure 5-11. Final segment slope variation

5.5 The proposed simplified model

After understanding the importance of each of the key components it was possible to come up with a first approach to find a suitable way to easily model the out-of-plane rotation phenomenon. Figure 5-12 shows the proposed simplified model for the mean rotations profile. It contains the different components that were found to have particular importance, as mentioned before.

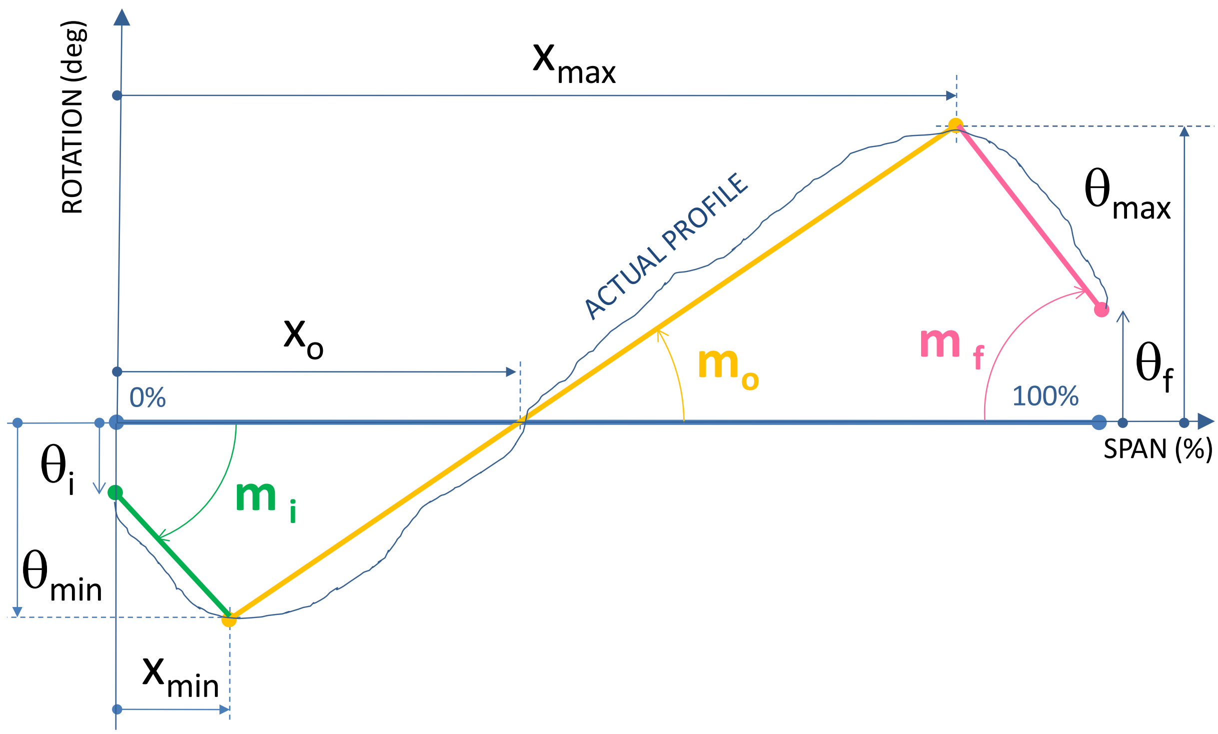

Figure 5-12. Proposed simplified model for mean values

It is worth mentioning that since the available data was limited only to two bridges it was found to be appropriate to determine an upper and lower bound, in an effort to more accurately represent the rotation profile.

It has to be pointed out that rotations are the combination of a number of independent factors such as skew, geometric properties of the bridge, etc. Hence, it is likely their values are normally distributed. This hypothesis could not be determined throughout the investigation due to the limited data available. Nonetheless, it will be seen that assuming a confidence interval of 95 percent (two standard deviations to either side of the mean) the resultant intervals strongly agreed with the data from the models. Figure 5-13 presents what this region looks like.

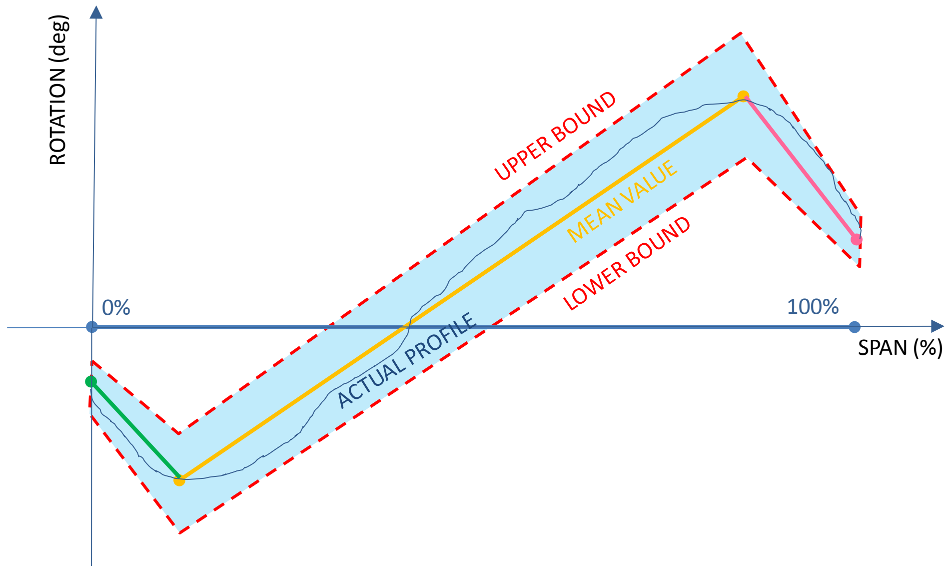

Figure 5-13. Proposed region of results for the rotation profile

5.5.1 Minimum and Maximum Locations (X_{min}, X_{max})

The locations for both the minimum and maximum rotation values can be determined by using a geometric relationship between the initial segment of the model and the middle one. An expression for X_{min} can be developed as given by,

$$X_{min} = \frac{\theta_i + m_0 X_0}{m_0 - m_i} \qquad \textbf{[Eq. 5-7]}$$

where θ_i is the initial end rotation in degrees, m_o and m_i are the middle segment and initial segment slopes respectively in degrees, and X_0 is the inflection point location in percent of span. Similarly, in order to determine the maximum rotation location, the resultant equation is,

$$X_{max} = \frac{m_0 X_0 - 100 m_f + \theta_f}{m_0 - m_f} \qquad \textbf{[Eq. 5-8]}$$

where θ_f is the final end rotation and m_f is the final segment slope.

When the values of X_{min} and X_{max} are compared for the three skew angles, the resultant data is shown on Figure 5-14 and Figure 5-15.

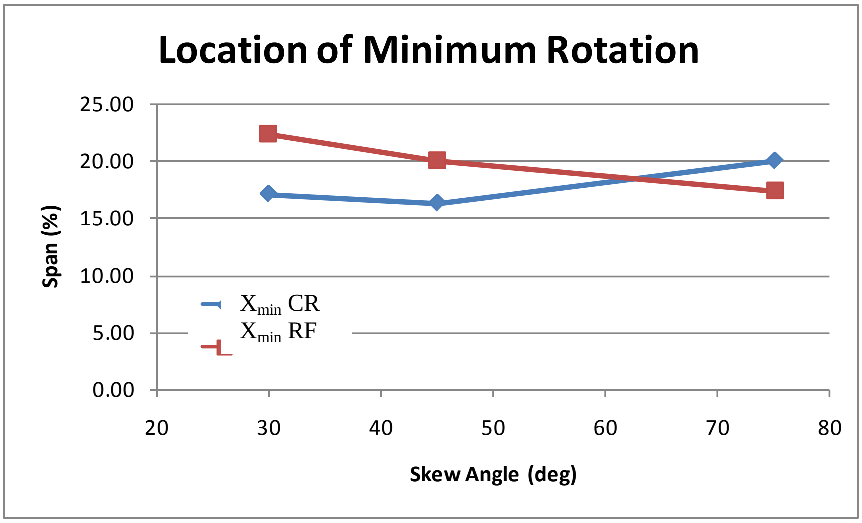

Figure 5-14. Distribution of locations of minimum rotations

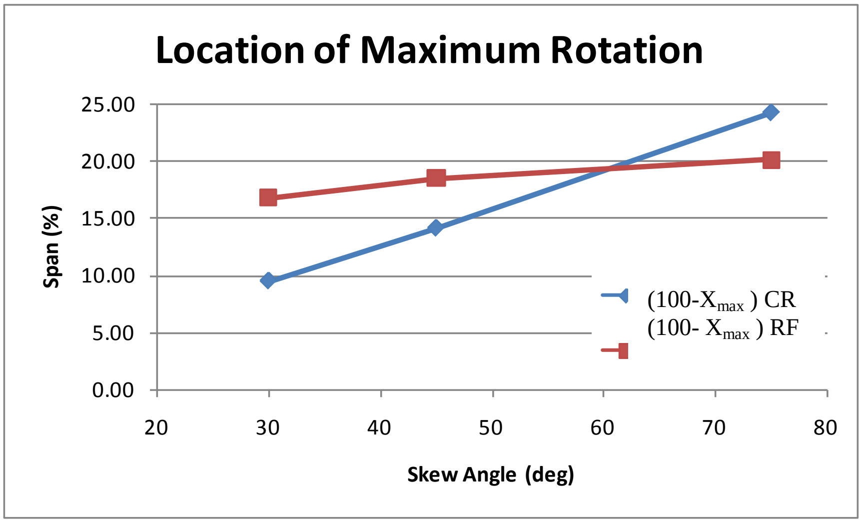

Figure 5-15. Locations of maximum rotations with respect to the final end of the two bridges

From the statistical analysis of this data it was found that a good approximation for the location of the minimum and maximum rotation points is 20 percent from each end, as shown in Table 5-1. However, due to the inherent scatter the upper and lower bounds can be found at 5 percent away from the median.

Table 5-1. Summary of minimum and maximum locations

Skew (deg)	X_{min} CR (%)	X_{min} RF (%)	(100 - X_{max}) CR (%)	(100 - X_{max}) RF (%)
30	16.98	22.38	9.42	16.82
45	16.29	20.09	14.11	18.54
75	20.01	17.41	24.24	20.12
Average	**17.76**	**19.96**	**15.92**	**18.49**
Std Dev	**1.98**	**2.48**	**7.57**	**1.65**

5.5.2 *Minimum and Maximum Values (θ_{min}, θ_{max})*

Once the key points were identified and its behavior understood it was possible to determine both the location and values of the minimum and maximum rotations. The process by which these values were determined is depicted in Figure 5-16.

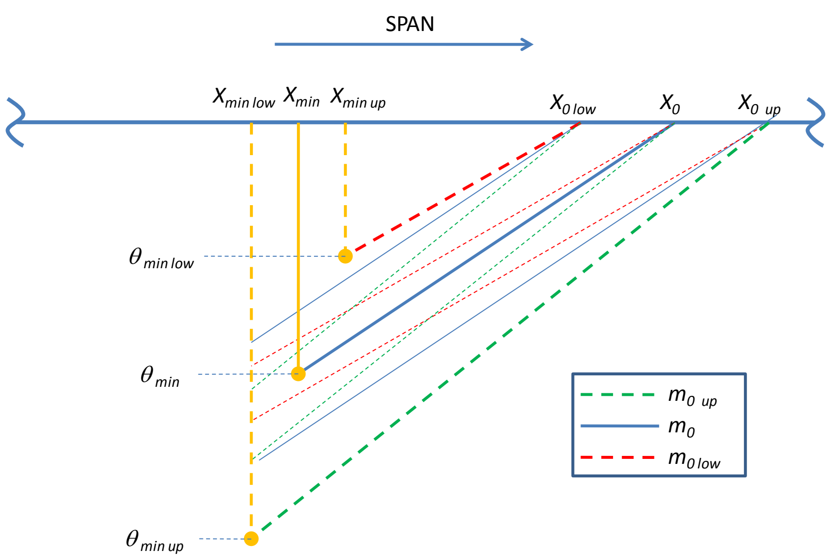

Figure 5-16. Low and upper bound points for the minimum values

First the upper and lower bound values of the inflection point location (X_0) are determined. Using the expressions found for m_0, X_{min} using Eq. 5.5 and Eq. 5.7 respectively, and simply following a geometrical analysis it is possible to solve for the lower minimum rotation, mean minimum rotation, and upper minimum point rotations.

Three straight lines with slopes of $m_{0\ \mathrm{low}}$, m_0, and $m_{0\ \mathrm{up}}$ are drawn from each of the three points, and intersected with those vertical from $X_{min\ low}$, X_{min}, and $X_{min\ up}$ to finally obtain $\theta_{min\ low}$, θ_{min} and $\theta_{min\ up}$.

Likewise, the maximum rotations can be found. For this case the three points are determined by intersecting the three lines with slopes $m_{0\ \mathrm{low}}$, m_0, and $m_{0\ \mathrm{up}}$ with the vertical lines $X_{max\ low}$, X_{max}, and $X_{max\ up}$, as shown on Figure 5-17.

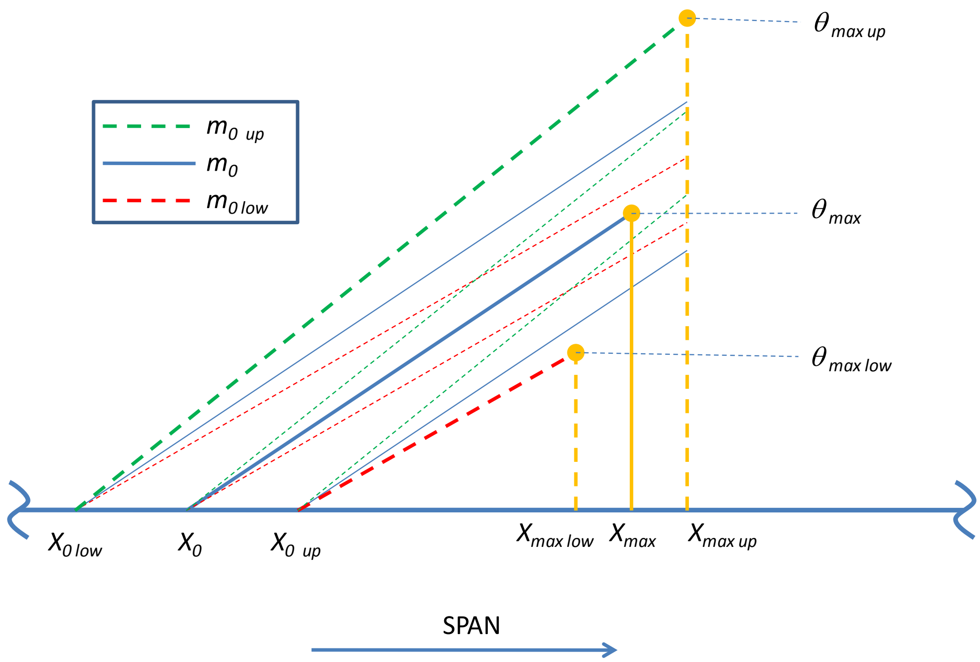

Figure 5-17. Lower and upper bound rotations for the maximum values

These numbers, in absolute value, are shown on Table 5-2 for different values of skew between 30 and 75 degrees, which is the allowable range of values where the equations are deemed to be valid.

Table 5-2. Values and Location of minimum and maximum rotations

Skew (deg)	X_{min} low	X_{min} (%)	X_{min} up	$X_{0\ low}$	X_0 (%)	$X_{0\ up}$	X_{max} low	X_{max} (%)	X_{max} up	θ min low	θ min (deg)	θ min up	θ max low	θ max (deg)	θ max up
30.0	15	20	25	40.50	55.50	70.50	75	80	85	0.205	0.937	2.198	0.059	0.647	1.762
35.0	15	20	25	38.75	53.75	68.75	75	80	85	0.165	0.812	1.939	0.075	0.631	1.668
40.0	15	20	25	37.00	52.00	67.00	75	80	85	0.130	0.694	1.693	0.087	0.608	1.562
45.0	15	20	25	35.25	50.25	65.25	75	80	85	0.099	0.585	1.459	0.094	0.576	1.444
50.0	15	20	25	33.50	48.50	63.50	75	80	85	0.072	0.485	1.237	0.098	0.536	1.313
55.0	15	20	25	31.75	46.75	61.75	75	80	85	0.049	0.392	1.027	0.097	0.487	1.170
60.0	15	20	25	30.00	45.00	60.00	75	80	85	0.031	0.308	0.830	0.092	0.431	1.015
65.0	15	20	25	28.25	43.25	58.25	75	80	85	0.016	0.231	0.646	0.083	0.366	0.847
70.0	15	20	25	26.50	41.50	56.50	75	80	85	0.006	0.163	0.473	0.070	0.293	0.667
75.0	15	20	25	24.75	39.75	54.75	75	80	85	-0.001	0.104	0.313	0.053	0.211	0.474

Generally speaking, what this procedure is aiming to do is to determine a region in which the out-of-plane rotations are expected to lie within. Additionally, linear interpolations are permitted. Figure 5-18 portrays what this region looks like for one of the bridges.

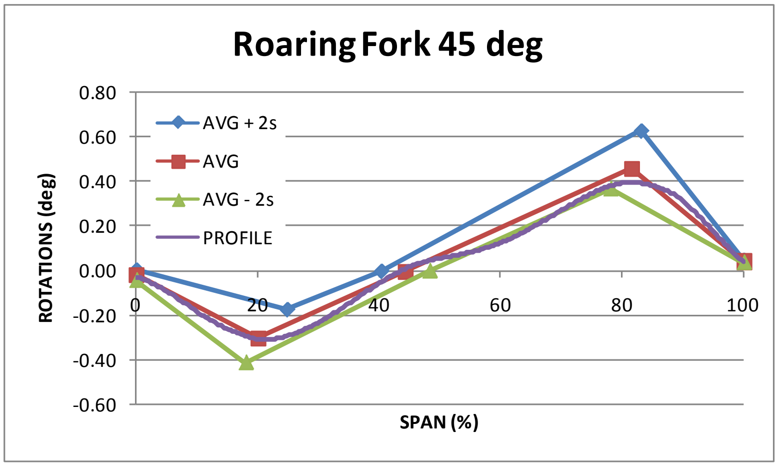

Figure 5-18. Example of the lower and upper bounds on one of the bridges

5.5.3 Example.

Let's consider a 60 degrees skewed bridge. According to this procedure all that is needed to do is to enter Table 5-3 with this skew angle and identify the corresponding minimum and maximum mean rotations as well as the lower and upper bounds.

Table 5-3. Values for 60 degrees skew

Skew (deg)	X_{min} low	X_{min} (%)	X_{min} up	$X_{0\ low}$	X_0 (%)	$X_{0\ up}$	X_{max} low	X_{max} (%)	X_{max} up	m_0 low	m_0 (deg)	m_0 up	θ_{min} low	θ_{min} (deg)	θ_{min} up	θ_{max} low	θ_{max} (deg)	θ_{max} up
55.0	15	20	25	31.75	46.75	61.75	75	80	85	0.73	1.47	2.20	0.049	0.392	1.027	0.097	0.487	1.170
60.0	**15**	**20**	**25**	**30.00**	**45.00**	**60.00**	**75**	**80**	**85**	**0.62**	**1.23**	**1.85**	**0.031**	**0.308**	**0.830**	**0.092**	**0.431**	**1.015**
65.0	15	20	25	28.25	43.25	58.25	75	80	85	0.50	1.00	1.49	0.016	0.231	0.646	0.083	0.366	0.847

For this case, the minimum rotation is 0.031 degrees for the lower bound, 0.308 degrees for the mean, and 0.83 degrees for the upper bound. As far as the maximum rotations are concerned, the lower bound is 0.092, the mean value is 0.431, and the upper bound is 1.015 degrees

5.6 Procedure to determine the Lateral Displacements (LD) on Steel skewed bridges due to lateral flange bending.

Step 1. Compute the skew offset of the bridge.

- If the bridge skew angle is smaller than 90 degrees, then:

SKEW OFFSET (deg) = bridge skew angle (deg)

- If the bridge skew angle is greater than 90 degrees, then:

SKEW OFFSET (deg) = 180 (deg) - bridge skew angle (deg)

Step 2. Find the location of the inflection point (X_0) and the slope of the middle portion (m_0) using Eq. 5-4 and Eq. 5-5:

$$X_0 = 66 - 0.35 \text{ x SKEW OFFSET (deg)}$$
$$m_0 = 4.05 - 0.047 \text{ x SKEW OFFSET (deg)}$$

Step 3. Determine the minimum and maximum rotations located at 20 percent of span and 80 percent of span respectively. Use:

$$\theta_{min} = m_0 (X_0 - 20) / 100 \text{ or } \theta_{max} = m_0 (80 - X_0) / 100$$

Step 4. Locate the Shear Center (S.C) of the girder cross-section at 20 percent and 80 percent of span.

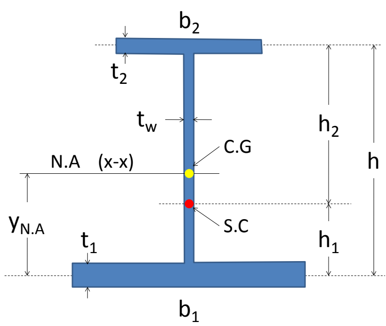

$$h_1 = \frac{h t_2 b_2^3}{t_1 b_1^3 + t_2 b_2^3}$$

$$h_2 = h - h_1 = \frac{h t_1 b_1^3}{t_1 b_1^3 + t_2 b_2^3}$$

Figure 5-19. Girder X section

Step 5. Find the maximum Lateral Displacements (LD), by computing:

$$\text{LD max} = \text{max of} \left| \begin{array}{l} h_2 \text{ x } \theta_{min} \text{ x } \pi / 180 \\ h_2 \text{ x } \theta_{max} \text{ x } \pi / 180 \end{array} \right.$$

5.6.1 Example.

Let's consider the case of Chicken Road Bridge, with an average skew angle of 137 degrees

Step 1.
Since 137 degrees > 90 degrees, then: SKEW OFFSET (deg) = 180 -137 = 43 degrees

Step 2.

$$X_0 = 66 - 0.35 \text{ x } 43 = 50.95 \text{ \%}$$

$$m_0 = 4.05 - 0.047 \text{ x } 43 = 2.029 \text{ degrees}$$

Step 3.

$$\theta_{min} = 2.029 (50.95 - 20) / 100 = 0.628 \text{ degrees}$$

$$\theta_{max} = 2.029 (80 - 50.95) / 100 = 0.589 \text{ degrees}$$

Step 4.
For Chicken Road Bridge:

b_1 (in)	t_1 (in)	h (in)	t_w (in)	b_2 (in)	t_2 (in)
18.11	0.87	57.1	0.63	14.17	0.87

Then:

$$h_1 = \frac{(57.1)(0.87)(14.17)^3}{(0.87)(18.11)^3 + (0.87)(14.17)^3} = 18.49 \text{ in}, \quad h_2 = 57.1 - 18.49 = 38.61 \text{ in}$$

Step 5.

$$\text{LD max} = \text{max of} \left| \begin{array}{l} h_2 \times \theta_{min} \times \pi / 180 \\ h_2 \times \theta_{max} \times \pi / 180 \end{array} \right. = \left| \begin{array}{l} 38.61 \times 0.628 \times \pi / 180 = 0.423 \text{ in} \\ 38.61 \times 0.589 \times \pi / 180 = 0.399 \text{ in} \end{array} \right.$$

$$\boxed{\text{LD max} = 0.423 \text{ in}}$$

6.0 PARAMETRIC ANALYSIS

6.1 Overview

This section discusses detailed information of the parametric study. To determine relationships between different bridge parameters and the cross-section rotations a comprehensive parametric study was conducted. One of the most important objectives was to determine the girders sensitivity to variations of one parameter at a time.

Due to the nature of the parameters considered on the investigation, it was considered appropriate and convenient to divide them into two different categories. The first group will include those parameters whose nature is such that they can be modified numerically. That is the case of the "girder spacing-to-span ratio", for example, on which the values of the parameter change from one number to another. However, some of the parameters cannot be varied in that fashion but non-numerically. A good example for this is the case of the "cross-frame type" parameter. It can be clearly seen this parameter can only be modified from one cross-frame type into another cross-frame type (i.e.: from K- type to X-type, or vice versa). Results from this parametric study are presented herein. Additional information related to the response of the bridges can be found on Morera (2010).

6.2 Numerical Parameters.

6.2.1 General

In an effort to determine the influence each parameter has on the bridge response a comparison between them and the original values of each skew angle was carried out. This was possible by determining the differential ratio between each case of study and its corresponding original value. This is:

$$RATIO = [(\theta_{case} - \theta_{original}) / \theta_{original}] \times 100 \qquad \textbf{[Eq. 6-1]}$$

where θ_{case} represents the rotation value when a given parameter is under study and $\theta_{original}$ is the rotation value of the original case where no parameters were modified. After determining which parameters induced important variations on the cross-section rotations it was possible to classify them in order of importance.

Parameters considered included exterior-to-interior moment of inertia (strong axis) ratio, exterior-to-interior load ratio, number of girders, number of transverse stiffeners, number of cross-frames, cross-frames stiffness, stay-in-place forms stiffness, and spacing-to-span ratio. In each of the following plots in this section each case will be identified with the initials of the bridge followed by the corresponding skew angle (i.e. CR 43 stands for Chicken Road 43 degrees skew).

Finally, a complete set of mitigation strategies was developed based upon a detailed comparison of the different results obtained and the development of a classifying criteria for the cases studied.

6.2.2 Exterior-to-interior Moment of Inertia Ratio (Strong Axis)

During previous investigations carried out by Whisenhunt (2004) and Fisher (2005) one of the most outstanding findings was the unusual deflection profile that steel skewed bridges presented. This unexpected behavior had to do with the fact that exterior girders experienced higher deflections than the interiors at a given section (Figure 6-1). Bearing that fact in mind it was considered a possibility that changing the exterior-to-interior girders flexural stiffness might have an important effect on the structure's behavior.

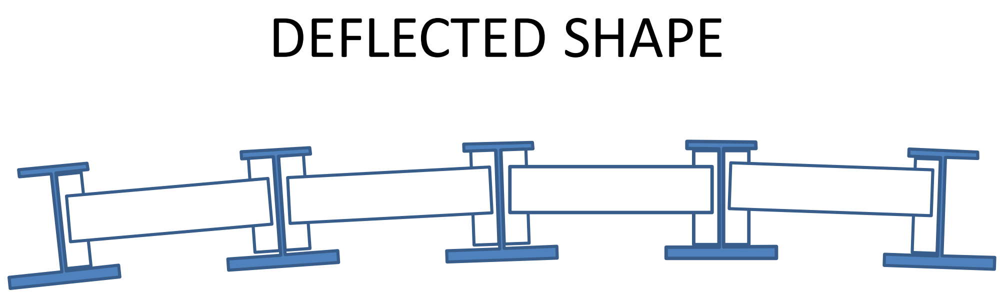

Figure 6-1. Typical cross-section on the deflected shape at a given section along the span

For both Chicken Road Bridge and Roaring Fork Road Bridge four different skew angles were considered. On Chicken Road 25, 43 (original), 75, and 90 degrees were considered whereas for Roaring Fork Road 23 (original), 45, 75, and 90 degrees were selected. For each skew angle three different conditions were studied and rotations were monitored at both flanges and the web.

The first condition included a 50 percent value for the parameter meaning the exterior girders moment of inertia was half the value of the rest of the girders. This was possible by changing the thicknesses for both the top and bottom flanges of the interior girders. The other cases included the original value of 100 percent and the final case studied the effect when this parameter is 200 percent.

Table 6-1 presents the rotation results.

Table 6-1. Rotation values for the "Exterior-to-interior Moment of Inertia" case

CASES	CR (25 DEG SKEW)		RF (23 DEG SKEW)	
	θ min CR 25	θ max CR 25	θ min RF 23	θ max RF 23
0.5X E-I INERTIA	-11%	-9%	-31%	-48%
ORIGINAL	0%	0%	0%	0%
2.0X E-I INERTIA	-31%	-27%	-31%	-17%

CASES	CR (43 DEG SKEW)		RF (45 DEG SKEW)	
	θ min CR 43	θ max CR 43	θ min RF 45	θ max RF 45
0.5X E-I INERTIA	-15%	-13%	-24%	-59%
ORIG	0%	0%	0%	0%
2.0X E-I INERTIA	-43%	-46%	-42%	1%

CASES	CR (75 DEG SKEW)		RF (75 DEG SKEW)	
	θ min CR 75	θ max CR 75	θ min RF 75	θ max RF 75
0.5X E-I INERTIA	-7%	-16%	51%	-80%
ORIGINAL	0%	0%	0%	0%
2.0X E-I INERTIA	-52%	-40%	-77%	66%

With the exception of the 75 degrees skew angle for the 0.5X case on θ_{min} and the 2.0X case for θ_{max}, all of the scenarios considered yielded good results. The change in the inertial properties of the girders seems to have a beneficial effect on the rotations profile since most of the resultant ratios were negative, meaning the rotations from each case were lower than the original. From Figure 6-2 and

Figure 6-3 it can be seen that the change in rotation values ranges between 20 percent and 40 percent. However, in some cases the changes reach the value of 80 percent.

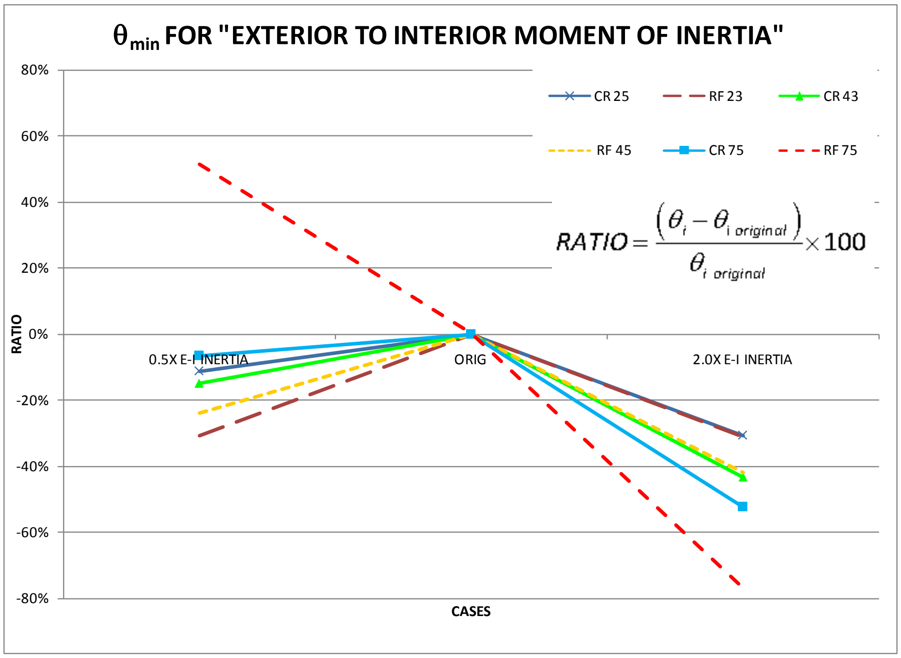

Figure 6-2. Minimum rotations for the "Exterior-to-Interior Moment of Inertia" case

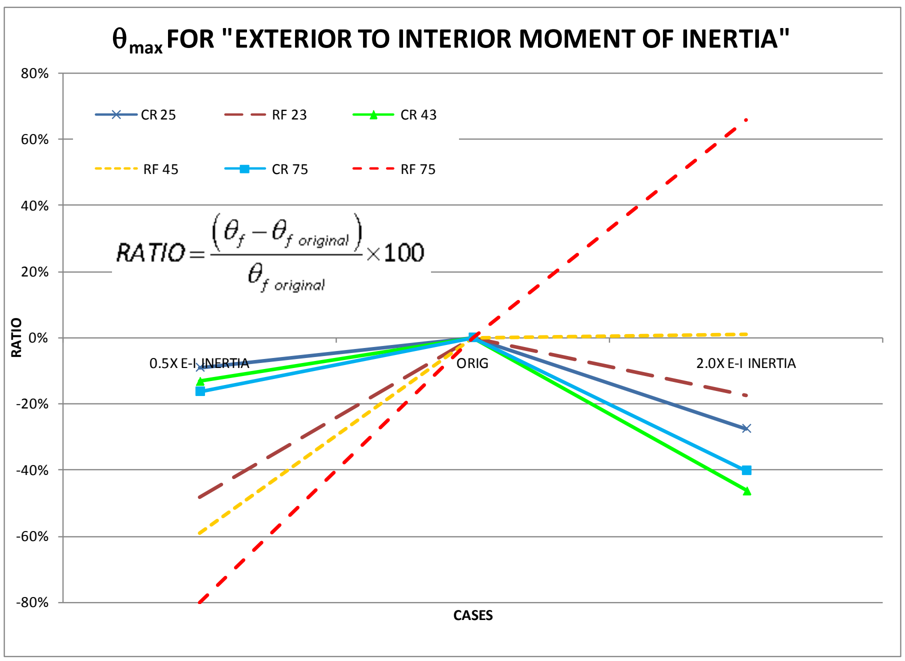

Figure 6-3. Maximum rotations for the "Exterior-to-Interior Moment of Inertia" case

6.2.3 Exterior-to-Interior Girder Load Ratio

Due to the difference in tributary load between exterior and interior girders it is reasonable to expect unequal rotational behavior of the exterior and interior girders.

A total of twenty-four finite element models were generated to investigate how exterior-to-interior girder load ratio affects steel girder rotations. For Chicken Road Bridge three different values were selected for this parameter: 50 percent, 85 percent (original), and 100 percent. Four different skews were included: 25, 43 (original), 75, and 90 degrees. As for the case of Roaring Fork Bridge, values of 50 percent, 67 percent (original), and 100 percent were considered along with skew angles of 23 (original), 45, 75, and 90 degrees. Table 6-2 presents results for this analysis.

Table 6-2. Rotation values for the "Exterior-to-interior Girder Load Ratio" case

CASES	CR (25 DEG SKEW)		RF (23 DEG SKEW)	
	θ_{min} CR 25	θ_{max} CR 25	θ_{min} RF 23	θ_{max} RF 23
E-I LOAD 50%	-25%	-20%	-14%	-3%
ORIGINAL	0%	0%	0%	0%
E-I LOAD 100%	13%	10%	19%	2%

CASES	CR (43 DEG SKEW)		RF (45 DEG SKEW)	
	θ_{min} CR 43	θ_{max} CR 43	θ_{min} RF 45	θ_{max} RF 45
E-I LOAD 50%	-23%	-14%	-16%	4%
ORIGINAL	0%	0%	0%	0%
E-I LOAD 100%	10%	7%	29%	-8%

CASES	CR (75 DEG SKEW)		RF (75 DEG SKEW)	
	θ_{min} CR 75	θ_{max} CR 75	θ_{min} RF 75	θ_{max} RF 75
E-I LOAD 50%	-28%	-8%	-56%	17%
ORIGINAL	0%	0%	0%	0%
E-I LOAD 100%	12%	4%	106%	-31%

For the case of the exterior-to-interior load parameter, results leave no doubt that increasing this number is not favorable in terms of the torsional effect it produces (see Figure 6-4 and Figure 6-5). A physical explanation relies upon the fact that an increase in this number represents a structure with wider overhangs, and all the forces transmitted to the exterior girders close to the bottom flanges via the falsework brackets generate undesirable horizontal forces that lead to twisting moments on the cross-section. Consequently, a higher tendency to rotate along the longitudinal axis occurs. Let's recall that a factor of 100 percent on this parameter represents an overhang width equal to one half the girders spacing, whereas a 50 percent factor means no overhang whatsoever.

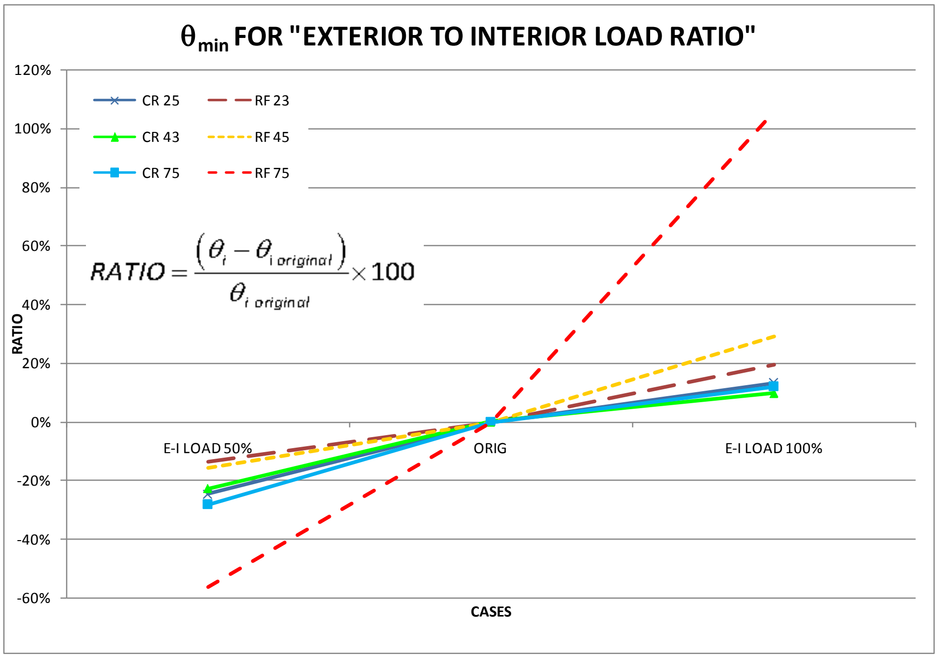

Figure 6-4. Minimum rotations distribution for the "Exterior-to-Interior Load Ratio" case

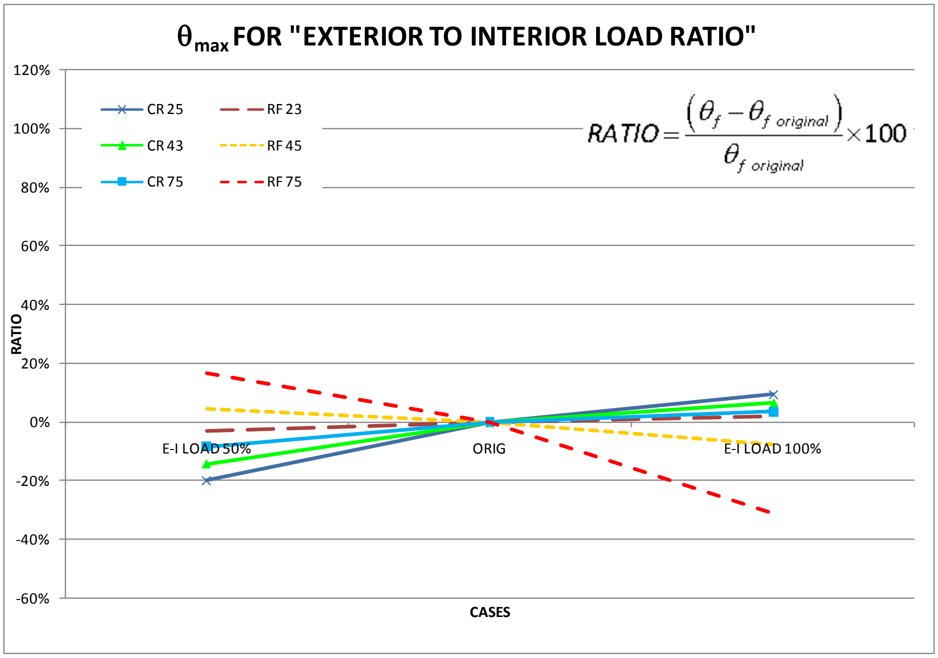

Figure 6-5. Maximum rotations distribution for the "Exterior-to-interior Load Ratio" case

6.2.4 Number of Girders

During Fisher's (2005) investigation it was found that the effect the number of girders has on the overall behavior of the steel skewed bridges was negligible. Nevertheless, it was worth reconsidering the potential sensitivity the structure has to rotations of the cross-section.

Four different values were selected for both Chicken Road and Roaring Fork Bridges. Calling "N" the number of girders, N-1, N (Original), N+2, and N+5 models were considered. For each value three skews were studied leading to a total of twenty four different finite element models studied. The skew angles involved were 30, 45, and 75 degrees. Results are presented on Table 6-3.

Table 6-3. Rotation values for the "Number of Girders" case

CASES	CR (25 DEG SKEW)		RF (23 DEG SKEW)	
	θ_{min} CR 25	θ_{max} CR 25	θ_{min} RF 23	θ_{max} RF 23
N-1	-3%	10%	-1%	-2%
ORIGINAL	0%	0%	0%	0%
N+2	-7%	-18%	-4%	-5%
N+5	-20%	-35%	-5%	-8%
CASES	CR (43 DEG SKEW)		RF (45 DEG SKEW)	
	θ_{min} CR 43	θ_{max} CR 43	θ_{min} RF 45	θ_{max} RF 45
N-1	-2%	0%	-5%	-3%
ORIGINAL	0%	0%	0%	0%
N+2	3%	0%	3%	3%
N+5	3%	3%	7%	3%
CASES	CR (75 DEG SKEW)		RF (75 DEG SKEW)	
	θ_{min} CR 75	θ_{max} CR 75	θ_{min} RF 75	θ_{max} RF 75
N-1	-1%	-4%	-3%	-5%
ORIGINAL	0%	0%	0%	0%
N+2	-1%	5%	-7%	6%
N+5	-2%	9%	4%	3%

Figure 6-6 and Figure 6-7 present the ratios of out-of-plane rotational change for the cases studied. Results obtained for this parameter suggest that as the number of girders is increased the out-of-plane rotations tend to increase, leading to positive ratios. However, this is not the case for low values of skew, of which the behavior is just the opposite.

In any case when the average change was computed for all of the cases studied the overall result was a change that ranged between ±5 percent. This results confirm what Fisher (2005) found for deflections. Figure 6-8 presents the bridge model for the case in which the number of girders is 10.

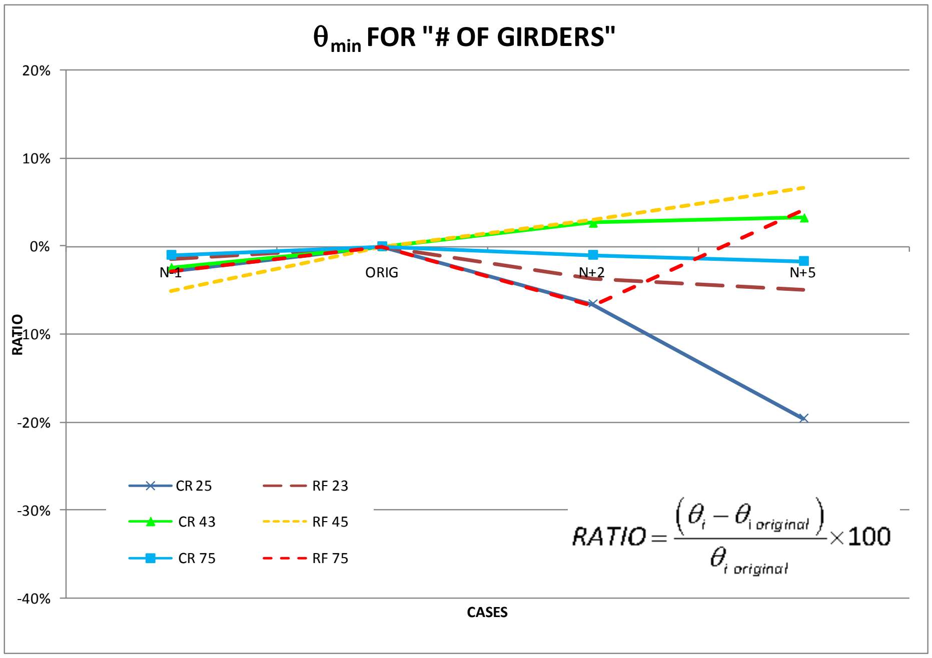

Figure 6-6. Minimum rotations distribution for the "Number of Girders" case

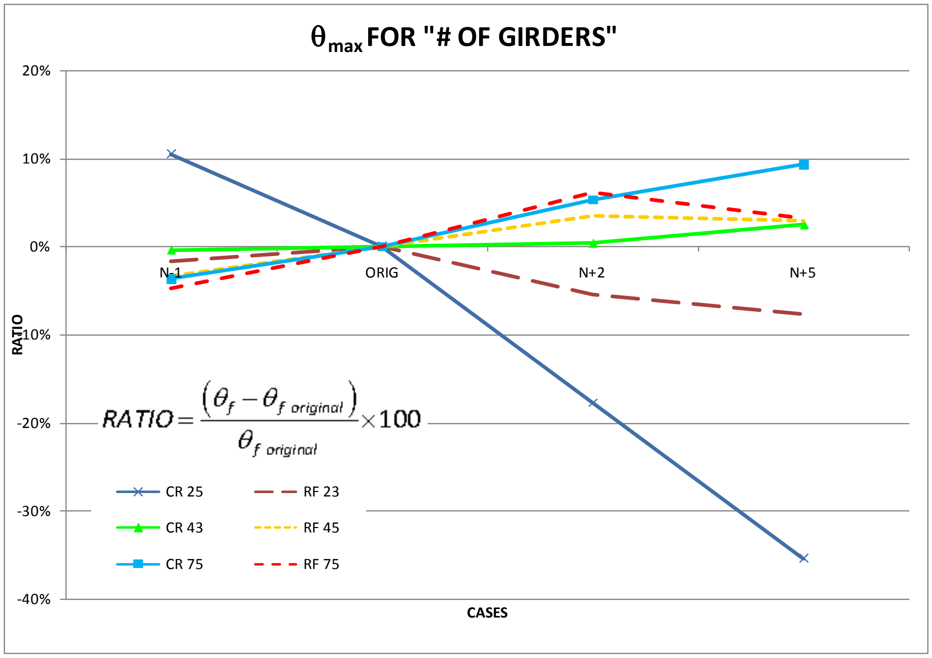

Figure 6-7. Maximum rotations distribution for the "Number of Girders" case

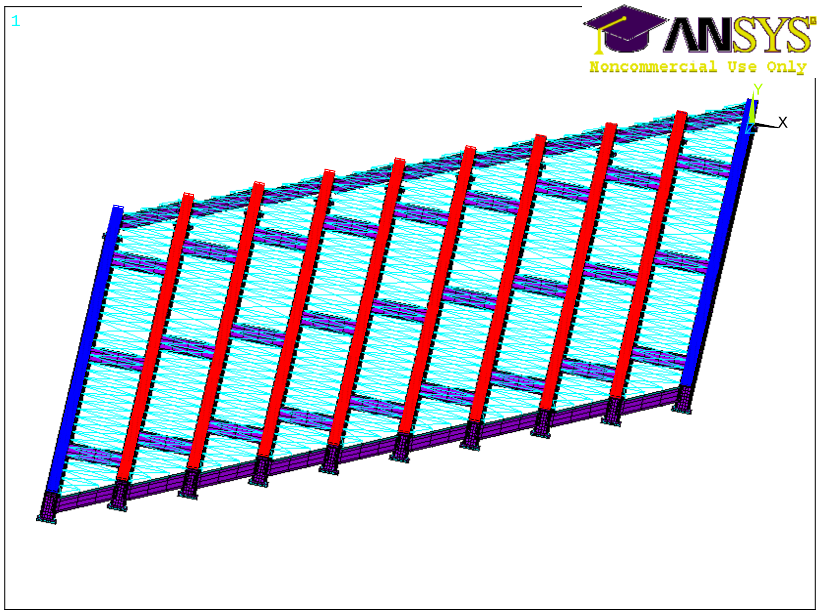

Figure 6-8. Roaring Fork Bridge with N+5 Girders (10 Girders)

6.2.5 Number of Transverse Stiffeners

Two of the main reasons why transverse stiffeners are used on steel girders is to control out-of-plane deformations at a given location and to prevent web buckling or crippling, etc. The possibility of modifying the torsional stiffness at discrete locations led to considering this parameter in the investigation.

Three values were analyzed for this parameter. However, the values were selected based upon the number of original intermediate stiffeners for each girder and increasing them by a given factor. For the case of Chicken Road, its original six stiffeners per side on the interior girders were modified by a factor of 11/6 and 14/6 while for Roaring Fork these factors were 5/3 and 7/3 because Roaring fork has three stiffeners per side of interior girder. Table 6-4 shows the results for this study.

Table 6-4. Rotation values for the "Number of Transverse Stiffeners" case

CASES	CR (25 DEG SKEW)		RF (23 DEG SKEW)	
	θ_{min} CR 25	θ_{max} CR 25	θ_{min} RF 23	θ_{max} RF 23
ORIGINAL	0%	0%	0%	0%
1.67X # STIFFENERS	-26%	-30%	-4%	-4%
2.33X # STIFFENERS	-5%	9%	-35%	-14%
CASES	**CR (43 DEG SKEW)**		**RF (45 DEG SKEW)**	
	θ_{min} CR 43	θ_{max} CR 43	θ_{min} RF 45	θ_{max} RF 45
ORIGINAL	0%	0%	0%	0%
1.67X # STIFFENERS	-11%	-3%	-1%	-2%
2.33X # STIFFENERS	-1%	-12%	-3%	-5%
CASES	**CR (75 DEG SKEW)**		**RF (75 DEG SKEW)**	
	θ_{min} CR 75	θ_{max} CR 75	θ_{min} RF 75	θ_{max} RF 75
ORIGINAL	0%	0%	0%	0%
1.67X # STIFFENERS	-16%	-17%	0%	-2%
2.33X # STIFFENERS	-12%	-13%	-2%	-5%

Similar to what happened with the Exterior-to-interior Moment of Inertia Ratio, the addition of stiffeners along the span of the girders proves to be effective as far as out-of-plane rotations are concerned, evidenced on Figure 6-9 and Figure 6-10. The results suggest that enhancing the torsional stiffness of the girders yields important changes in the cross-section rotational behavior, at least up to 20 percent. The values range between 5 percent and 25 percent, reaching a one time the value of 30 percent. Figure 6-11 presents an image of the additional transverse stiffeners along the span of the girder. Notice that for this case there is an extra transverse stiffener between intermediate and end bent cross-frames.

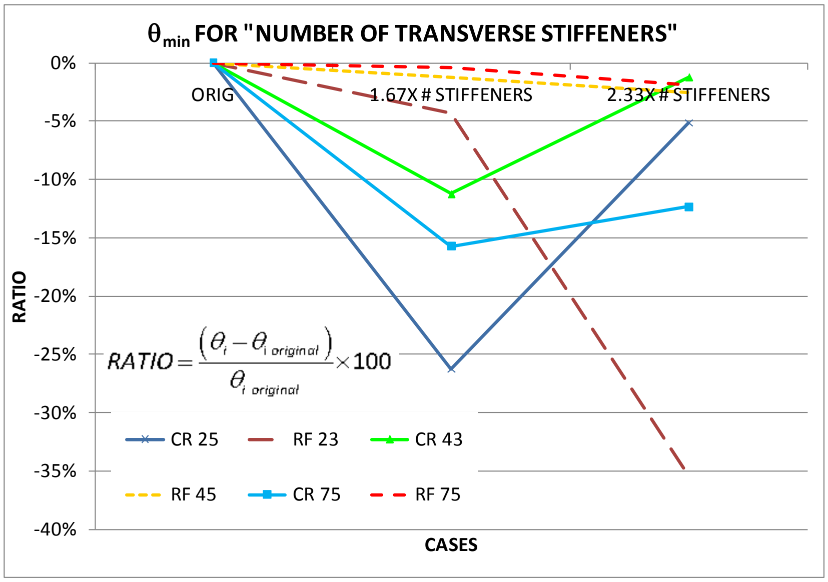

Figure 6-9. Minimum rotations distribution for the "Number of Transverse Stiffeners" case

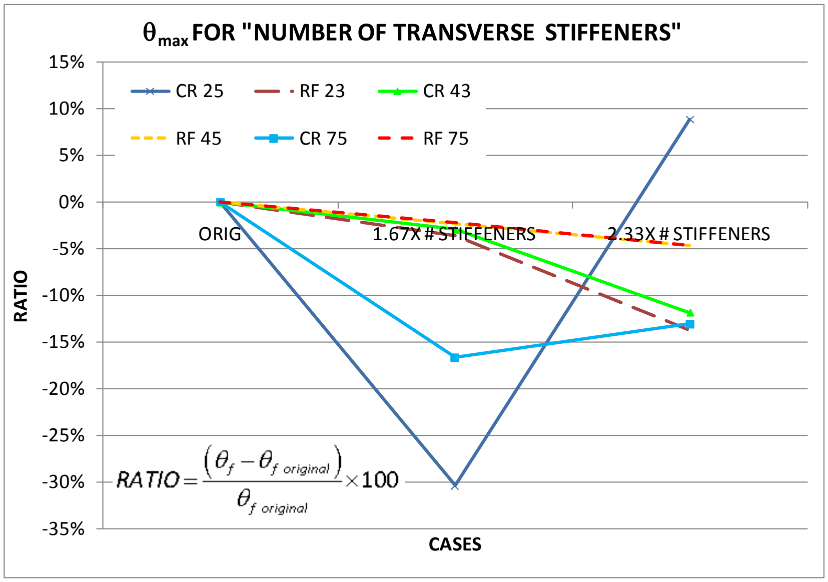

Figure 6-10. Maximum rotations distribution for the "Number of Transverse Stiffeners" case

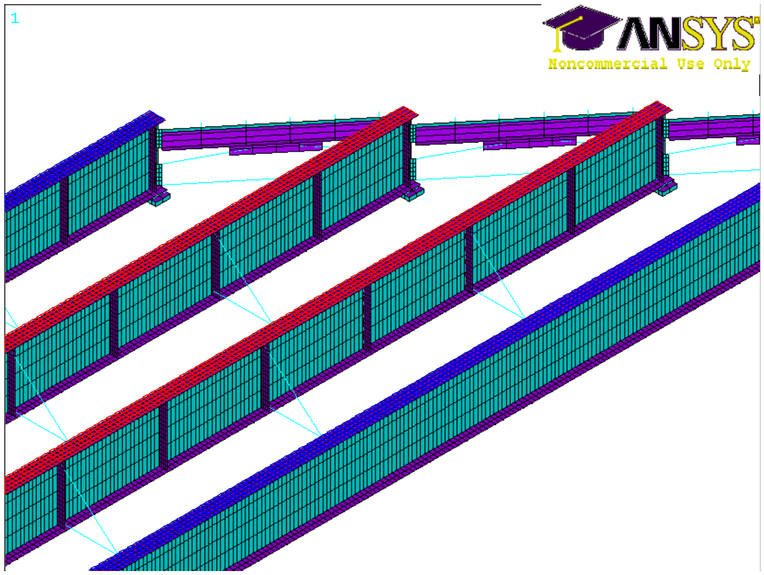

Figure 6-11. Detail of the stiffeners distribution for the 2.33X case on Chicken Road Bridge

6.2.6 Number of Cross-frames

In an effort to determine how sensitive steel skewed bridges are to the number of cross-frames or diaphragms a series of analyses were conducted. For the two bridges three values for this parameter were considered. They ranged from a structure with no cross-frames (#XF 0X) to a structure with twice the number of cross-frames (#XF 2.0X). Again, as it has been done with the rest of the parameters, three skew angles were considered for each bridge. Table 6-5 presents the results of the study on this parameter

Table 6-5. Rotation values for the “Number of Cross-frames” case

CASES	CR (25 DEG SKEW)		RF (23 DEG SKEW)	
	θ_{min} CR 25	θ_{max} CR 25	θ_{min} RF 23	θ_{max} RF 23
# XF 0X	-93%	-92%	-98%	-98%
ORIGINAL	0%	0%	0%	0%
# XF 2X	-48%	-48%	-20%	-37%
CASES	CR (43 DEG SKEW)		RF (45 DEG SKEW)	
	θ_{min} CR 43	θ_{max} CR 43	θ_{min} RF 45	θ_{max} RF 45
# XF 0X	-86%	-88%	-93%	-94%
ORIG	0%	0%	0%	0%
# XF 2X	-47%	-49%	0%	-22%
CASES	CR (75 DEG SKEW)		RF (75 DEG SKEW)	
	θ_{min} CR 75	θ_{max} CR 75	θ_{min} RF 75	θ_{max} RF 75
# XF 0X	-58%	-58%	-69%	-86%
ORIG	0%	0%	0%	0%
# XF 2X	-43%	-38%	23%	-21%

From the data obtained there are several observations. The fact that the best results were obtained when no cross-frames are provided may support the idea that the major cause of out-of-plane rotations are the presence of cross-frames along the bridge, either staggered or not. The fact that forces and stresses can be distributed along the girders via the cross-frames leads to the theory that rotations are the consequence of an inherent behavior of the steel skewed bridges, and rotations will always be part of their behavior (See Figure 6-12 and Figure 6-13).
Nevertheless, when the cross-frames are doubled the effect is interesting. The overall ability of the girders to rotate against the longitudinal axis is enhanced up to 30 percent on average, with values varying from 0 percent to almost 50 percent. Figure 6-14 presents Roaring Fork Bridge with twice the number of cross-frames for a 75 degrees skew angle case.

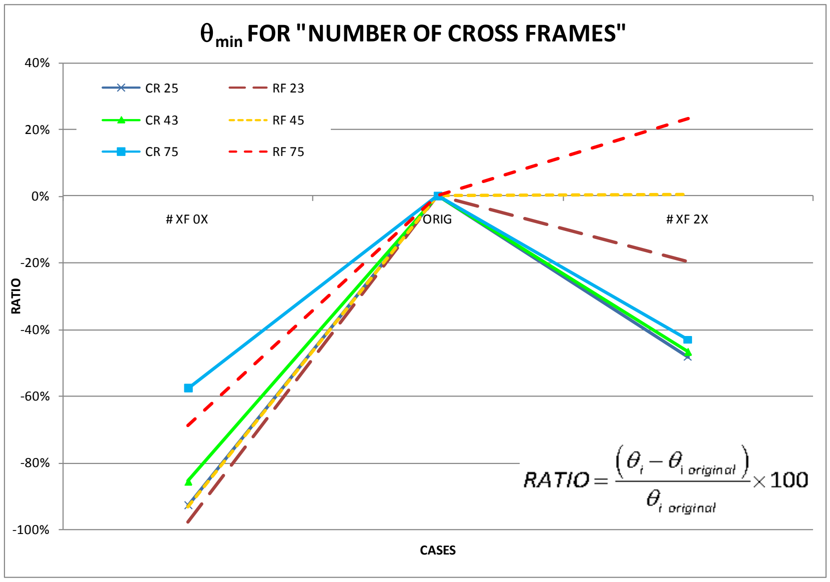

Figure 6-12. Rotations distribution for the "Number of Cross-frames" case

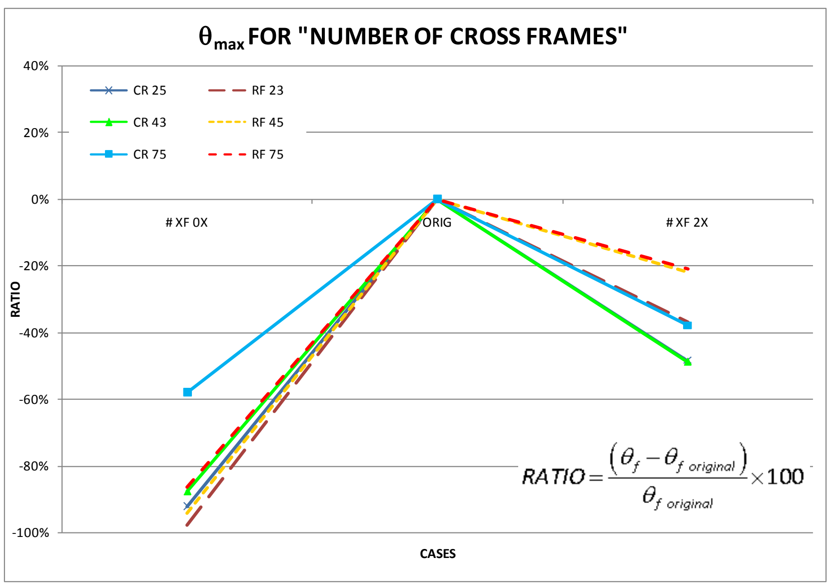

Figure 6-13. Maximum rotations distribution for the "Number of Cross-frames" case

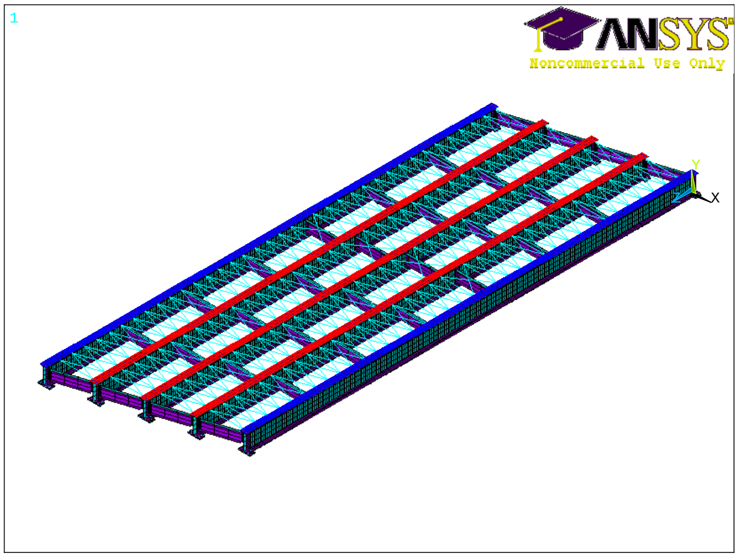

Figure 6-14. Roaring Fork Bridge at 75 degrees skew with twice the original number of Cross-frames

6.2.7 Cross-frame Stiffness

Another parameter considered in the analysis was the cross-frame stiffness. For Chicken Road Bridge this parameter was directly associated with the cross-frame members cross-section area, due to the fact that in a K-type or X-type cross-frame the overall stiffness is provided by the axial rigidity of each member. For Roaring Fork Road Bridge the situation is different since diaphragms provide both axial and flexural stiffness. Therefore both the cross-sectional area and the moment of inertia of the strong axis were evaluated.

For Chicken Road a total of three different stiffnesses, including the original, were considered. The cross-sectional areas of the members were modified to half of the original and twice the original. For Roaring Fork Road Bridge it was necessary to evaluate both the moment of inertia along the strong axis and cross-section area independently since the diaphragms provide both flexural and axial rigidity to the system. Both the moment of inertia and the cross-section area were modified independently to half and twice the original for the three different skew angles studied. Results obtained are presented on Table 6-6. Contrary to what could be thought, changes in the cross-frame stiffness do not show a unique trend. The idea that stiffer cross-frames could be beneficial to the structure is not necessary the case.

Table 6-6. Rotation values for the “Cross-frame Stiffness” case

			FLEX STIFFNESS		AXIAL STIFFNESS	
CASES	CR (25 DEG SKEW)		RF (23 DEG SKEW)		RF (23 DEG SKEW)	
	θ_{min} CR 25	θ_{max} CR 25	θ_{min} RF 23	θ_{max} RF 23	θ_{min} RF AX 23	θ_{max} RF AX 23
0.5X INERTIA X-F	0%	0%	-5%	-9%	-5%	0%
ORIGINAL	0%	0%	0%	0%	0%	0%
2.0X INERTIA X-F	0%	0%	-3%	5%	-1%	-4%
CASES	CR (43 DEG SKEW)		RF (45 DEG SKEW)		RF (45 DEG SKEW)	
	θ_{min} CR 43	θ_{max} CR 43	θ_{min} RF 45	θ_{max} RF 45	θ_{min} RF AX 45	θ_{max} RF AX 45
0.5X INERTIA X-F	0%	0%	-1%	1%	-4%	-7%
ORIGINAL	0%	0%	0%	0%	0%	0%
2.0X INERTIA X-F	0%	0%	3%	0%	7%	5%
CASES	CR (75 DEG SKEW)		RF (75 DEG SKEW)		RF (75 DEG SKEW)	
	θ_{min} CR 75	θ_{max} CR 75	θ_{min} RF 75	θ_{max} RF 75	θ_{min} RF AX 75	θ_{max} RF AX 75
0.5X INERTIA X-F	0%	0%	-7%	5%	5%	-9%
ORIGINAL	0%	0%	0%	0%	0%	0%
2.0X INERTIA X-F	0%	0%	28%	-8%	12%	6%

Figure 6-15 and Figure 6-16 demonstrate that modifying either the axial or the flexural stiffness does not provide the desired response when the cross-frames system is composed of diaphragms. There are cases in which these changes produce a less stiff structure, evidenced by the increase in rotational values. Based upon the data obtained it seems that it is better to enhance the flexural stiffness of a diaphragm by increasing its moment of inertia rather than its cross-section area. Changes in the stiffness of the K-type cross-frames did not show significant variations.

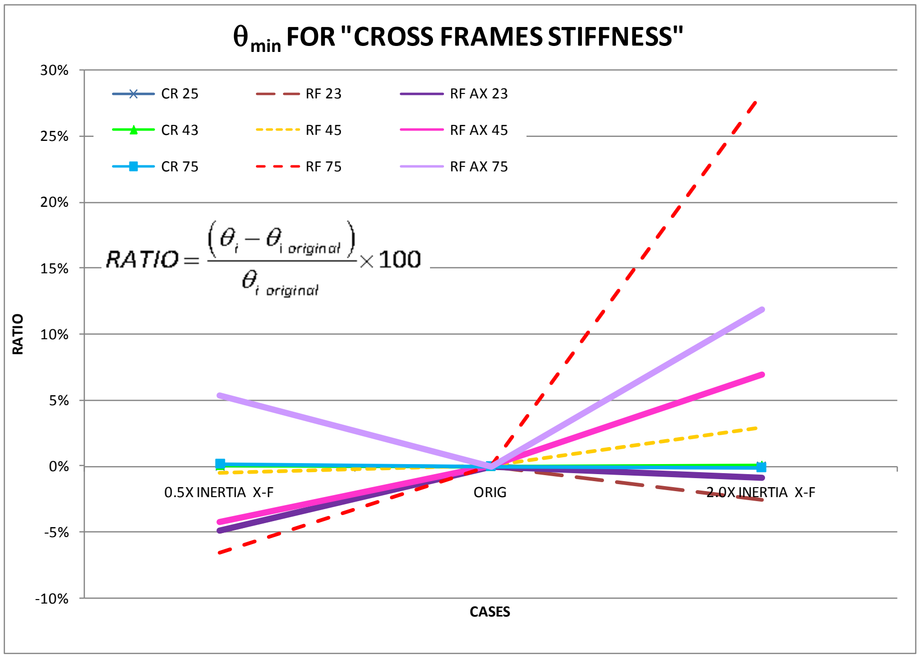

Figure 6-15. Minimum rotations distribution for the "Cross-frames Stiffness" case

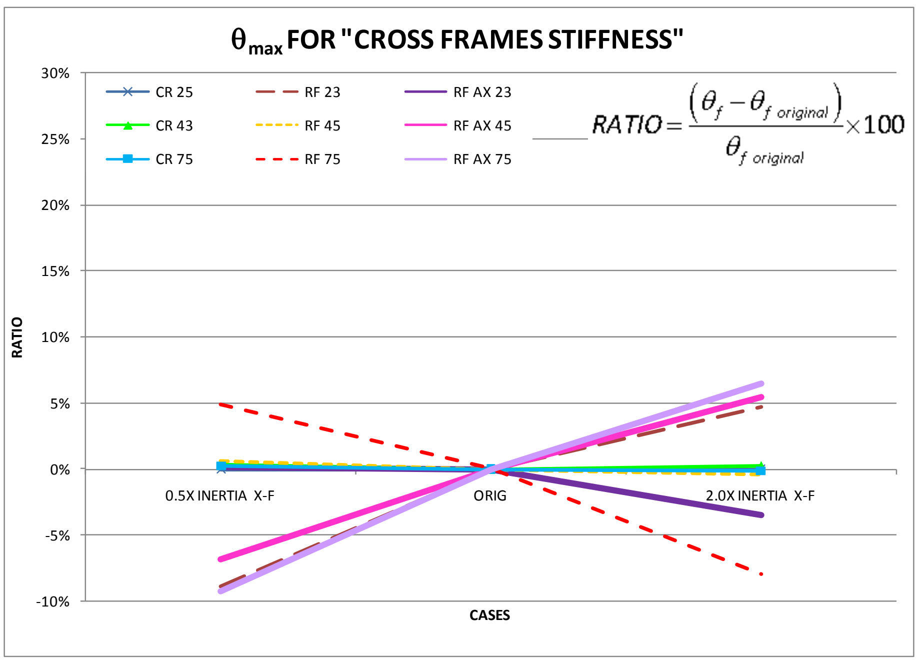

Figure 6-16. Maximum rotations distribution for the "Cross-frames Stiffness" case

6.2.8 Stay-in-place Forms Stiffness

Although not included in current design codes, it has been demonstrated that the stay-in-place metal deck forms provide some lateral stiffness to the structure before the composite behavior of the bridge slab. (Jetann et al, 2002; Egilmez et al, 2003 and 2006). Considering this, it makes sense to modify the stay-in-place form stiffness to determine how these changes affect the overall behavior of the bridge.

To investigate this parameter for each of the two bridges and the three skew angles in the study, three different stay-in-place form stiffnesses were considered, including the original. Table 6-7 summarizes these cases mentioned.

Table 6-7. Rotation values for the "Stay-in-place Forms Stiffness" case

CASES	CR (25 DEG SKEW)		RF (23 DEG SKEW)	
	θ_{min} CR 25	θ_{max} CR 25	θ_{min} RF 23	θ_{max} RF 23
SIP 0.1X	37%	11%	18%	23%
ORIGINAL	0%	0%	0%	0%
SIP 10X	-13%	-21%	-17%	-10%

CASES	CR (43 DEG SKEW)		RF (45 DEG SKEW)	
	θ_{min} CR 43	θ_{max} CR 43	θ_{min} RF 45	θ_{max} RF 45
SIP 0.1X	12%	6%	3%	9%
ORIGINAL	0%	0%	0%	0%
SIP 10X	-1%	-2%	-2%	-4%

CASES	CR (75 DEG SKEW)		RF (75 DEG SKEW)	
	θ_{min} CR 75	θ_{max} CR 75	θ_{min} RF 75	θ_{max} RF 75
SIP 0.1X	-2%	6%	-24%	17%
ORIGINAL	0%	0%	0%	0%
SIP 10X	4%	-4%	22%	-11%

Results from the study of this parameter are presented on Figure 6-17 and Figure 6-18. These results present a clear trend in which the higher the cross-section area of the SIP elements the lower the rotations on the structure. These values reach up to 10 percent to 15 percent average for skew angles lower than 75 degrees. This is clear evidence that even though the SIP forms provide some lateral bracing especially during the construction phase, a small improvement on the connection system, which is usually the weakest part of the system, would be beneficial for the entire structure.

These results are in good agreement with those obtained by Egilmez et al. (2007). They suggested that by enhancing the connection details between the SIP forms and the girders, which is the weakest point of this structural component, it is possible to improve the strength, stiffness and overall performance of the system.

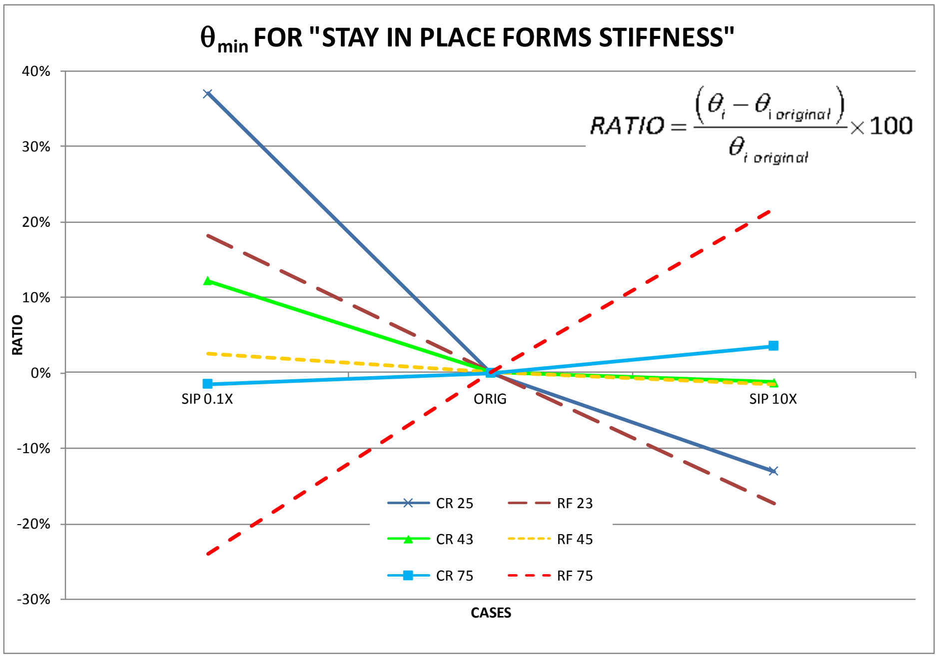

Figure 6-17. Minimum rotations distribution for the "Stay-in-place Forms Stiffness" case

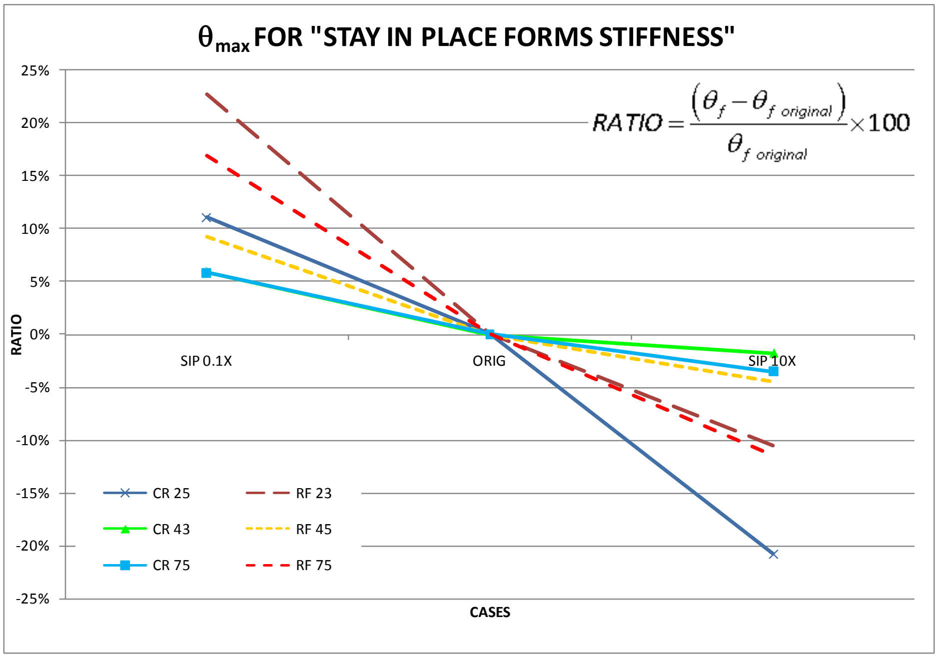

Figure 6-18. Maximum rotations distribution for the "Stay-in-place Forms Stiffness" case

6.2.9 Girder Spacing-to-Span Ratio

Previous investigations regarding differential deflections carried out by Wisenhunt (2004) and Fisher (2005) came to the conclusion that this particular parameter has an important role on the deflection values. Likewise, it was considered worth checking whether this condition is also applicable to torsional out-of-plane rotations.

Four different spacing-to-span ratio values were studied for the two bridges, which are 0.5 times the original, the original, 1.25 times the original, and two times the original. However, due to the geometric constraints associated with each bridge cases with a skew angle lower than 30 degrees could not have values determined. Table 6-8 presents the results for all the above cases.

Table 6-8 Rotation values for the "Girder Spacing-to-span Ratio" case

CASES	CR (25 DEG SKEW)		RF (23 DEG SKEW)	
	θ_{min} CR 25	θ_{max} CR 25	θ_{min} RF 23	θ_{max} RF 23
SPC-SPN 0.5X	30%	68%	11%	17%
ORIGINAL	0%	0%	0%	0%
SPC-SPN 1.25X	11%	-24%	-12%	-35%

CASES	CR (43 DEG SKEW)		RF (45 DEG SKEW)	
	θ_{min} CR 43	θ_{max} CR 43	θ_{min} RF 45	θ_{max} RF 45
SPC-SPN 0.5X	3%	0%	6%	-10%
ORIGINAL	0%	0%	0%	0%
SPC-SPN 1.25X	-1%	-2%	0%	1%
SPC-SPN 2X	-15%	-33%	-5%	-9%

CASES	CR (75 DEG SKEW)		RF (75 DEG SKEW)	
	θ_{min} CR 75	θ_{max} CR 75	θ_{min} RF 75	θ_{max} RF 75
SPC-SPN 0.5X	3%	-7%	7%	-31%
ORIGINAL	0%	0%	0%	0%
SPC-SPN 1.25X	-2%	1%	1%	5%
SPC-SPN 2X	-6%	4%	5%	0%

From Figure 6-19 and Figure 6-20 it was observed that the worst scenario occurs when this parameter is changed to values lower than one. However, when those values are increased above one there seems to be a slight decrease in the rotations values, particularly for skew angles lower than 75 degrees. Although the change is within 15 percent to 20 percent of average, it represents an alternative to be considered for controlling out-of-plane rotations of the structure. Although it may sound logical to modify the amount of dead load on the structure when the spacing-to-span ratio is modified, this was not the case since the main objective was to evaluate changes in the response for one variable at a time. Nevertheless results suggest that when this parameter is set less than one, the stiffness of the intermediate diaphragms is increased and therefore their capacity to transfer forces from one girder to its adjacent promoting transverse deformations along the span. Conversely, when the value of this parameter is set greater than one, the diaphragms become more slender and therefore more flexible, decreasing their ability to transfer lateral loads. Figure 6-21 presents a picture of one of the bridges when this parameter is set to 0.5.

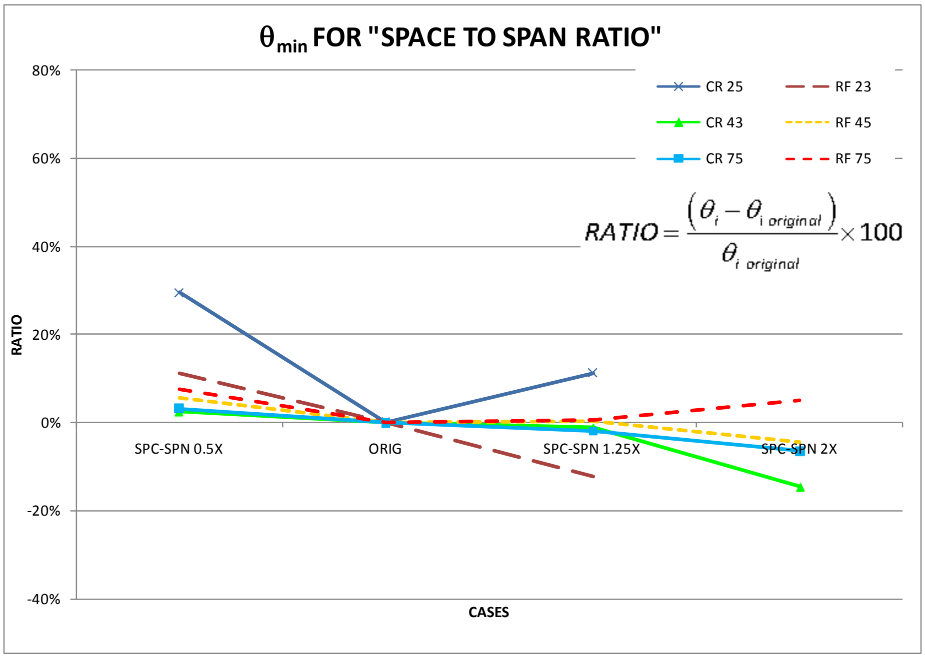

Figure 6-19. Minimum rotations distribution for the "Spacing-to-Span Ratio" case

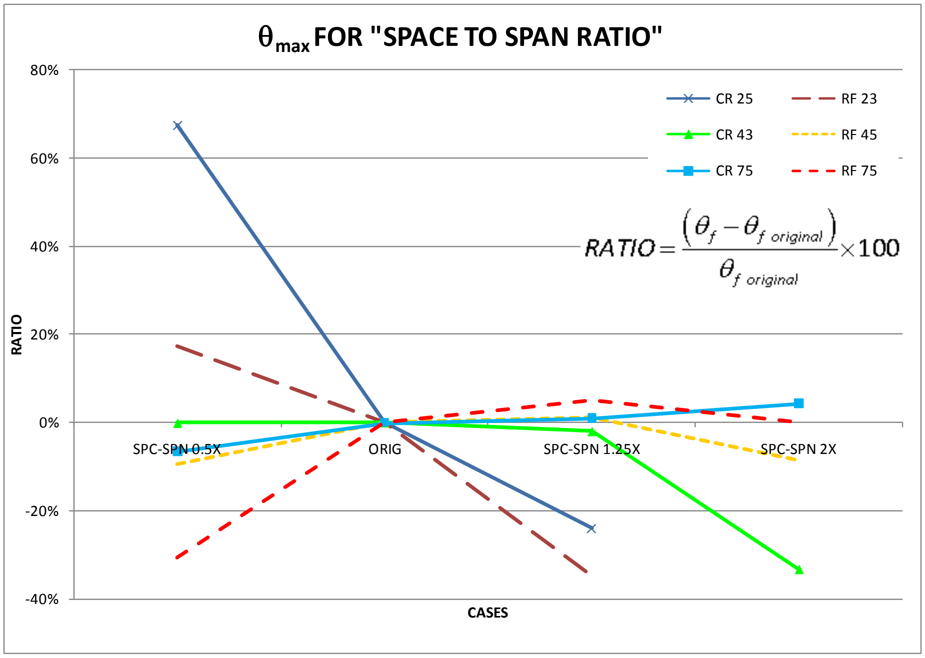

Figure 6-20. Maximum rotations distribution for the "Spacing-to-Span Ratio" case

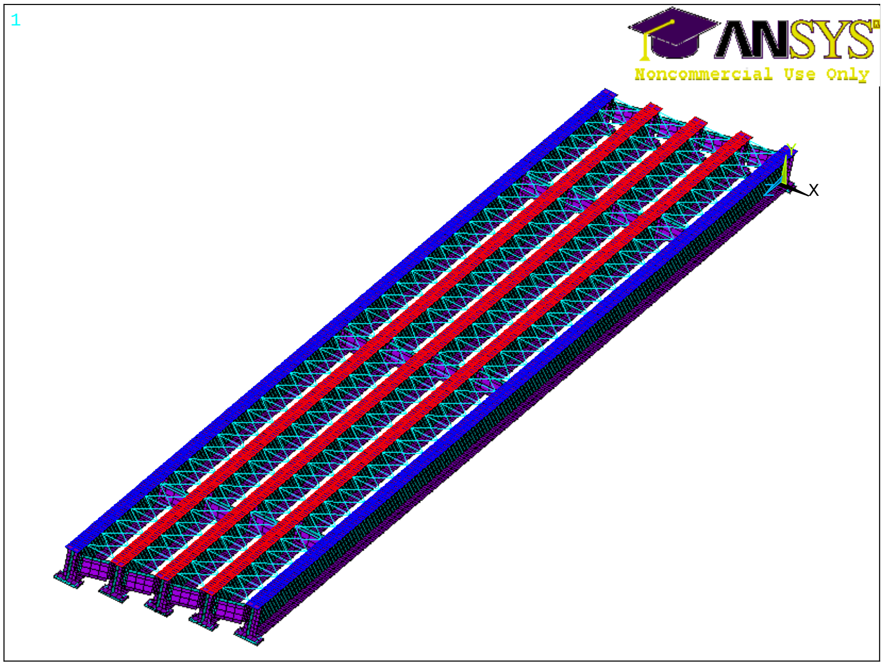

Figure 6-21. Roaring Fork Bridge with a 75 degrees skew and a Spacing-to-Span Ratio half of the original

6.2.10 Analysis of Results

From the parametric analysis it can be determined, among other things, how sensitive the structure is to changes of a particular variable. Some of the parameters demonstrated to be less effective and some proved to be of vital importance in the final rotational response of the steel girders.

In an effort to provide a better understanding of the out-of-plane rotations effects of each variable the parameters were classified in order of effectiveness in modifying the response.

The criteria utilized to classify the parameters was based on a tolerance margin set to plus minus 5 percent; where those situations that led to changes higher than 5 percent were considered to be unfavorable and those that fell under -5 percent were defined as favorable. Regardless of the values selected as boundaries, perhaps the most important outcome was related to the idea of establishing possible mitigation strategies and criteria oriented towards controlling the out-of-plane rotations phenomenon. The proposed classification is as follows:

6.2.10.1 Favorable Parameters (Ratio > 5%)

Parameters are considered favorable if when modified, the behavior of the structure is torsionally stiffer structure. This is a structure whose out-of-plane rotations are lower than those on the original.

6.2.10.1.1 Increase either the exterior girders or the interior girders moments of inertia

The best effects were obtained by changing the values of this parameter. On average, by increasing the internal girders moment of inertia the rotations were decreased by 20 percent, whereas by increasing the exterior girders moment of inertia the change produced a reduction of 28 percent of the out-of-plane rotations.

6.2.10.1.2 Increase the number of cross-frames

After modifying this variable by a factor of 2 the average rotation reductions was around 28 percent, which is similar than what the previous condition generated.

6.2.10.1.3 Increase the Number of Transverse Stiffeners

This condition, on average, was capable of reducing the rotations up to 10 percent for the three skew angles and on both bridges.

6.2.10.2 Neutral Parameters (-5% ≤ Ratio ≤ 5%)

This classification was intended to cover those cases in which changes in the corresponding parameters did not produce, on average, significant changes in the girder response, either positive or negative. These cases are:

6.2.10.2.1 Modify the number of girders

Although it may be reasonable to think that the larger the number of girders the smaller the maximum rotations, this does not seem to be true. This is based on the idea that as we increase the number of girders, the “local” effect of both the skewness and the unbalanced tributary load should fade off. However results do not agree with this theory. In fact, for the three values considered (N-1, N+2 and N+5) the highest or lowest average change for any case was 3 percent.

6.2.10.2.2 Modify the stiffness of the cross-frames

Another condition somewhat unexpected was that increasing or decreasing the cross-frame stiffness by factors of 2 and ½ respectively, did not produce substantial changes on the rotation values. In any case, the results demonstrated that the maximum absolute change was 2 percent.

6.2.10.2.3 Increase the stiffness of the SIPs

By increasing this variable by a factor of 10 the average change in rotation values was only 2 percent, which means that as long as this parameter is not modified, there will not be any undesirable effects as it is the case when the value of this parameter is reduce, that will be discussed in the following section.

6.2.10.3 Unfavorable Parameters (Ratio < -5%)

When the value of one parameter is modified such that it yields increments of the out-of-plane rotation, then it is defined as an unfavorable parameter. Following there is a list of those that satisfy this condition.

6.2.10.3.1 Increase in the exterior-to-interior load ratio

When this parameter was changed to the extreme amount of 100 percent, the original idea was to monitor the effect of increasing the sizes of overhangs on the structure as well as to verify how effective this condition is in modifying the average out-of-plane rotations of the girders. It turns out that the worst change that can be done to a bridge, as far as out-of-plane rotations are concerned, is this condition. The average increase in rotations for all the skews and bridges studied was 14 percent.

6.2.10.3.2 Decrease in the stiffness of the Stay-in-place metal deck forms

It was mentioned before that increasing the SIPs stiffness by a factor of 10 did not produce major changes on the rotational values. However, when this condition is inversed the outcome is not the same. Indeed, decreasing the SIPs stiffness by a factor of 10 causes the rotations to increase by 10 percent.

6.2.10.4 Summary of Numerical Cases

After analyzing all the different results obtained from the parametric study it was possible to identify potential sources for mitigation strategies. For example, if for a given bridge potential torsional rotation problems are identified then one possible solution would be to increase the torsional stiffness of the girders by increasing the moment of inertia of the exterior ones. Figure 6-22 depicts the average rotation ratios for all the parameters considered in this investigation. It can be noted that some cases lie within the neutral zone (ie. N+2), whereas others fall outside, either on the unfavorable area above +5 percent (ie. SIP 0.1X) or on the favorable area below -5 percent (ie. #XF 2X). Although some of the values adopted for the parameters are not technically reasonable, their study suggests a possible trend on the results that is necessary to understand the degrees of influence a parameter has on the girder response.

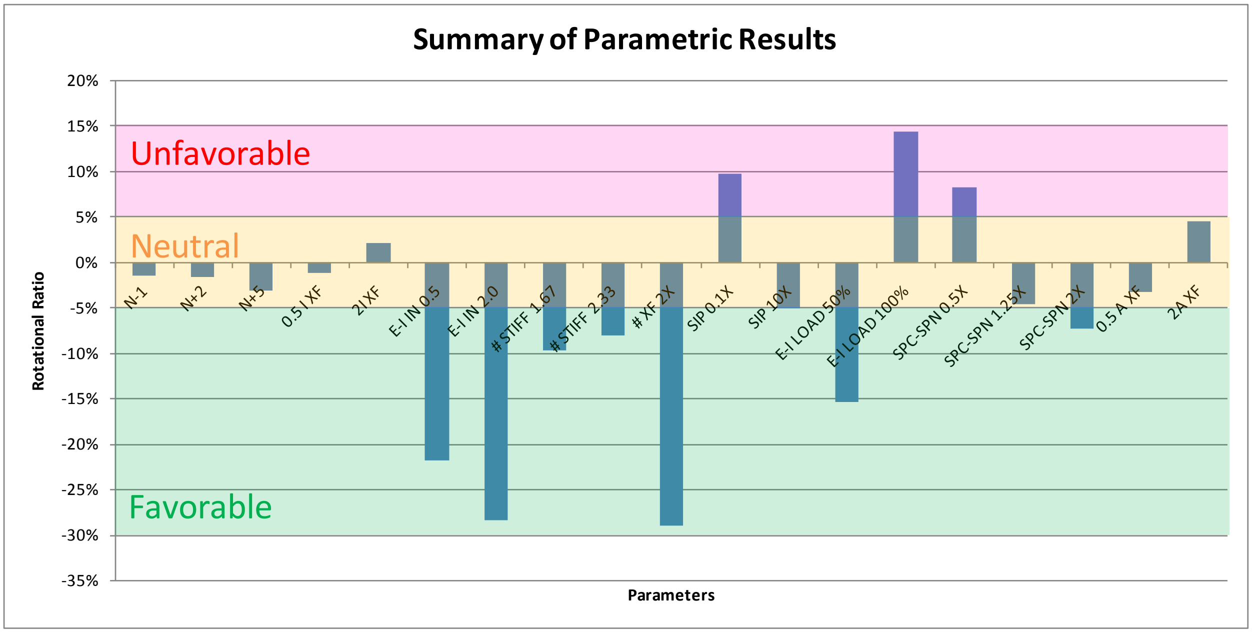

Figure 6-22. Results from the study on numerical parameters

6.3 Non-numerical Parameters

6.3.1 Cross-frame Layout.

6.3.1.1 Overview

A preliminary parametric analysis was conducted in order to determine the influence of the cross-frame layout on the overall behavior of the structure. Three different layouts were considered on this investigation, which include the original staggered case, the case where cross-frames are perpendicular to the girder web and aligned with each other and finally the case where cross-frames are laid out parallel to the abutments and aligned to one another. Figure 6-23 presents these three layouts.

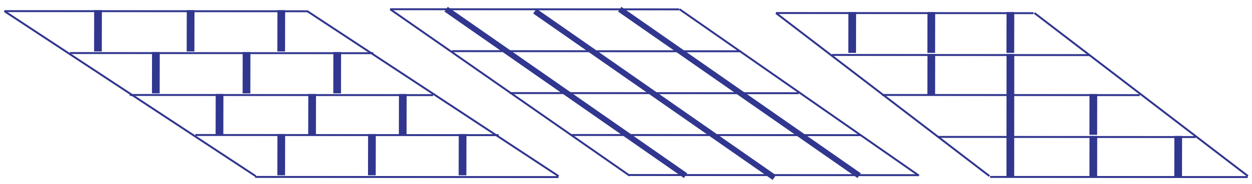

Figure 6-23. Layouts considered: Staggered (left), Parallel (center) and Perpendicular (right)

Additionally, each layout was evaluated for three different skew angles on each of the two bridges included along the investigation. These skew angles were 25, 43 and 75 degrees for Chicken Rd. Bridge and 23, 45 and 75 degrees for Roaring Fork. Bridge. The results were compared for both the out-of-plane rotations and longitudinal stresses and the most interesting findings are presented.

6.3.1.2 Comparison of Results

The initial analysis consisted of determining both maximum rotations and average stresses along the structure for the each of the three skew angles selected. For each case the values were compared in an effort to identify possible trends that might lead to useful conclusions. Figure 6-24 presents the distribution of the maximum average out-of-plane rotations for both Chicken Rd. Bridge and Roaring Fork. Bridge. It can be seen that the staggered option is the one that shows the highest rotational values for most of the cases included. This is also evidenced when comparing the average maximum stresses on the girders.

In this sense Figure 6-25 presents the average maximum stresses measured along the girders. It is possible to notice that the staggered alternative provides the highest average stresses for almost the entire data. This result strongly agrees with the rotation results evidencing the fact that perhaps the staggered scenario is not the most adequate for this type of steel bridges.

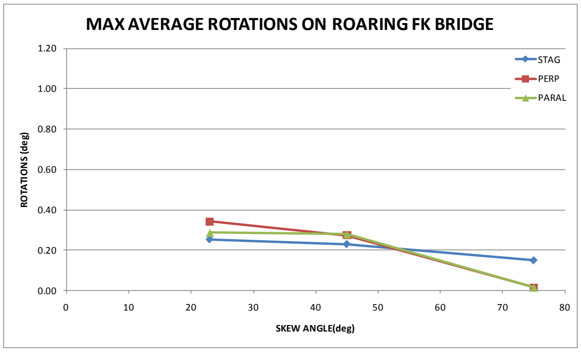

Figure 6-24. Rotations on Chicken Rd. (left) and Roaring Fk. Rd (right) Bridges

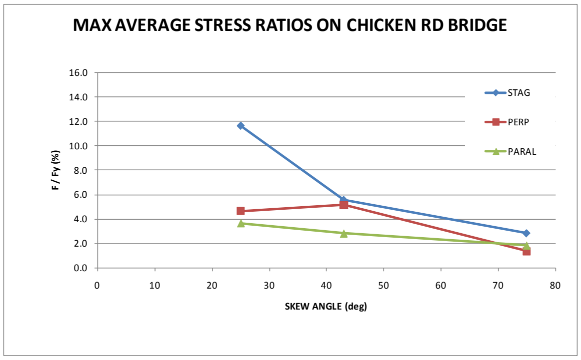

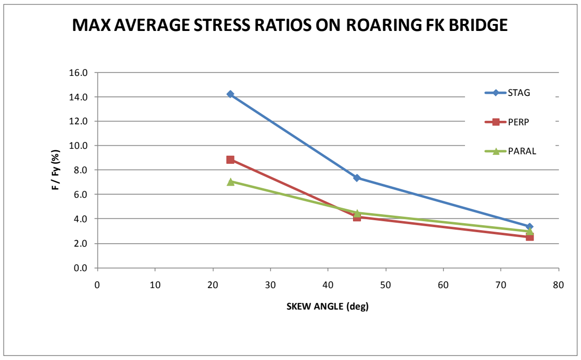

Figure 6-25. Average maximum stresses on Chicken Rd. (left) and Roaring Fork Rd. (right) Bridges

Nonetheless, in an effort to have a broader picture of the situation, another parameter was considered in the analysis. Figure 6-26 presents the total cross-frame forces for each scenario. In this Figure each point represents the summation of all the total forces on each cross-frame located between the corresponding girders. It can be observed that the staggered alternative is not the best option for two of the three skew angles studied on Chicken Road Bridge. However, the case on Roaring Fork Bridge is somewhat different. This is due to the fact that the diaphragm system has not only the possibility of transferring forces from one girder to the other as it is the case of the cross-frames but its flexural stiffness also contributes to the force flow between adjacent girders by its capability of transferring moments. Results show that while perpendicular layout produced the highest forces on all cases the parallel configurations produced the lowest. For all the cases studied, as the skew angle moves towards 90 degrees the forces are smaller, indicating less interaction between girders and cross-frames. The situation regarding the 75 degrees configuration is also particular. It can be seen from Figure 6-27 that the three layouts are so similar and so close to each other that it could be anticipated that any of the options would give the best results. This is expected to be the case as the skew angle approaches to 90 degrees.

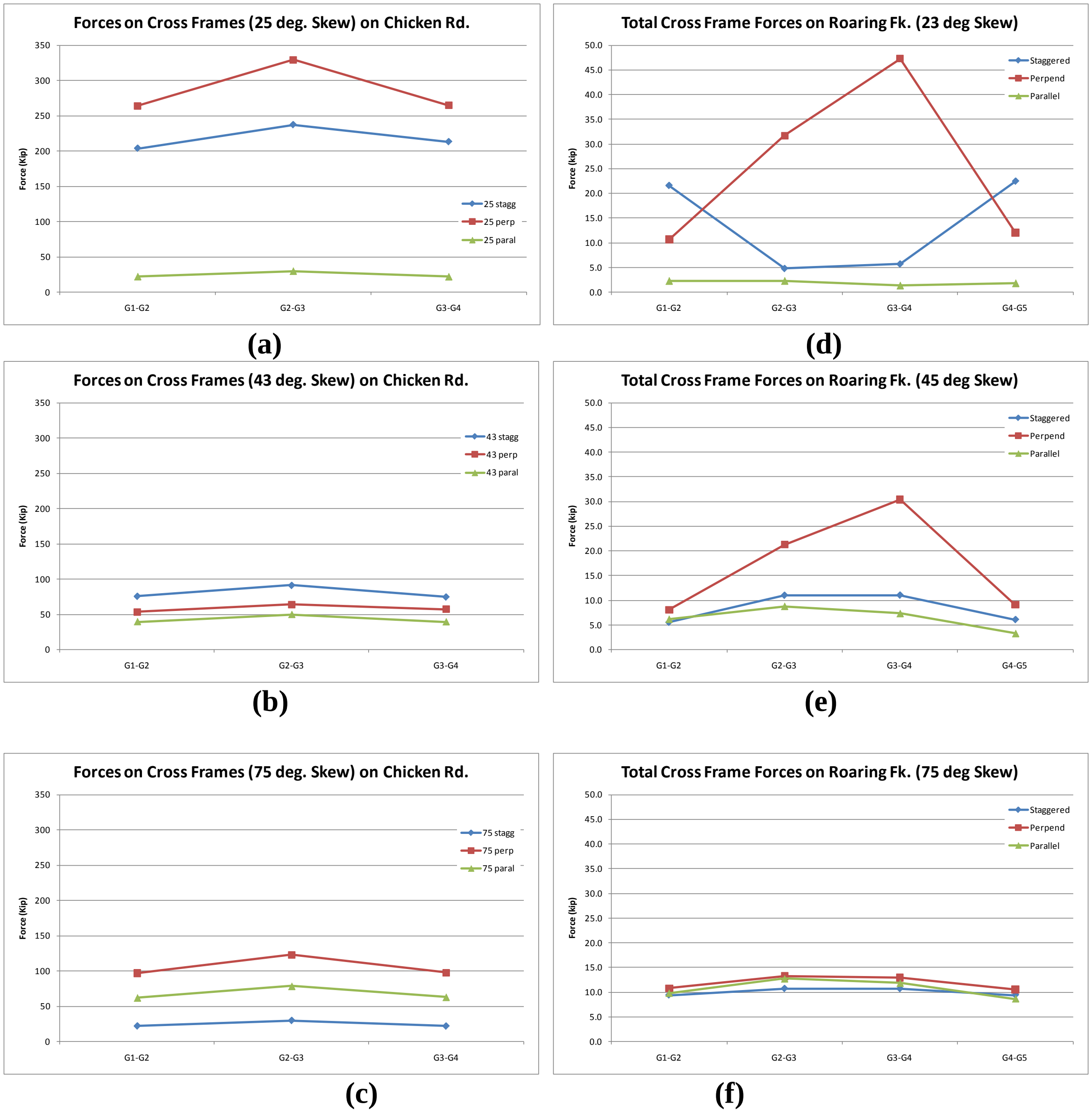

Figure 6-26. Total Cross-frame forces for the three skew angles studied. (a) CR 25 (b) CR 43 (c) CR 75 (d) RF 23 (e) RF 45 (f) RF 75

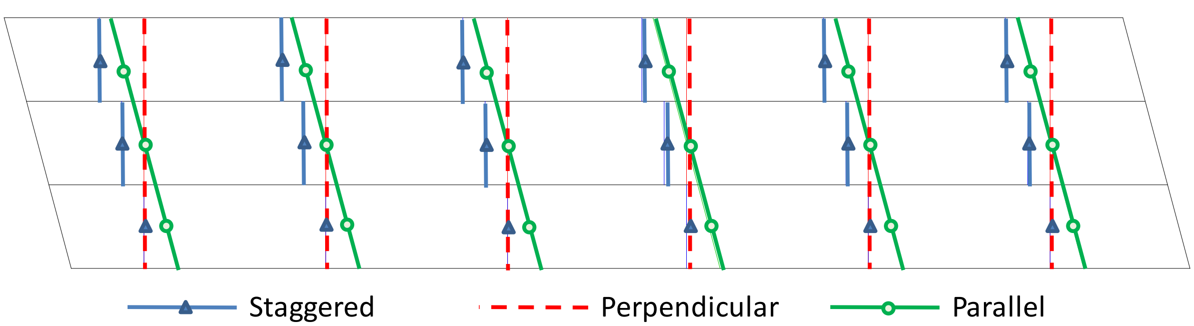

Figure 6-27. Plan view of the three cross-frame layouts overlapped for 75 degrees skew on Chicken Rd. Bridge

6.3.2 Cross-frame Type (X-Type versus K-Type)

6.3.2.1 General

A parametric analysis was conducted to determine the influence of the type of cross-frame in the overall response of the bridge. Two types of cross-frame configurations were included (K-type and X-type) and three different skew angles (25, 43 and 75 degrees) were selected to determine the sensitivity of the system to these parameters. Additionally, for both types of cross-frames, the same cross-section was selected (L 3 ½ x 3 ½ x ½). In order to study the response, cross-section rotations were selected as the comparison criteria. It is worth mentioning that the analysis was carried only for Chicken Road Bridge, because it was the only bridge that was designed with one of these cross-frame geometries.

6.3.2.2 Preliminary Analysis

To have an initial idea of how the system behaves with each of the cross-frame configurations selected, a preliminary study was conducted by subjecting each configuration to a unit load in both the horizontal and vertical directions, as it is shown on Figure 6-28. Whisenhunt (2004) carried out a similar analysis but only considering vertical deflection. He found that both systems yielded relatively similar results.

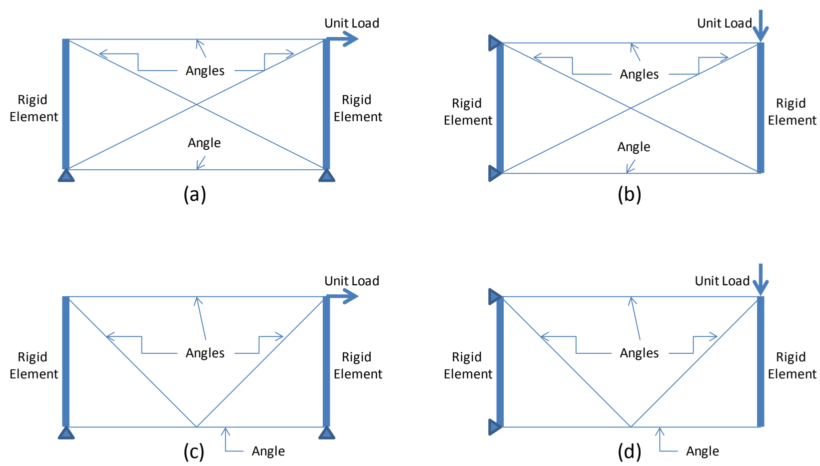

Figure 6-28. Cross-frame and unit load configurations

Each truss system was composed of diagonals and struts with the actual angle cross-section, whereas the vertical elements that correspond to the girders cross-sections were considered to be much stiffer than the angles. Although the assumptions related to the top strut as well as the girders cross-section are not entirely true, the main purpose was to perform a relative analysis, on which both truss systems are subjected to the same load and boundary conditions.

After performing the analysis it was found that both systems yielded almost the same vertical deflections for cases (b) and (d) on Figure 6-28. However, when the lateral deformations were studied, which corresponds to cases (a) and (c) on Figure 6-28, the outcome was much different. It turns out that the X-type system yielded lateral deformations 50 percent smaller than the K-type. Having this in mind it is possible to expect higher rotations on the K-type system, but same vertical deflections on both, as it was mentioned by Whisenhunt (2004).

6.3.2.3 Comparison of Results

Figure 6-29 presents what was found to be the distribution of maximum rotations with respect to the skew angle. It can be clearly seen that, as expected, the X-type of cross-frame yielded much lower values of rotations than the K-type. However as we approach a non-skewed bridge (90 degrees), the difference tends to reduce. This agrees with the fact that out-of-plane rotations for a non-skewed bridge are negligible when compared to the skewed configuration. As a general recommendation, it seems reasonable to select X-type cross-frames for those bridges with severe skew angles in order to have a more efficient control of the rotations.

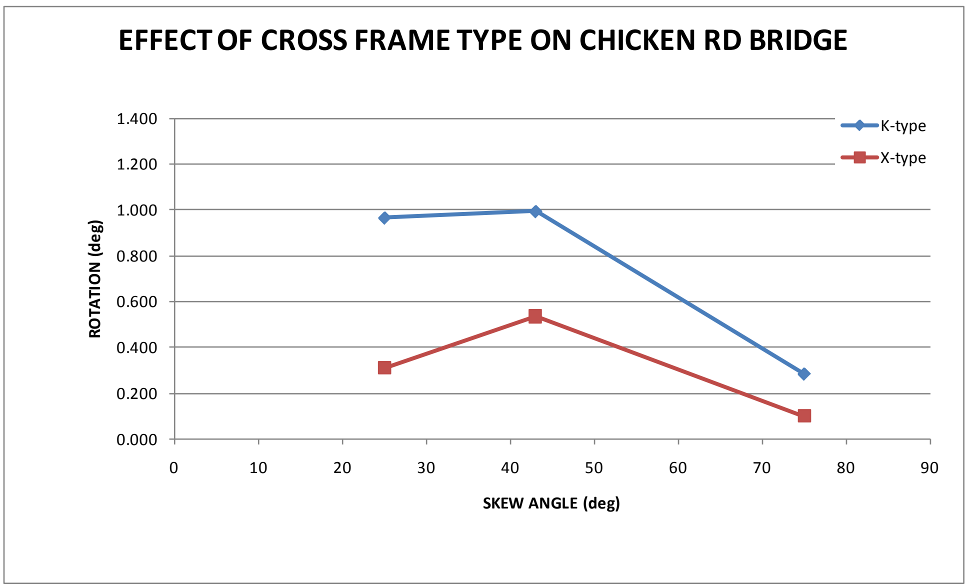

Figure 6-29. Distribution of out-of-plane rotations versus skew angle on Chicken Road Bridge

6.3.3 Dead Load Fit

6.3.3.1 Overview

Some of the topics related to differential deflections on steel skewed bridges have been addressed in several documents. In particular AASHTO/NSBA (2003) accounts for this condition by stating, among other things, that designers should indicate the condition under which diaphragms fit (no-load fit, full dead load fit or any condition in between). When designers consider full dead load, they must anticipate the out-of-plane rotations if girders need to be plumb, however AASHTO/NSBA (2003) admits that the rotations are only a prediction and therefore at the final stage of the loading process the girders may end up being somewhat out-of-plumb. It can be inferred from the aforementioned statement that the current knowledge on the rotational response of steel skewed bridges is not sufficient to provide more accurate guidelines.

In an effort to address these issues a parametric analysis was implemented. A description of the procedure adopted as well as results and observations are presented herein.

6.3.3.2 General Procedure.

To determine the influence of the dead load fit condition on the bridge behavior, a general but simple procedure was implemented. In essence, the main objective was to compare the responses for both the out-of-plane rotations and the longitudinal stresses on the following cases:

- When dead loads were applied to the original straight structure.
- When dead loads were applied to the cambered structure.

To achieve this objective, the following methodology was adopted to model the cambered structure. First, it was required to compute the deformations on the initially straight girders in all of the three directions (x, y and z). Once these deformations were obtained, they were subtracted from the nodal coordinates of the original straight structure to create the nodal coordinates on the cambered structure. Although this methodology may sound quite simple, it proved to be very effective. Equation 6-2 presents this calculation.

$$\lambda_i^{\text{cambered}} = \lambda_i^{\text{straight}} - \Delta\lambda_i^{\text{straight}} \qquad \textbf{[Eq. 6-2]}$$

where λ represents either the x, y or z coordinate and *i* is the node number.

Figure 6-30 and Figure 6-31 present a cross-section of a girder at four different stages, and for simplicity only one node was identified. For the straight girder case the initial condition, labeled as State A, and the final stage, labeled as State B are presented on Figure 6-30. For the selected node (TF right) both the transverse and the vertical deflections were identified as $\Delta X_{\text{TF RIGHT STR}}$ and $\Delta Y_{\text{TF RIGHT STR}}$ respectively. On the other hand, Figure 6-31 shows the same situation but for the cambered case. In this condition, State C represents the initial situation whereas State D accounts for the final one, with the correspondent transverse and vertical deformations, identified as $\Delta X_{\text{TF RIGHT CAMB}}$ and $\Delta Y_{\text{TF RIGHT CAMB}}$ respectively.

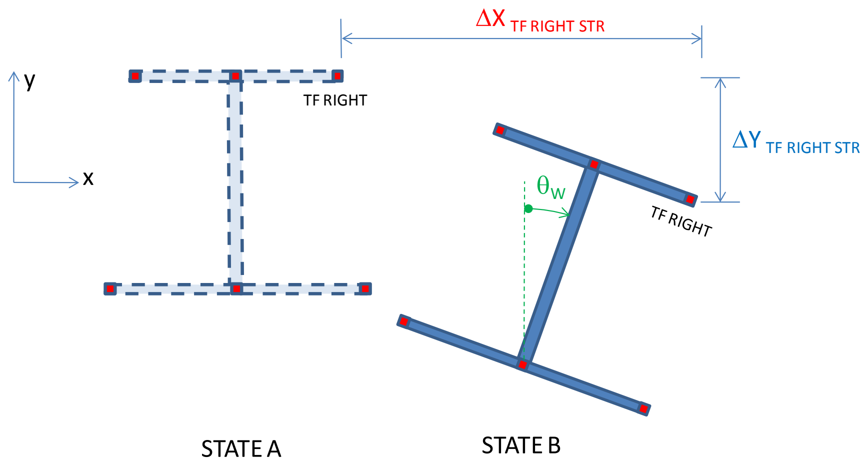

Figure 6-30. Initial (State A) and final (State B) conditions of a cross-section on a straight skewed bridge.

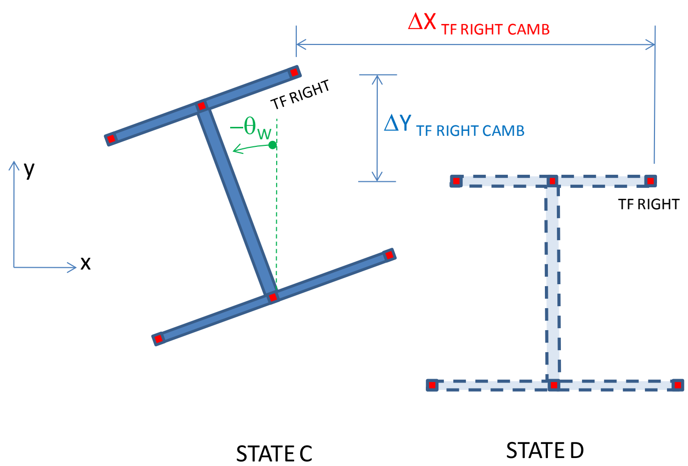

Figure 6-31. Initial (State C) and final (State D) conditions of a cross-section on a cambered skewed bridge

Part of the investigation was focused on determining whether or not the deflections and stresses that take place on the straight case are similar to the ones obtained on the cambered model. Perhaps the most important reason for this has to do with the typical asymmetry of both the plan view and the cross-section view of a skewed bridge. Hence, predictions on the response were not easy and it was required to perform a sensitivity study that could help us in clarifying this issue.

In order to have a better picture of the potential influence of designing the girders specifying a full dead load fit, a parametric analysis was carried out on which the skew angle of one of the bridges was selected as the variable. In this sense, three different skew angles were selected, including the original angle, and the rotational and stress responses were normalized with respect to the non-skewed case.

6.3.3.3 Analysis of Results

Figure 6-32 and Figure 6-33 present what it was found to be the typical stress response obtained when comparing the straight and the cambered cases. In both figures the plotted data represent the stress distribution of the difference between two cases in study for an exterior girder.

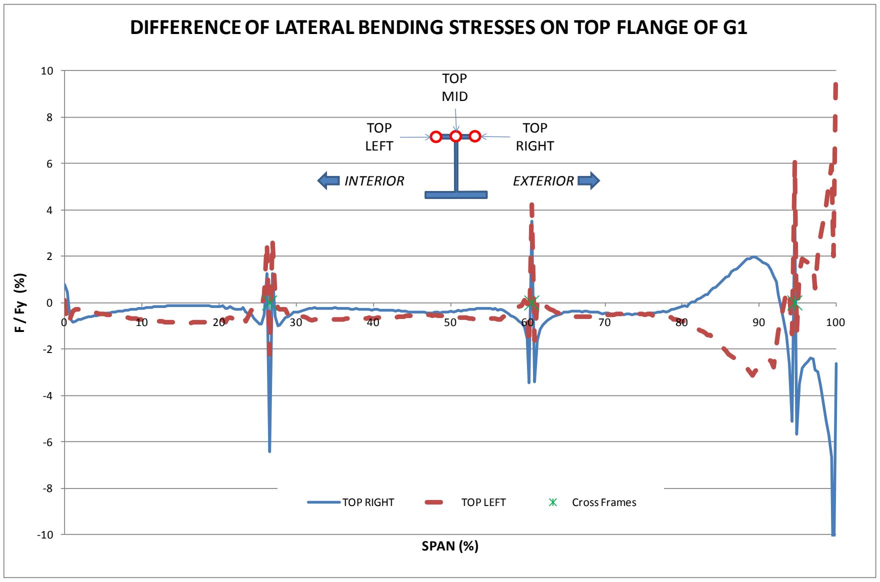

Figure 6-32. Distribution of the difference in stresses on an exterior girder between the cambered and the straight models at the top flange on a 23 degrees skew angle bridge

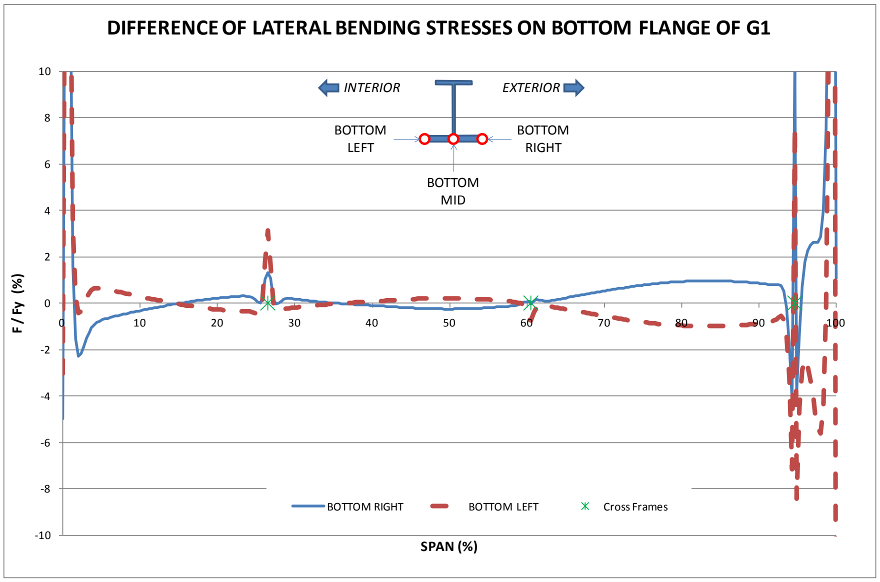

Figure 6-33. Distribution of the difference in stresses on an exterior girder between the cambered and the straight models at the bottom flange on a 23 degrees skew angle bridge.

It can be seen that both behaviors look very similar, in particular along the stable region. In fact, it was found that the maximum stress difference at this region was within ±5 percent for the three skew angles selected on the parametric analysis. In the case of rotations the situation is quite similar. Figure 6-34 and Figure 6-35 depict this condition for two contiguous girders. The dashed line represents the normalized difference obtained from the two cases. As in the stresses distributions, the maximum difference observed was within ±5 percent.

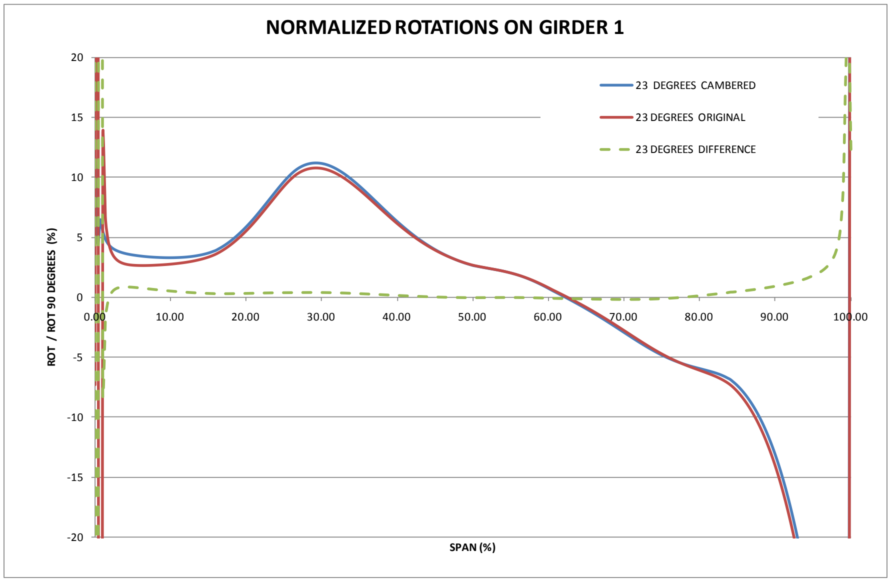

Figure 6-34. Distribution of normalized rotations and their difference for an exterior girder on a 23 degrees skew angle

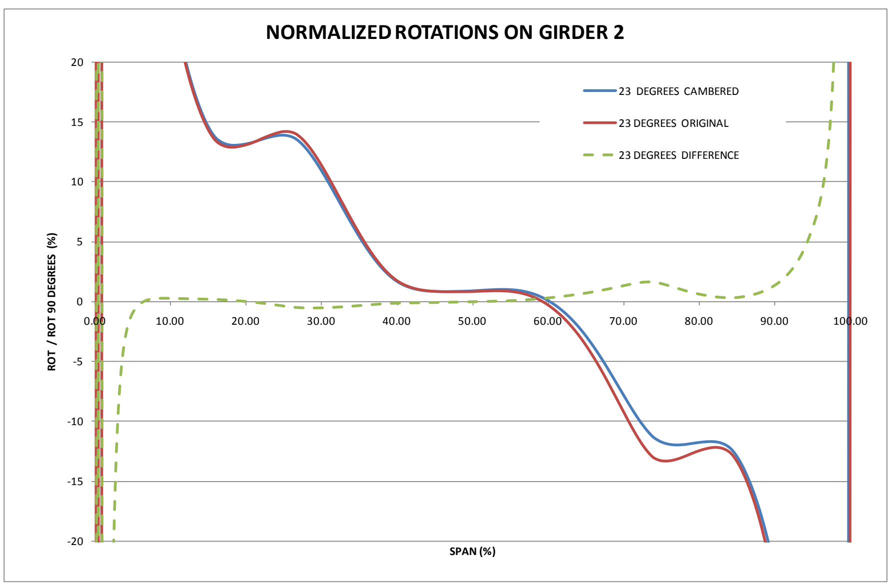

Figure 6-35. Distribution of normalized rotations and their difference for an interior girder on a 23 degrees skew angle.

6.3.4 Pouring Sequence

6.3.4.1 Overview

The issues related to the pouring sequence on steel bridges have been the subject of study in several investigations. The National Cooperative Highway Research Program (NCHRP) (2005) has accounted for this condition through a publication that presented the results of a survey study on the steel bridge erection practices nationwide. Some of the interesting concerns that arose from that study had to do with the pouring sequence practices. As a result, in an effort to address those concerns a parametric analysis was carried out on which the skew angle was selected as the main parameter. The objective was to determine whether or not adopting a different pouring sequence could affect the response of the structures as far as rotations and longitudinal stresses are concerned.

In this sense, the pouring sequence adopted in the investigation only considered the case when the central half of the slab is cast. The reason lays in the fact that it is not only common practice particularly in continuous span steel bridges but also it is highly expectable that rotations and stresses induced by this condition will be close to those obtained from the full dead load. The study incorporated three different skew angles (23, 45 and 75 degrees) and the non-skewed case (90 degrees) for normalization purposes out-of-plane rotations as well as longitudinal stresses were considered as the comparison parameters.

6.3.4.2 Analysis of Results

As it was the case on the Dead Load Fit analysis carried out on section 6.3.3, the normalized rotations and the longitudinal stresses were compared to the correspondent original full load case. By doing this it was possible to have an idea of how sensitive the structure is to changes in the loading scenarios, in this case addressed by the pouring sequence. Figure 6-36 and Figure 6-37 present what was found to be the stress profiles for an exterior girder at both the top and bottom flanges.

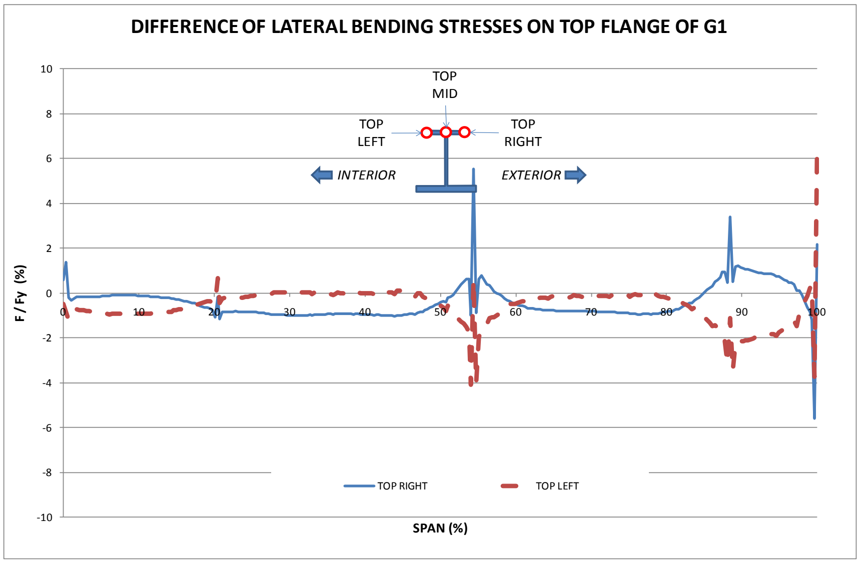

Figure 6-36. Distribution of the difference in LFB stresses on an exterior girder between the pouring sequence adopted and the original model at the top flange on a 45 degrees skew angle bridge.

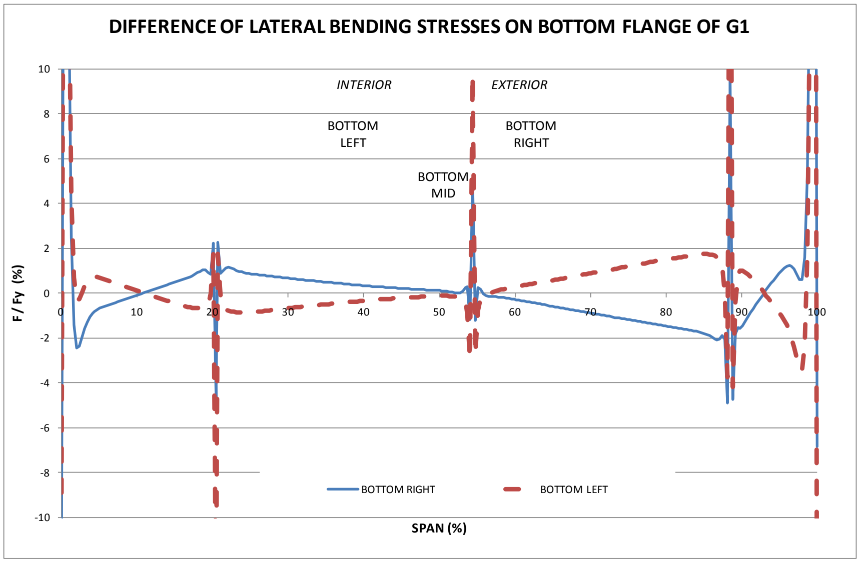

Figure 6-37. Distribution of the difference in LFB stresses on an exterior girder between the pouring sequence adopted and the original model at the bottom flange on a 45 degrees skew angle bridge.

From both previous figures it is apparent that with the exception of the peak values at the cross-frame locations, the difference in stresses is very low. In fact, the maximum stress difference along the stable region was found to be within a ±5 percent for all the three different skew angles considered. This particular behavior highlights the idea that the magnitude of the longitudinal stresses that take place within the girders when concrete is cast on the middle section of the bridge are in the same order of magnitude than those obtained by casting the whole structure. Figure 6-38 shows what it was found to be the average percent reduction in both deflections and rotations when using the proposed pouring sequence. It can be seen that while deflection reduction seems to be constant around 25 percent, rotations reductions tend to be sensitive upon the skew angle. In fact, as the skew angle approaches to 90 the average percent reduction seems to be less. However, we must bear in mind that absolute rotations values for a non-skewed bridge are insignificant, as it was shown before.

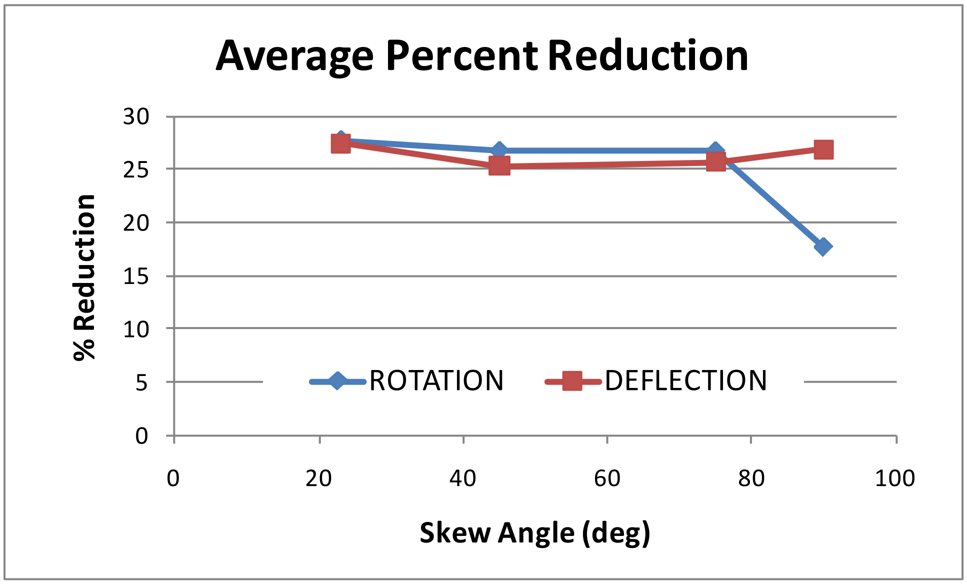

Figure 6-38. Comparison between average percent reduction in deflections and rotations with respect to the original pouring sequence

Although no composite effect was considered throughout this investigation, it is expected that once the middle strip of concrete is poured approximately 75 percent of the total dead load deflections and rotations (for skew angles between 30 and 75 degrees) will be locked in once the concrete hardens. This means that by adopting this proposed pouring sequence significant improvements will be achieved in controlling rotations and deflections resulting from casting the remainder of the slab and therefore it is less likely that the bridge might experience excessive deformations that could lead to other potential problems.

Figure 6-39 and Figure 6-40 show what was found to be the distribution of normalized rotations along the span for an exterior and interior girder respectively, including the difference between them (dashed line). As it was expected, along the stable zone (see Section 7) the difference obtained is almost zero. This, along with the stress distribution already covered, demonstrates that a great deal of the total out-of-plane rotations take place by loading the central zone of the bridge.

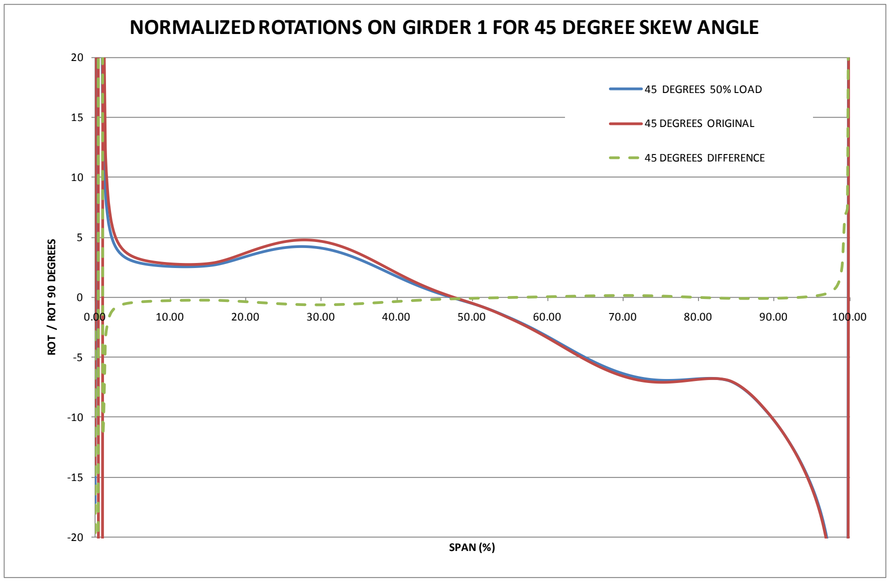

Figure 6-39. Distribution of normalized rotations and their difference for an exterior girder on a 45 degrees skew angle

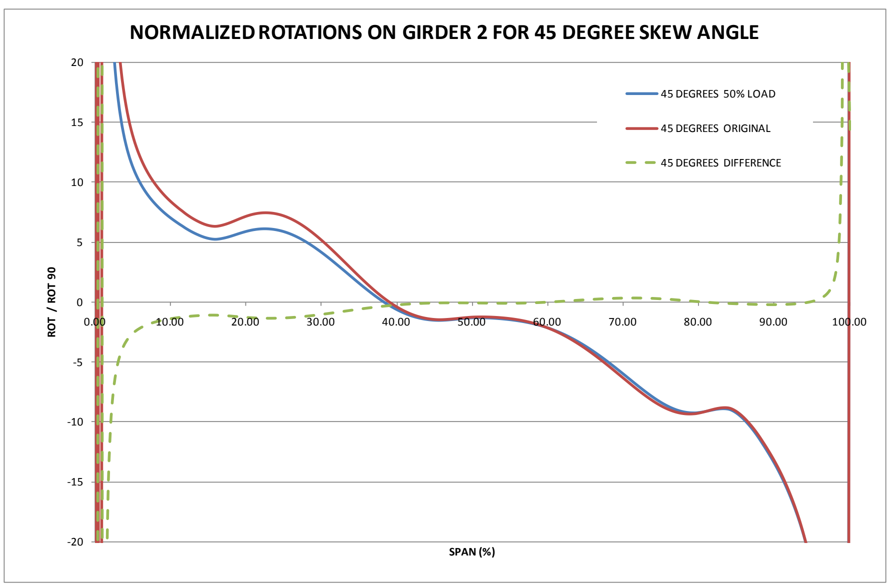

Figure 6-40. Distribution of normalized rotations and their difference for an interior girder on a 45 degrees skew angle.

7.0 LATERAL FLANGE BENDING STRESSES

7.1 General

Current design codes related to structures in the transportation field, such as the AASHTO Guidelines for Design for Constructability (2003), have stated that designers are required to consider the possible effects that differential deflections may have on a bridge structure. Particularly, design codes are concerned with the unexpected issues that might arise due to the lateral flange bending phenomenon typical of skewed bridges with staggered cross-frames. A comprehensive study was conducted to verify and quantify the overall flexural stresses that take place in the flanges under this condition.

In Section 5 of this report it was stated that it seems reasonable to consider the cross-section torsional rotation as a rigid body rotation and therefore consider web rotations as the representation of the overall torsional behavior of the girder. With this assumption it was possible to determine the stress profile due to Lateral flange bending (LFB) for both the top and bottom flanges. It was found that in no case did these stresses exceed 10 percent of the corresponding yield strength, and that the shape of the stress profile was particularly affected by the stress concentrations occurring at the vicinity of the cross-frames and supports.

7.2 Sources of Stress Concentration

Throughout the investigation, and particularly during the three-dimensional finite element modeling phase, the presence of stress concentrations due to either geometric or structural constraints were observed. The locations of the concentrations were identified as the primary sources of variation of the stress results profile. Hence, it was required to characterize these modeling anomalies inherent to the process and make sure they were accurately described during the analysis stage.

7.2.1 Stress concentrations at the End Bents.

The end bents of the girders consisted of a series of shell elements that defined each component of the bridge at this location. These components are the girder flanges and web, the end bent stiffener (or connector), the sole plates, the elastomeric pad, the gusset plates, and the diaphragm. Particular attention must be given to the end connector, which must not carry the load transmitted by the diaphragm but also transfer the typically high forces from the supports across the cross-section of the girder.

Figure 7-1 shows how the stresses flow in the vicinity of the supports. It can be noticed that besides the gusset plates that link the diaphragms to the girders, the highest stress concentrations are located towards the ends of the top and bottom flanges and spread along the span. This was later evidenced in the erratic behavior of the stress profile at the end bent surroundings.

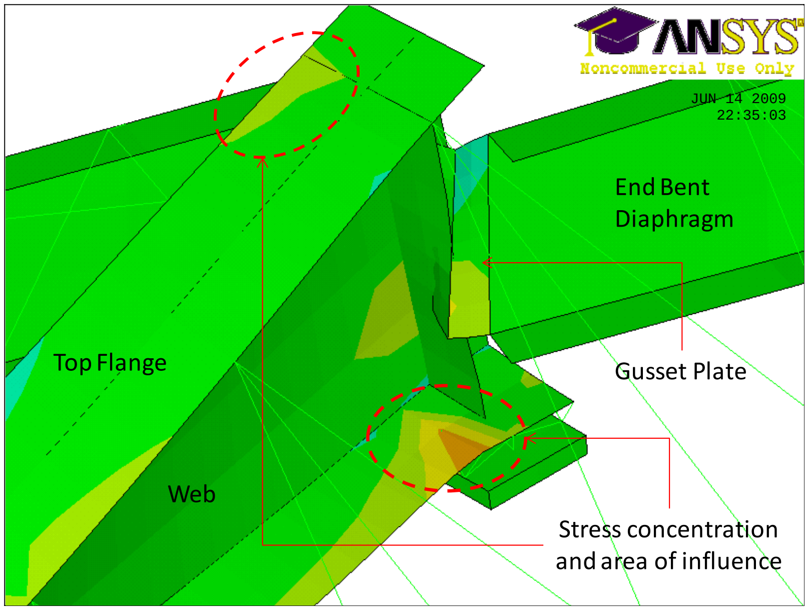

Figure 7-1. Longitudinal stress contours at the end bents.

7.2.2 Stress concentrations at the Intermediate Cross-frames or Diaphragms

The intermediate cross-frames not only have the function of providing adequate lateral bracing to the structure, but also guarantee enough redundancy to distribute forces and stresses throughout the bridge. Hence, it is expected that high stress concentrations will develop at their connections within the superstructure considering they are discretely distributed along the span of the girders. In other words, the flow of forces and moments that are developed continuously along the span of the girder has only a discrete number of locations to get transferred from one girder to the other, leading to an important force flow density at the vicinity of the intermediate connectors. Figure 7-2 depicts this situation. Although the contours do not show a stress variation as important as they were on the end bents, the localized effect of the connectors spreads along the span.

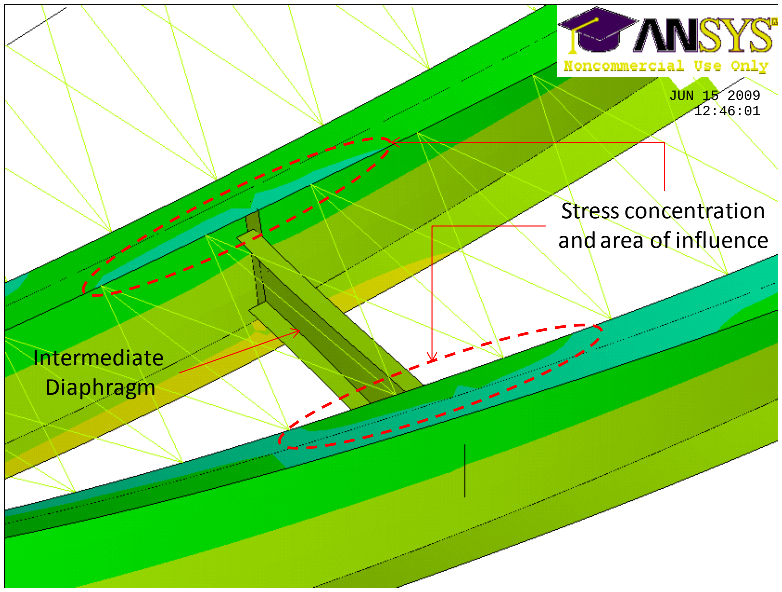

Figure 7-2. Stress concentrations along the span on top and bottom flanges

7.2.3 Other possible sources

Although the previous two conditions seemed to be the most determinant on the stress profile, other possible sources, such as the stay-in-place forms, were observed. However, this particular component did not prove to be crucial in any of the cases included in the analysis and their effect was considered negligible.

7.3 The LFB stress profile

One of the things we must bear in mind when studying the lateral flange bending stress problem is the need to isolate the lateral stress component from the total stresses acting on both the bottom and the top flanges. This means that it is required to identify the two sources of longitudinal stresses that take part in the analysis. From solid mechanics, the total longitudinal stresses that act on a beam subjected to multi-axial loading come from both the web flexure and from the lateral flange flexure.

Figure 7-3 shows a decomposition of the two different stresses acting on the flanges. First the flexural stress coming from the action of moments perpendicular to the plane of the web (M_{web}) and last, but not least, stresses due to moments perpendicular to the plane of the flanges (M_{flange}). In order to determine the stresses due to M_{flange} (σ_{LFB}), solid mechanics tells us the following:

$$\sigma_{LFB} = \sigma_{TOTAL} - \sigma_{WEB} \qquad \textbf{[Eq. 7-1]}$$

where σ_{TOTAL} is the total stress at the point and σ_{WEB} is the stress due to M_{web}.

With this relationship it is possible to determine the actual stress that is caused by the LFB condition.

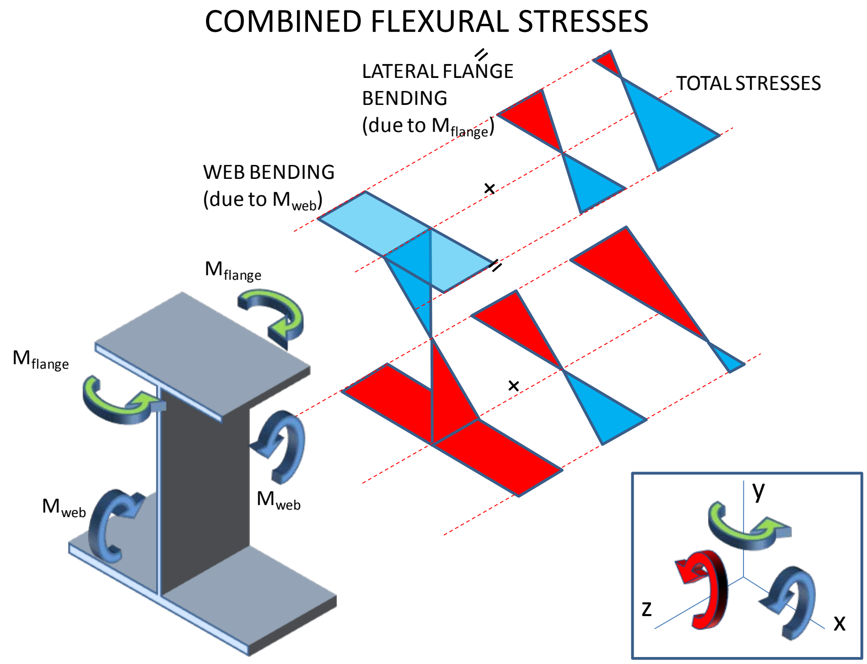

Figure 7-3. Combined Longitudinal stresses on a girder section

Figure 7-4 and Figure 7-5 present what is found to be the typical total stress distribution along the span for an external girder and the corresponding LFB stress profile. It can be noticed the recurrent presence of disturbances evidenced in the peak values for both the top and bottom flanges. For the bottom flange, disturbances were more drastic at the end bents.

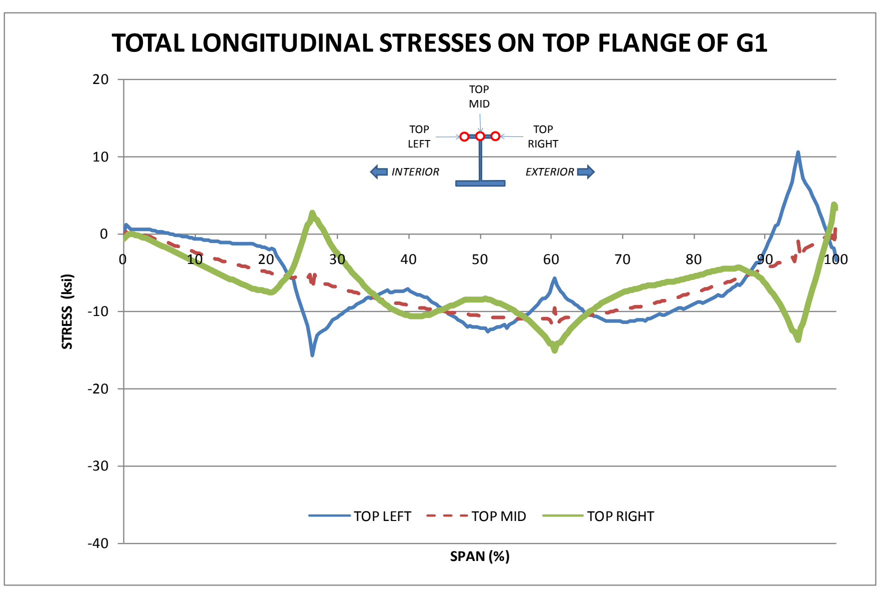

Figure 7-4. Total stress distribution on top flange of an exterior girder

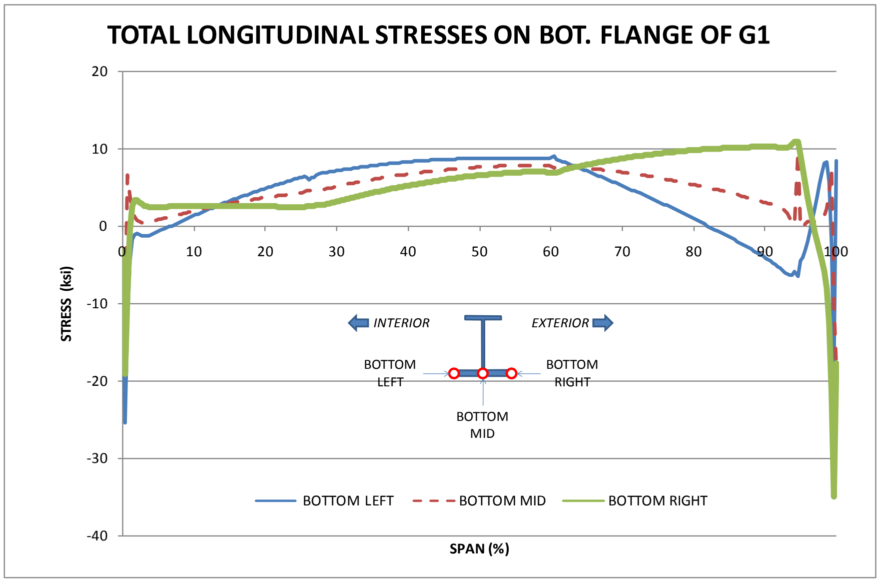

Figure 7-5. Total stress distribution on bottom flange of an exterior girder

When this analysis is carried out on an interior girder, the situation is different. The existence of cross-frames on both sides of the girder has a major influence on the stress response. See Figure 7-6 and Figure 7-7.

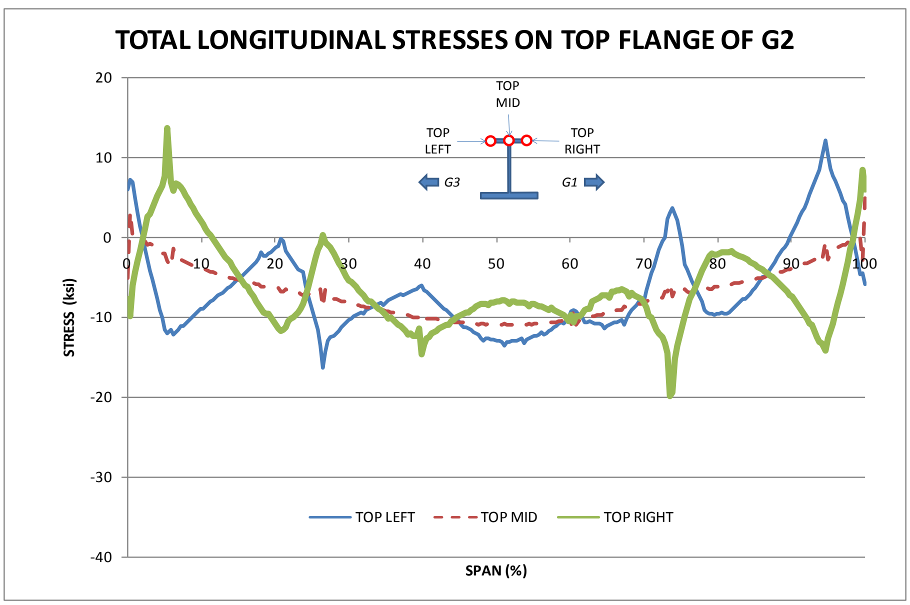

Figure 7-6. Total stress distribution on top flange of an interior girder

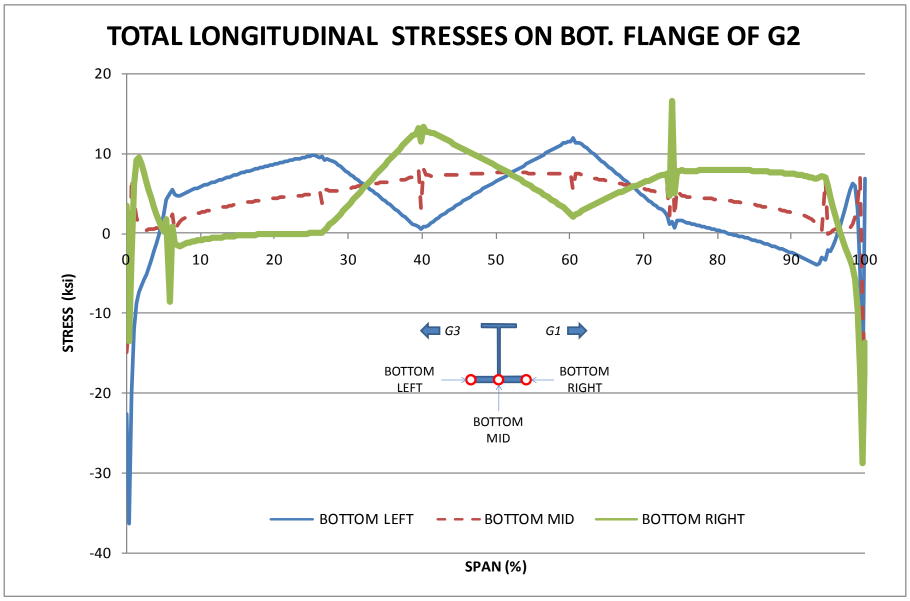

Figure 7-7. Total stress distribution on bottom flange of an interior girder

When the σ_{WEB} element is "filtered" from the total, it is then possible to visualize the σ_{LFB} component.

In order to normalize the results related to LFB stresses the ratios of LFB stress versus the yield stress (F_y) were also monitored, which aid to determine whether the stresses would lie within certain values. The location of the cross-frames along the span was included in order to compare them with the peak values on the stress profile, as it is shown on Figure 7-8 and Figure 7-9 for the exterior girders. Figure 7-10 and Figure 7-11, on the other hand, show what is found to be the general profile for the LFB stresses on an interior girder for both bridges.

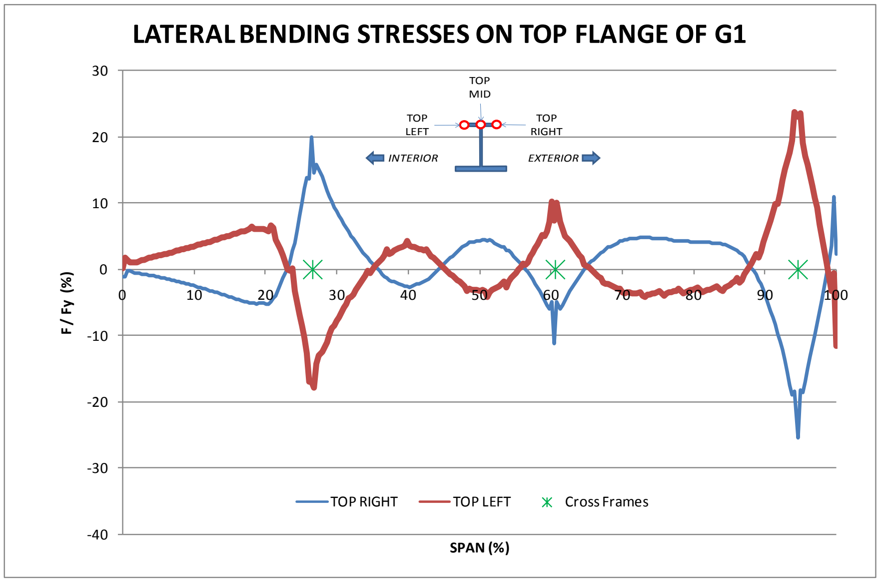

Figure 7-8. Normalized LFB stress profile for on the top flange of an exterior girder

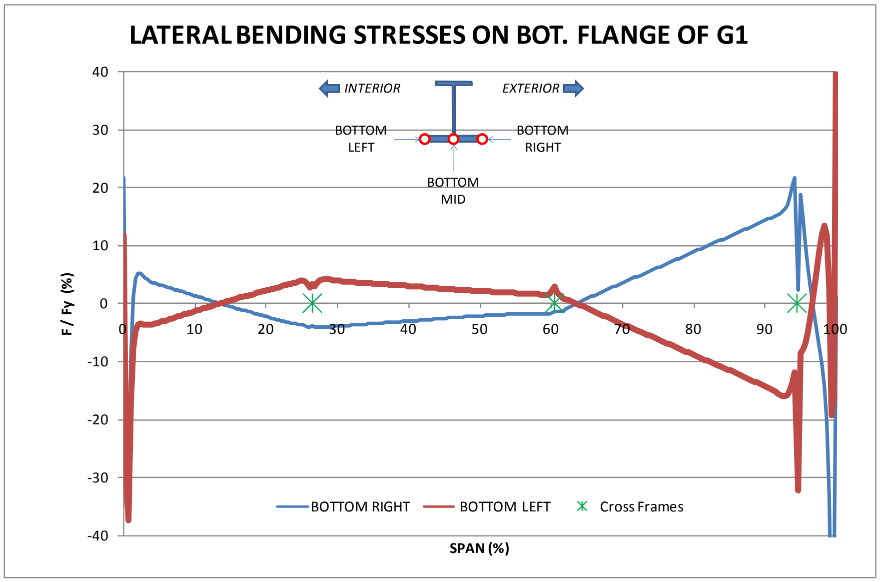

Figure 7-9. Normalized LFB stress profile for on the bottom flange of an exterior girder

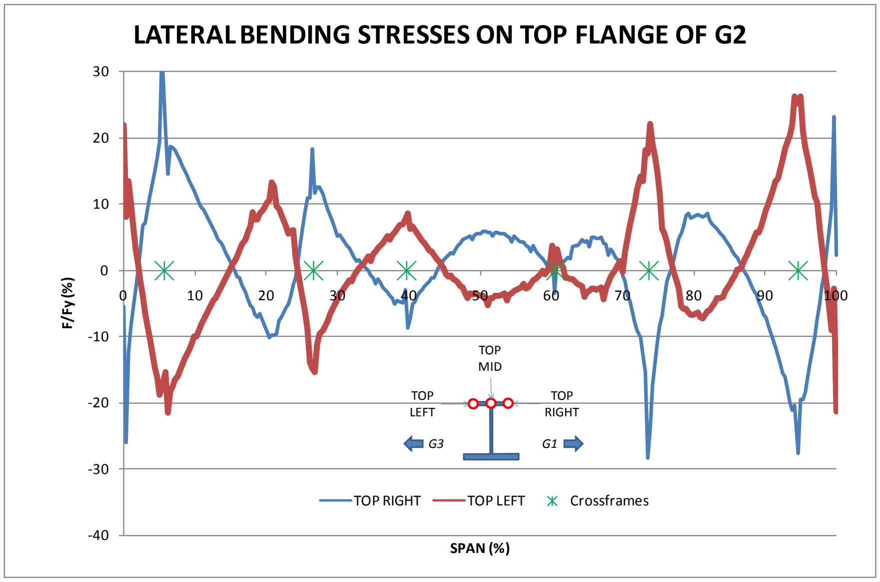

Figure 7-10. Normalized LFB stress profile for on the top flange of an interior girder

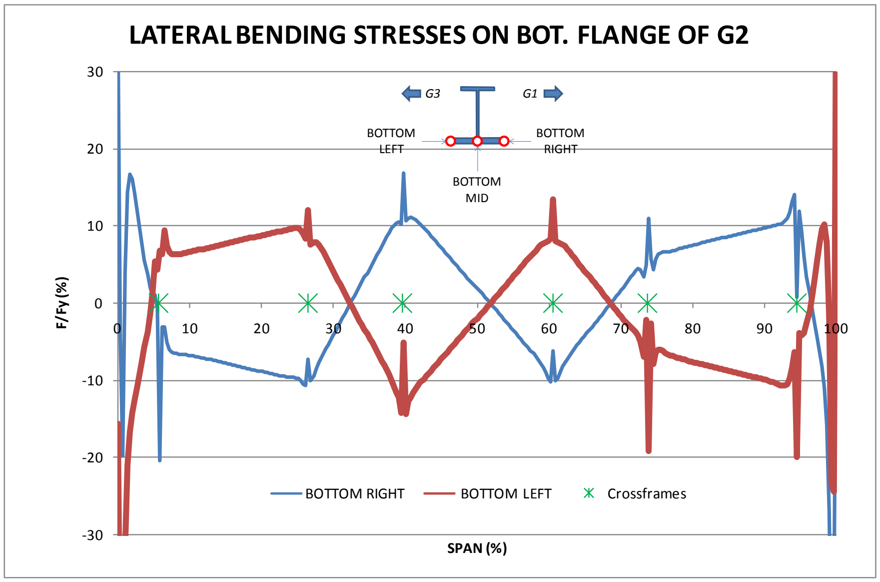

Figure 7-11. Normalized LFB stress profile for on the bottom flange of an interior girder

7.4 LFB stress profile characteristics

From the stress profiles obtained during the investigation it was possible to identify some of the key characteristics of its behavior.

7.4.1 Key Regions

Figure 7-12 shows the two different regions that can be pinpointed. It can be clearly noted a region, typically on the central part of the span in which stresses tend to be less disturbed. This “stable” zone range varies depending on whether we consider the bottom or top flange. Results also show this value is sensitive to the location of the girder in the structure, whether it is an exterior or an interior girder. Table 7-1 presents the values found for this stable range along the span in percent.

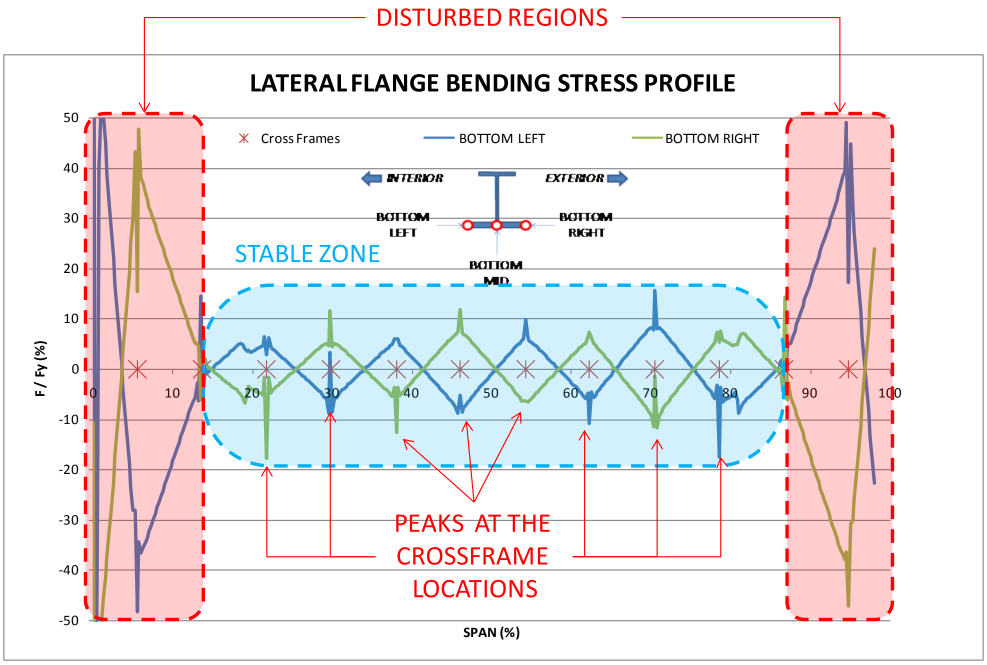

Figure 7-12. Key regions on a typical LFB stress profile

Table 7-1. Bounds for the stable region.

BRIDGE	PARAMETER	GIRDER	BOTTOM FLANGE		TOP FLANGE	
			MIN (%)	MAX (%)	MIN (%)	MAX (%)
Chicken Road	43 deg Skew	G1	25	82	17	88
Chicken Road	43 deg Skew	G2	14	87	16	79
Chicken Road	E-I LOAD 100% (43 deg)	G1	20	77	17	88
Chicken Road	E-I LOAD 100% (43 deg)	G2	20	80	16	79
Chicken Road	E-I INERTIA 2X (43 deg)	G1	20	81	18	88
Chicken Road	E-I INERTIA 2X (43 deg)	G2	21	87	15	84
Roaring Fork	23 deg Skew	G1	13	63	23	87
Roaring Fork	23 deg Skew	G2	7	96	33	70
Roaring Fork	23 deg Skew	G3	5	97	34	64
Roaring Fork	E-I LOAD 100% (23 deg)	G1	14	66	23	87
Roaring Fork	E-I LOAD 100% (23 deg)	G2	6	96	15	86
Roaring Fork	E-I LOAD 100% (23 deg)	G3	6	96	14	86
Roaring Fork	E-I INERTIA 2X (23 deg)	G1	9	47	23	86
Roaring Fork	E-I INERTIA 2X (23 deg)	G2	6	97	44	70
Roaring Fork	E-I INERTIA 2X (23 deg)	G3	6	96	34	66

The case of the disturbed regions shows stress peaks that tend to be higher the closer we get to the supports. This condition evidences the unstable behavior developed close to the supports where stress concentrations seem to be critical. Evidently, the stress values in this region were disregarded as far as the conclusions were concerned, since the accumulation of stress concentration places distort the actual values.

It is worth mentioning that the parameters considered for this analysis were limited to one favorable (Section 6), one neutral, and one unfavorable case in an effort to evaluate the correspondence between the mitigation criteria based upon the rotation profile and the LFB stress profile.

7.4.2 "Locked-in" Stresses due to LFB

As mentioned previously, once the LFB stress profile is determined it is possible to identify the magnitude of these stresses within the stable region. This is particularly important when the time comes to establish the most efficient and adequate mitigation strategy.

It was observed that regardless of the bridge considered there is no indication of a possible trend to determine the locations of these maximum and minimum stress points within the stable region. In some cases they are close to the midspan but in other cases they are towards the ends of the stable zone. However, as far as the stress values are concerned, they proved to be higher on the bottom flange.
Table 7-2 and 7-3 present a summary of the maximum and minimum stresses due to LFB within the stable zone. The values are presented in percent from the yield stress (F/Fy) and the location on the span is also presented as LOC (%). It can be observed that the values lie below 18 percent.

Table 7-2. Summary of Stresses on the Bottom Flange

BRIDGE	PARAMETER	GIRDER	BOTTOM FLANGE			
			LOW STRESS		HIGH STRESS	
			LOC (%)	VALUE (%)	LOC (%)	VALUE (%)
Chicken Road	43 deg Skew	G1	20	**-4**	80	**4**
Chicken Road	43 deg Skew	G2	70	**-9**	71	**8**
Chicken Road	E-I LOAD 100% (43 deg)	G1	20	**-5**	78	**5**
Chicken Road	E-I LOAD 100% (43 deg)	G2	70	**-6**	71	**5**
Chicken Road	E-I INERTIA 2X (43 deg)	G1	20	**-2**	20	**3**
Chicken Road	E-I INERTIA 2X (43 deg)	G2	46	**-6**	46	**5**
Roaring Fork	23 deg Skew	G1	27	**0**	28	**4**
Roaring Fork	23 deg Skew	G2	41	**-11**	40	**11**
Roaring Fork	23 deg Skew	G3	40	**-8**	58	**7**
Roaring Fork	E-I LOAD 100% (23 deg)	G1	15	**-2**	31	**2**
Roaring Fork	E-I LOAD 100% (23 deg)	G2	92	**-5**	7	**6**
Roaring Fork	E-I LOAD 100% (23 deg)	G3	92	**-6**	92	**6**
Roaring Fork	E-I INERTIA 2X (23 deg)	G1	25	**-4**	23	**4**
Roaring Fork	E-I INERTIA 2X (23 deg)	G2	41	**-18**	41	**16**
Roaring Fork	E-I INERTIA 2X (23 deg)	G3	40	**-18**	0	**15**

Table 7-3. Summary of Stresses on the Top Flange

BRIDGE	PARAMETER	GIRDER	TOP FLANGE			
			LOW STRESS		HIGH STRESS	
			LOC (%)	VALUE (%)	LOC (%)	VALUE (%)
Chicken Road	43 deg Skew	G1	34	**-3**	34	**5**
Chicken Road	43 deg Skew	G2	24	**-2**	24	**5**
Chicken Road	E-I LOAD 100% (43 deg)	G1	33	**-2**	33	**5**
Chicken Road	E-I LOAD 100% (43 deg)	G2	24	**-3**	24	**6**
Chicken Road	E-I INERTIA 2X (43 deg)	G1	36	**-4**	36	**4**
Chicken Road	E-I INERTIA 2X (43 deg)	G2	26	**-4**	26	**5**
Roaring Fork	23 deg Skew	G1	20	**-5**	21	**7**
Roaring Fork	23 deg Skew	G2	24	**-8**	24	**8**
Roaring Fork	23 deg Skew	G3	47	**-3**	49	**3**
Roaring Fork	E-I LOAD 100% (23 deg)	G1	41	**-2**	40	**3**
Roaring Fork	E-I LOAD 100% (23 deg)	G2	21	**-6**	21	**6**
Roaring Fork	E-I LOAD 100% (23 deg)	G3	27	**-6**	27	**7**
Roaring Fork	E-I INERTIA 2X (23 deg)	G1	62	**-5**	61	**7**
Roaring Fork	E-I INERTIA 2X (23 deg)	G2	51	**-5**	50	**6**
Roaring Fork	E-I INERTIA 2X (23 deg)	G3	60	**-4**	39	**4**

7.5 LFB stress profile analysis

7.5.1 LFB versus Torsional displacements

One of the questions that arise once the LFB stress profile is known is what determines its behavior. Is it due to the rotational phenomena or not? In order to answer this question the stress profiles were compared to both the LFB rotational and displacement profiles.

In Section 5 it was demonstrated that rigid body motion controls the rotational behavior of the cross-section of the girders particularly in those regions away from the cross-frame connections. Knowing that fact, comparisons were carried out between the total lateral displacement, the lateral displacements due to out-of-plane rotations, and the lateral displacements due to LFB. The reason to do this was to determine what component of the total displacement is the one that agrees with the stress profile.

Figure 7-13 presents one of these comparisons. It reflects the typical behavior for all of the cases studied. Hence, from this comparison it is clearly stated that it is the torsional behavior that seems to control the lateral displacements of the girders of steel skewed bridges.

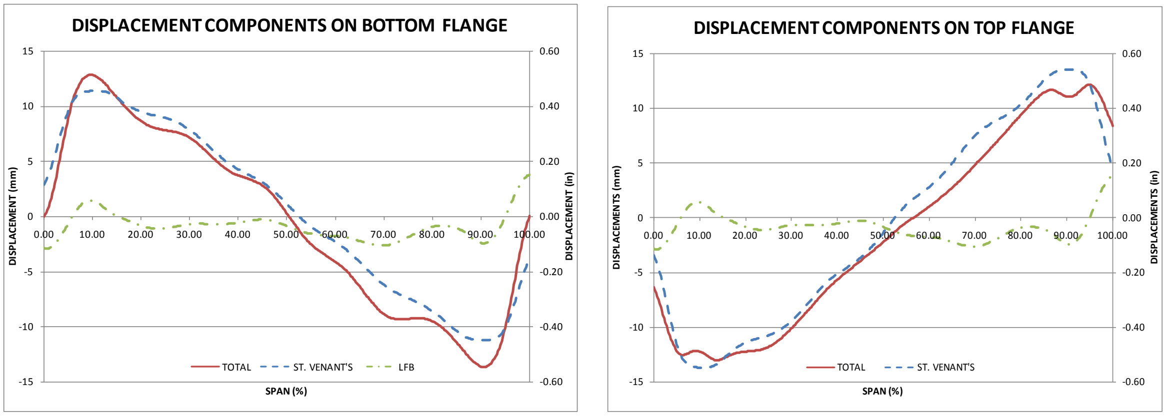

Figure 7-13. Bottom flange (left) and Top flange (right) displacements

Table 7-4 and Table 7-5 present a summary of the peak displacements from the total lateral displacements for both the bottom and top flanges. Likewise, Table 7-6 shows the peak displacements obtained from the LFB displacements profile.

Table 7-4. Summary of Lateral Displacements on the Bottom Flange

BRIDGE	PARAMETER	GIRDER	TOTAL DISPLECEMENTS BOTTOM FLANGE			
			MIN DISPLACEMENT		MAX DISPLACEMENT	
			LOC (%)	VALUE	LOC (%)	VALUE
Chicken Road	43 deg Skew	G1	88	-0.63 in	17	0.47 in
Chicken Road	43 deg Skew	G2	90	-0.54 in	9	0.50 in
Chicken Road	E-I LOAD 100% (43 deg)	G1	17	-0.54 in	88	0.65 in
Chicken Road	E-I LOAD 100% (43 deg)	G2	10	-0.55 in	91	0.57 in
Chicken Road	E-I INERTIA 2X (43 deg)	G1	16	-0.21 in	87	0.31 in
Chicken Road	E-I INERTIA 2X (43 deg)	G2	10	-0.27 in	89	0.24 in
Roaring Fork	23 deg Skew	G1	29	-0.10 in	82	0.30 in
Roaring Fork	23 deg Skew	G2	18	-0.20 in	81	0.20 in
Roaring Fork	23 deg Skew	G3	18	-0.20 in	83	0.20 in
Roaring Fork	E-I LOAD 100% (23 deg)	G1	15	-0.03 in	79	0.20 in
Roaring Fork	E-I LOAD 100% (23 deg)	G2	61	-0.04 in	40	0.07 in
Roaring Fork	E-I LOAD 100% (23 deg)	G3	61	-0.04 in	40	0.07 in
Roaring Fork	E-I INERTIA 2X (23 deg)	G1	14	-0.01 in	74	0.20 in
Roaring Fork	E-I INERTIA 2X (23 deg)	G2	18	-0.02 in	46	0.20 in
Roaring Fork	E-I INERTIA 2X (23 deg)	G3	61	-0.05 in	40	0.08 in

Table 7-5. Summary of Lateral Displacements on the Top Flange

BRIDGE	PARAMETER	GIRDER	TOTAL DISPLACEMENTS TOP FLANGE			
			MIN DISPLACEMENT		MAX DISPLACEMENT	
			LOC (%)	VALUE	LOC (%)	VALUE
Chicken Road	43 deg Skew	G1	94	-0.52 in	14	0.47 in
Chicken Road	43 deg Skew	G2	91	-0.54 in	8	0.49 in
Chicken Road	E-I LOAD 100% (43 deg)	G1	95	-0.50 in	15	0.57 in
Chicken Road	E-I LOAD 100% (43 deg)	G2	94	-0.52 in	14	0.55 in
Chicken Road	E-I INERTIA 2X (43 deg)	G1	94	-0.30 in	35	0.34 in
Chicken Road	E-I INERTIA 2X (43 deg)	G2	94	-0.33 in	26	0.35 in
Roaring Fork	23 deg Skew	G1	95	-0.10 in	30	0.20 in
Roaring Fork	23 deg Skew	G2	91	-13.70 in	10	12.80 in
Roaring Fork	23 deg Skew	G3	92	-0.20 in	8	0.20 in
Roaring Fork	E-I LOAD 100% (23 deg)	G1	15	0.00 in	79	0.20 in
Roaring Fork	E-I LOAD 100% (23 deg)	G2	61	-0.04 in	40	0.07 in
Roaring Fork	E-I LOAD 100% (23 deg)	G3	61	-0.04 in	40	0.07 in
Roaring Fork	E-I INERTIA 2X (23 deg)	G1	14	-0.01 in	74	0.20 in
Roaring Fork	E-I INERTIA 2X (23 deg)	G2	18	-0.02 in	46	0.20 in
Roaring Fork	E-I INERTIA 2X (23 deg)	G3	61	-0.50 in	40	0.08 in

Table 7-6. Summary of LFB Displacements

BRIDGE	PARAMETER	GIRDER	LFB DISPLECEMENTS			
			MIN DISPLACEMENT		MAX DISPLACEMENT	
			LOC (%)	VALUE	LOC (%)	VALUE
Chicken Road	43 deg Skew	G1	87	-0.18 in	18	0.27 in
Chicken Road	43 deg Skew	G2	69	-0.11 in	9	0.06 in
Chicken Road	E-I LOAD 100% (43 deg)	G1	25	-0.08 in	100	0.09 in
Chicken Road	E-I LOAD 100% (43 deg)	G2	15	0.00 in	78	0.01 in
Chicken Road	E-I INERTIA 2X (43 deg)	G1	13	0.00 in	52	0.15 in
Chicken Road	E-I INERTIA 2X (43 deg)	G2	12	-0.03 in	48	0.12 in
Roaring Fork	23 deg Skew	G1	14	-0.02 in	78	0.20 in
Roaring Fork	23 deg Skew	G2	20	-0.02 in	47	0.12 in
Roaring Fork	23 deg Skew	G3	18	-0.04 in	40	0.07 in
Roaring Fork	E-I LOAD 100% (23 deg)	G1	14	-0.02 in	80	0.20 in
Roaring Fork	E-I LOAD 100% (23 deg)	G2	61	-0.04 in	40	0.07 in
Roaring Fork	E-I LOAD 100% (23 deg)	G3	61	-0.04 in	82	0.06 in
Roaring Fork	E-I INERTIA 2X (23 deg)	G1	14	-0.01 in	73	0.20 in
Roaring Fork	E-I INERTIA 2X (23 deg)	G2	19	-0.02 in	46	0.17 in
Roaring Fork	E-I INERTIA 2X (23 deg)	G3	60	-0.04 in	40	0.07 in

7.5.2 LFB stresses versus Torsional displacements.

Throughout the investigation of the LFB stresses on steel skewed bridges it was found, among other things, that from the total lateral displacements, the values that seem to be determinant are those coming from the out-of-plane rotations. To verify this condition both the stress and rotation profiles were compared to determine a possible agreement in the overall behavior that could confirm the original hypothesis of a torsional controlled phenomenon. Figure 7-14 shows what is found to be a typical comparison between the LFB stress profile and the rotation profile.

There can clearly be seen a strong degrees of correspondence between them. Both profiles seem to experience maximum and minimum values within the same regions.

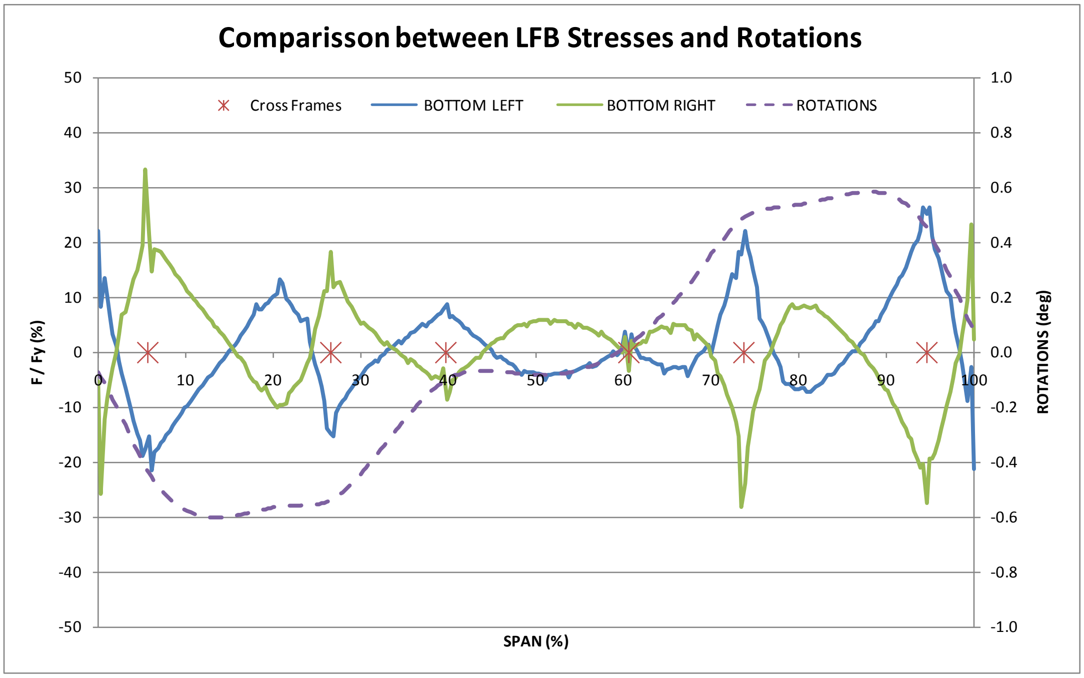

Figure 7-14. LFB stresses versus Rotations on the bottom flange

7.5.3 LFB Stresses versus Skew Angle

The skew angle has proven to be a paramount parameter as far as the structural behavior of steel skewed bridges, with the case of LFB stresses being no exception. Once the stress analysis was finalized on four different skew angles for both bridges, it was possible to evaluate how relevant the skew angle was on the behavior. Figure 7-15 shows this situation for Chicken Road Bridge. Likewise, Figure 7-16 depicts the maximum stress values for Roaring Fork Road Bridge. It can be clearly noticed from both figures that regardless of the bridge in question, the trend suggests that as the skew angle is increased the total stress increases while the LFB stresses decrease. As the values of the skew angle get closer to 90 degrees both behaviors tend to stabilize.

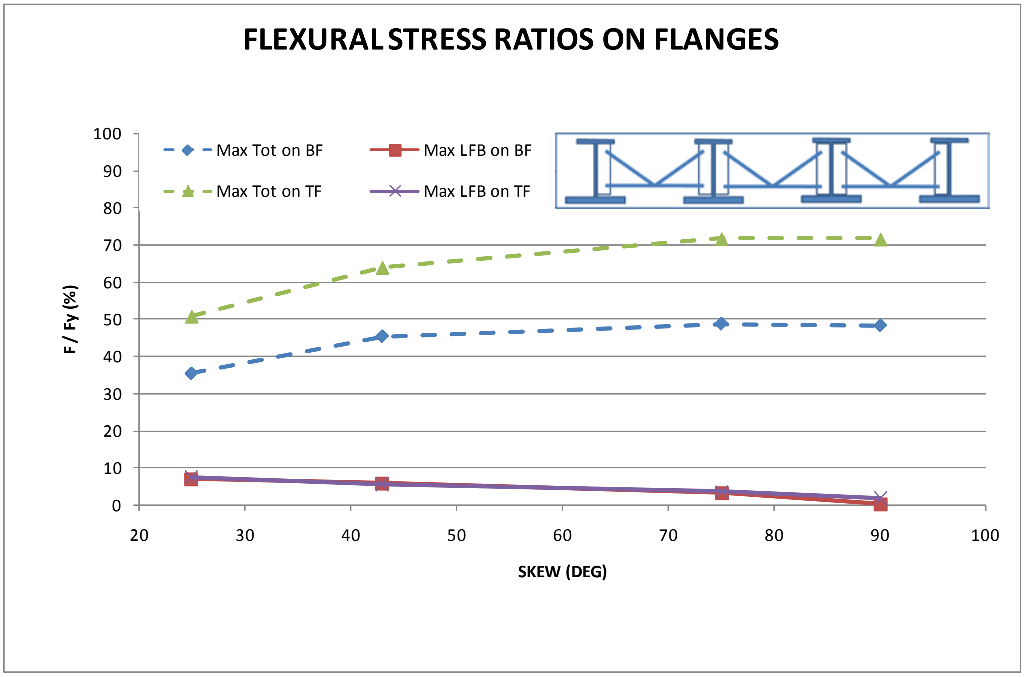

Figure 7-15. Maximum stress values for Chicken Road bridge versus skew angle.

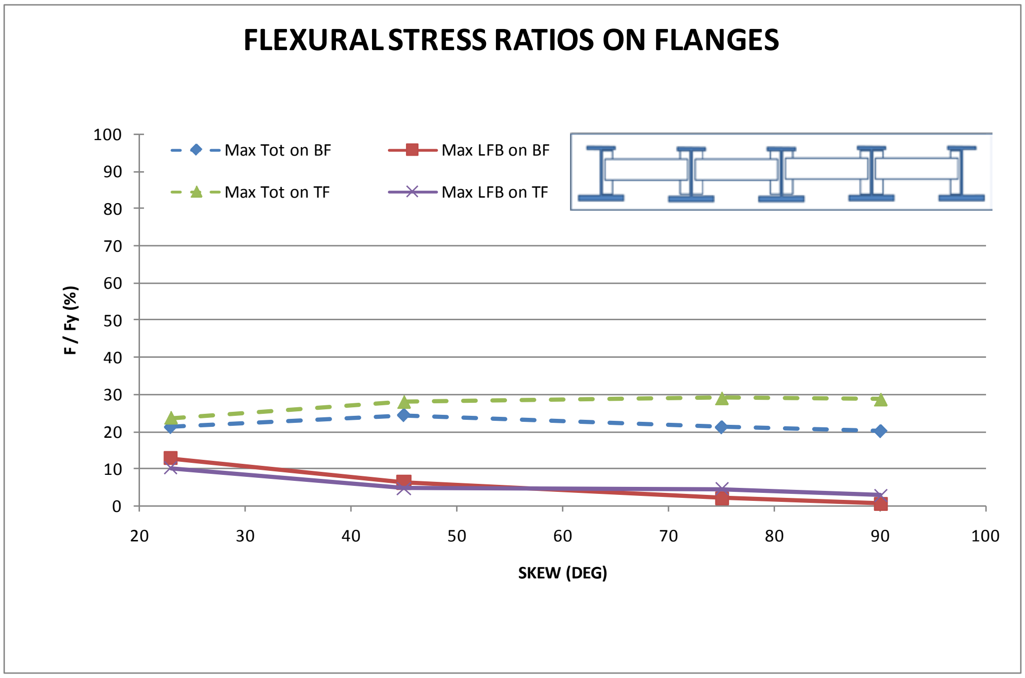

Figure 7-16. Maximum stress values for Roaring Fork Road bridge versus skew angle.

8.0 SUMMARY, OBSERVATIONS, RECOMMENDATIONS AND CONCLUSIONS

8.1 General

This section presents a summary of the present investigation and a review of the most important observations found during this research. In addition, it contains a list of primary recommendations and conclusions related to the lateral flange bending and out-of-plane girder rotations of skewed steel plate girder bridges.

8.2 Summary

The primary objectives of the proposed research are to quantify the lateral flange bending of steel plate girders in heavily skewed bridges, develop a methodology for predicting the magnitude of lateral translation of the girder flanges due to this effect, and establish recommended strategies for mitigating the effect of heavy skew. To achieve these objectives an extensive literature review was carried out and presented in Section 2. The review was classified into four major categories, construction issues, parametric studies, steel bridge studies and NCSU / NCDOT related studies. Some of the most advanced research approaches and techniques were carefully selected through the literature review stage and adopted to develop the current limited knowledge.

Section 3 summarizes all the steps adopted through the field investigation during the construction process, including the instrumentation and procedures utilized in order to validate the numerical techniques required to develop the investigation. Section 4 presents the finite element modeling approach taken to develop a reliable and accurate model that could serve as a useful tool to characterize the behavior of the steel skewed bridges. This included the model evolution necessary to determine that most suitable approach for the level of accuracy required.

As a result of the analytical investigation it was possible to identify trends on the bridge response with respect to out-of-plane rotations. Section 5 presents these findings acknowledging that it is possible to predict the response by means of simplified model. Section 6 represents the main analytical phase of the research. A total of eight numerical and four non-numerical parameters were incorporated. For most of them variations included changes in the parameter itself combined with changes in the skew angle for the two bridges leading to more than 180 cases studied. The out-of-plane rotations and corresponding lateral flange bending stresses were monitored throughout the parametric study.

8.3 Observations

Following will be presented the most important observations related to field measurements and finite element modeling that were found throughout this investigation.

- The torsional rotation phenomenon is not random and can be accurately predicted using three-dimensional finite element modeling.

- The results of the finite element modeling were improved by improving the original finite element model through the inclusion of additional structural details and the use of higher order elements in some locations. The final finite element model accounted for the effect of parameters that were not considered on previous investigations such as elastomeric pads, gusset plates, bolts, etc.

- With the exception of the end bent and the vicinity of the cross-frames connection locations, the girders cross-sections behave in a rigid body fashion. The differences in rotation between flanges and web were less than ten percent, hence they are considered negligible.

- The field measured rotations for Chicken Road Bridge matched the rotations obtained from the finite element model. However, for Roaring Fork Road Bridge, this observation cannot be stated with the same degree of certainty due to the site constraints that led to a lack of enough rotation readings along the span of each girder.

- The location of the inflection point along the span can be predicted with relatively high accuracy. This can be achieved by means of a linear equation that is a function of the bridge skew angle.

- The parametric analysis for the numerical parameters provided the necessary information to classify the results into three groups. The first group contains the unfavorable cases, the second group related to the neutral cases, and the third group dealt with the favorable cases.

- The presence of cross-frames on the end bents as well as along the span produces stress concentrations at the top and bottom flanges.

- The total longitudinal stress in the girder flanges is a combination of those coming from the web flexure and those from the lateral flange bending.

8.4 Recommendations

Based on the findings presented in this report, the following mitigation strategies are recommended to decrease the out-of-plane girder rotations and the lateral flange bending stresses.

- Use X-type of cross-frames instead of K-type.
- Increase the torsional stiffness of the exterior bridge girders.
- Reduce the width of the bridge deck overhang.
- Consider using cross-frames laid out perpendicular to the girders and aligned with each other. Cross-frames aligned to the abutments rendered the best results. However, due to

the difficulties related to construction and erection for the particular configuration in heavily skewed bridges, it may be convenient to use the aforementioned alternative.

- Increase the number of cross-frames.

8.5 Conclusions

After analyzing all the information obtained from the field and the modeling processes, it was possible to develop the following conclusions:

- Vertical girder deflections can be accurately predicted as a function of the skew angle and other parameters.
- The out-of-plane (torsional) rotation of the girders in skewed steel plate girder bridges can be accurately predicted.
- The locations along the span of the girders of the maximum and minimum rotations and the inflection point are a function of the bridge skew. These values were found to be approximately 20 percent span from each end for the minimum and maximum rotations and near 50 percent span for the inflection point.
- The mid-segment slope of the simplified model can be estimated with a linear equation that is dependent on the bridge skew angle.
- The lower and upper bounds of the simplified model can be determined by considering amplitude of two standard deviations.
- The effects of the parameters selected for analysis turned out to be skew dependent. Hence, the affect of the bridge skew could not be isolated from the rest of the parameters, particularly during the comparison process.
- The unfavorable numerical parameters variations were found to be the increase of exterior-to-interior load ratio, decrease in the stiffness of the stay-in-place metal deck forms,.
- The neutral parameters variations were the number of girders, the increase or decrease in the stiffness of the stay-in-place metal deck forms, and either to increase or to decrease the overall stiffness of the cross-frames.
- The favorable variations were found to be the increase of either the exterior girders or the interior girders moments of inertia, increase the number of cross-frames, and increase the number of transverse stiffeners along the span.
- The X-type of cross-frames yielded the best results as far as controlling the girder's out-of-plane (torsional) rotations.

- Laying the cross-frames aligned and perpendicular to the girders produced the highest forces and as the skew angle changes towards the non-skewed condition these forces tend to decrease regardless of the cross-frame layout adopted.

- Determining the stresses and rotations from a finite element model that considers straight girders seems to mach to the stresses and rotations from the cambered structure. This suggests that to account for the dead load fit, rotations can be predicted using models with straight girders.

- The pouring sequence on which the concrete is cast on the central half of the bridge produced similar stresses and rotations to those obtained from the full load case, suggesting it does not enhance the response of the structure.

- The disturbed zone on the LFB stress profile is on average along the first 20 percent of the span at each end of the girder.

- The maximum LFB stress found was 18 percent on the bottom flange whereas the maximum value observed on the top flange was 8 percent.

- The skew angle proved to be a dominant parameter on the LFB behavior. It was shown that as it is changed from high values to 90 degrees, the total stresses increase but the LFB stresses decrease, up to a point that at 90 degrees skew their values are negligible.

8.6 Future Research

It is recommended that additional bridges be incorporated into the future studies of lateral flange bending to decrease the variability of the results. In addition, the investigation of lateral flange bending in continuous span bridges is recommended.

REFERENCES

AASHTO LRFD Bridge Design Specifications (2004). Published by the *American Association of State Highway and Transportation Officials*. Third Edition. ISBN: 1-56051-250-4. Publication Code: LRFDUS-3.

AASHTO/NSBA (2003). *Guidelines for Design for Constructability, G 12.1-2002, Draft for Ballot*, American Association of State Highway and Transportation Officials/National Steel Bridge Alliance.

Akay, H.U. Johnson, C.P., Will, K.M. (1977) "Lateral and Local Buckling of Beams and Frames" *Journal of the Structural Division*, ASCE, ST9, September, pp. 1821-1832

Bakht, B. (1988). "Analysis of Some Skew Bridges as Right Bridges," *Journal of Structural Engineering*, ASCE, 114(10), 2307-2322

Beckmann and Medlock (2005). "Skewed Bridges and Girder Movements Due to Rotations and Differential Deflections", *Proceeding 2005 World Steel Bridge. Symposium and Workshops. November 29 – December 2.*

Berglund, E.M., Schultz, A.E. (2006)."Girder Differential Deflection and Distortion-Induced Fatigue in Skewed Steel Bridges, *Journal of Bridge Engineering*, ASCE, 11(2), 169-177

Bishara, A.G., Elmir, W.E. (1990). "Interaction Between Cross-frames and Girders," *Journal of Structural Engineering*, ASCE, 116(5), 1319-1333.

Bishara, A.G. (1993). "Cross-frames Analysis and Design," *FHWA/OH-93/004*, Federal Highway Administration, Washington, D.C. and Ohio Department of Transportation, Columbus, OH.

Brockenbrough, R.L. (1986). "Distribution Factors for Curved I-Girder Bridges," *Journal of Structural Engineering*, ASCE, 112(10), 2200-2215.

Burke Jr, Martin P.(1983) "Abnormal Rotations of Skewed and Curved Bridges" *Transportation Research Record. Transportation Research Board. Issue 903, 59-64.*

Choo, K.M, (1987) "Buckling Program BASP for Use on a Microcomputer", Thesis presented to The University of Texas at Austin, May.

Choo, T.W., Linzell, D.G., Lee, J.I., Swanson, J.A. (2005). "Response of Continuous, Skewed, Steel Bridge during Deck Placement," *Journal of Construction Steel Research*, Science Direct, N° 61. 567-586.

Chung, W., Sotelino, E.D. (2005). “Nonlinear Finite-Element Analysis of Composite Steel Girder Bridges,” Journal *of Structural Engineering*, ASCE, 131(2), 304-313.

Currah, R.M. (1993). “Shear Strength and Shear Stiffness of Permanent Steel Bridge Deck Forms,” M.S. Thesis, Department of Civil Engineering, University of Texas, Austin, TX

Ebeido, T., Kennedy, J.B. (1995). “Shear Distribution in Simply Supported Skew Composite Bridges,” *Canadian Journal of Civil Engineering*, National Research Council of Canada, 22(6), 1143-1154.

Ebeido, T., Kennedy, J.B. (1996). “Girder Moments in Simply Supported Skew Composite Bridges,” *Canadian Journal of Civil Engineering*, National Research Council of Canada, 23(4), 904-916.

Egilmez, O.O., Jetann, C.A., Helwig, T.A. (2003). “Bracing Behavior of Permanent Metal Deck Forms,” *Proceedings of the Annual Technical Session and Meeting*, Structural Stability Research Council

Egilmez, O.O., Helwig, T.A, (2004) “Buckling Behavior of Steel Bridge Girders Braced with Permanent Metal Deck Forms” *Proceedings of the Annual Technical Session and Meeting,* Structural Stability Research Council

Egilmez, O.O., Helwig, T.A, Herman, H. (2005) “Strength of Metal Deck Forms Used for Stability Bracing of Steel Bridge Girders” *Proceedings of the Annual Technical Session and Meeting,* Structural Stability Research Council

Egilmez, O.O., Helwig, T.A., Herman, R. (2006). “Stiffness Requirements for Metal Deck Forms Used for Stability Bracing of Steel Bridge Girders,” *Proceedings of the Annual Technical Session and Meeting,* Structural Stability Research Council

Egilmez, O.O., Helwig, T.A., Jetann, C.A., Lowery, R. (2007). “Stiffness and Strength of Metal Bridge Deck Forms” *Journal of Bridge Engineering*, ASCE, 12(4), 429-437

Fisher, S.T. (2005). “Measurement and Finite Element Modeling of the Non- Composite Deflections of Steel Plate Girder Bridges,” M.S. Thesis, Department of Civil, Construction and Environmental Engineering, North Carolina State University, Raleigh, NC.

Fu, K.C., Lu, F. (2003). “Nonlinear Finite-Element Analysis for Highway Bridge Superstructures,” *Journal of Bridge Engineering*, ASCE, 8(3), 173-179.

Gupta, Y.P., Kumar, A. (1983). “Structural Behaviour of Interconnected Skew Slab-Girder Bridges,” *Journal of the Institution of Engineers (India), Civil Engineering Division*, 64, 119-124.

Helwig, T. (1994). “Lateral Bracing of Bridge Girders by Metal Deck Forms,” Ph.D. Dissertation, Department of Civil Engineering, The University of Texas at Austin, Austin, TX.

Helwig, T., Wang, L. (2003). “Cross-Frame and Diaphragm Behavior for Steel Bridges with Skewed Supports,” *Research Report No. 1772-1, Project No. 0-1772*, Department of Civil and Environmental Engineering, University of Houston, Houston, TX.

Herman, R; Helwig, T; Holt, J; Medlock, R; Romage, M; Zhou, C. (2005) “Lean-on Cross-frame bracing for steel girders with skewed supports,” *Proceeding 2005 World Steel Bridge. Symposium and Workshops. November 29 – December 2.*

Hilton, M.H. (1972). “Factors Affecting Girder Deflections During Bridge Deck Construction,” *Highway Research Record*, HRB, 400, 55-68.

Huang, H., Shenton, H.W., Chajes, M.J. (2004). “Load Distribution for a Highly Skewed Bridge: Testing and Analysis,” *Journal of Bridge Engineering*, ASCE, 9(6), 558-562.

Jetann, C.A., Helwig, T.A., Lowery, R. (2002). “Lateral Bracing of Bridge Girders by Permanent Metal Deck Forms,” *Proceedings of the Annual Technical Session and Meeting*, Structural Stability Research Council.

Jofriet, J. C., and McNeice, G. M. (1971). “Finite element analysis of reinforced concrete slabs.” *Journal of the Structural Division, ASCE*, 97(3), 785–806.

Kathol, S., Azizinamini, A., and Luedke, J. (1995). “Strength capacity of steel girder bridges.” *Nebraska Department of Roads (NDOR) Research Project No. RES1 90099*, Nebraska Department of Roads, Lincoln, NE.

Mabsout, M.E., Tarhini, K.M., Frederick, G.R., Tayar, C. (1997a). “Finite-Element Analysis of Steel Girder Highway Bridges,” *Journal of Bridge Engineering*, ASCE, 2(3), 83-87.

Mabsout, M.E., Tarhini, K.M., Frederick, G.R., Kobrosly, M. (1997b). “Influence of Sidewalks and Railings on Wheel Load Distribution in Steel Girder Bridges,” *Journal of Bridge Engineering*, ASCE, 2(3), 88-96.

Mabsout, M.E., Tarhini, K.M., Frederick, G.R., Kesserwan, A. (1998). “Effect of Continuity on Wheel Load Distribution in Steel Girder Bridges,” *Journal of Bridge Engineering*, ASCE, 3(3), 103-110.

Morera, F. (2010) “Lateral Flange Bending in Heavily Skewed Steel Bridges” Ph.D. Dissertation. Department of Civil, Construction and Environmental Engineering, North Carolina State University, Raleigh, NC.

Muscarella, J.V., Yura, J.A (1995) " An experimental study of elastomeric bridge bearings with design recommendations" Texas DOT. *Research Report 1304-3.* Research and Technology Transfer Office, TX

National Cooperative Highway Research Program (NCHRP) (2005). "Steel Bridge Erection Practices: A Synthesis of Highway Practice" Synthesis 345. *Transportation Research Board*, Washington D.C.

Norton, E.K. (2001). "Response of a Skewed Composite Steel-Concrete Bridge Floor System to Placement of Deck Slab," M.S. Thesis Proposal, Department of Civil and Environmental Engineering, The Pennsylvania State University, University Park, PA.

Norton, E.K., Linzell, D.G., Laman, J.A. (2003). "Examination of Response of a Skewed Steel Bridge Superstructure During Deck Placement," *Transportation Research Record 1845,* Transportation Research Board, Washington D.C.

Paoinchantara, N. (2005). "Measurement and Simplified Modeling Method of the Non-Composite Deflections of Steel Plate Girder Bridges," M.S. Thesis, Department of Civil, Construction and Environmental Engineering, North Carolina State University, Raleigh, NC.

Sahajwani, K. (1995). "Analysis of Composite Steel Bridges With Unequal Girder Spacings," M.S. Thesis, Department of Civil and Environmental Engineering, University of Houston, Houston, TX.

Samaan, M., Sennah, K., Kennedy, J.B. (2002). "Distribution of Wheel Loads on Continuous Steel Spread-Box Girder Bridges," *Journal of Bridge Engineering*, ASCE, 7(3), 175-183.

Schilling, C.G. (1982). "Lateral-Distribution Factors for Fatigue Design," *Journal of the Structural Division*, ASCE, 108(ST9), 2015-2033.

Sennah, K. M., and Kennedy, J. B. (1998). ''Shear distribution in simply supported curved composite cellular bridges.'' *Journal of Bridge Engineering,* ASCE 3(2), 47–55.

Sennah, K. M., and Kennedy, J. B. (1999).''Load distribution factors for composite multicell box girder bridges.'' *Journal of Bridge Engineering,* ASCE 4(1), 71–78.

Shi, J. (1997). "Brace Stiffness Requirements of Skewed Bridge Girders," M.S. Thesis, Department of Civil and Environmental Engineering, University of Houston, Houston, TX

Soderberg, E.G. (1994). "Strength and Stiffness of Stay-in-Place Metal Deck Form Systems," M.S. Thesis, Department of Civil Engineering, University of Texas, Austin, TX.

Swett, G.D. (1998). “Constructability Issues With Widened and Stage Constructed Steel Plate Girder Bridges,” M.S. Thesis, Department of Civil and Environmental Engineering, University of Washington, Seattle, WA.

Swett, G.D., Stanton, J.F., Dunston, P.S. (2000). “Methods for Controlling Stresses and Distortions in Stage-Constructed Steel Bridges,” *Transportation Research Record 1712*, Transportation Research Board, Washington D.C.

Tabsh, S., Sahajwani, K. (1997). “Approximate Analysis of Irregular Slab-on-Girder Bridges,” *Journal of Bridge Engineering*, ASCE, 2(1), 11-17.

Tarhini, K.M., Frederick, G.R. (1992). “Wheel Load Distribution in I-Girder Highway Bridges,” *Journal of Structural Engineering*, ASCE, 118(5), 1285-1294.

Whisenhunt, T.W. (2004). “Measurement and Finite Element Modeling of the Non- Composite Deflections of Steel Plate Girder Bridges,” M.S. Thesis, Department of Civil,Construction and Environmental Engineering, North Carolina State University, Raleigh, NC.

Yam, L. C. P., and Chapman, J. C. (1972). ‘‘The inelastic behavior of continuous composite beams of steel and concrete.’’ *Proceedings, Inst. Civ.Eng., Struct. Build.*, 53, 487–501.

Yura, J. A. (1993), “Fundamentals of Beam Bracing”, *Proceedings, Structural Stability Research Council Conference*, “ Is Your Structure Suitably Braced?”.Milwaukee

Yura, J. A (1999) “Bracing for Stability – State-of-the-Art”. From the material of “Bracing for Stability” sponsored by American Institute of Steel Construction and Structural Stability Research Council.

APPENDICES

APPENDIX A

ANSYS Model Generation Program Flowchart.

This appendix contains a flow chart outlining the computational program developed using a Visual Basic 6.0™ Software platform to automate the model generation for the parametric analysis of skewed steel plate girder bridges.

This flowchart summarizes all the important steps that were taken in order to develop a comprehensive computational program to generate the input text files utilized by ANASYS to create the models. It was developed including many different features such as the capability of selecting the type of cross-frame or diaphragm, the number of girders, the skew angle, the girder spacing, etc. in such a way that the average time for creating one model from scratch was 4 minutes.

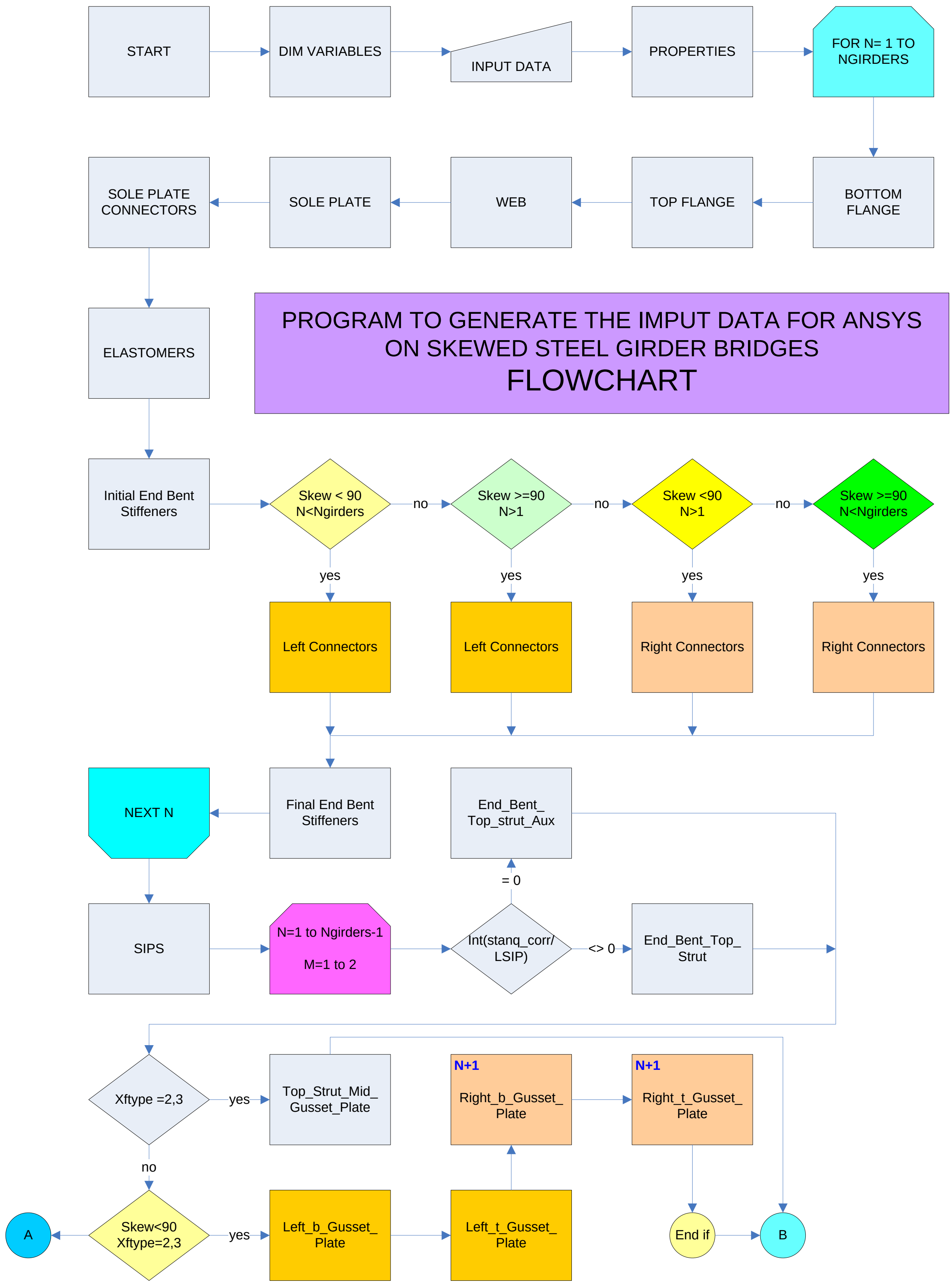
START
DIM VARIABLES
INPUT DATA
PROPERTIES
FOR N= 1 TO NGIRDERS
BOTTOM FLANGE
TOP FLANGE
WEB
SOLE PLATE
SOLE PLATE CONNECTORS
ELASTOMERS
PROGRAM TO GENERATE THE IMPUT DATA FOR ANSYS ON SKEWED STEEL GIRDER BRIDGES
FLOWCHART
Initial End Bent Stiffeners
Skew < 90 N<Ngirders
no
Skew >=90 N>1
no
Skew <90 N>1
no
Skew >=90 N<Ngirders
yes
yes
yes
yes
Left Connectors
Left Connectors
Right Connectors
Right Connectors
NEXT N
Final End Bent Stiffeners
End_Bent_ Top_strut_Aux
= 0
SIPS
N=1 to Ngirders-1
M=1 to 2
Int(stanq_corr/ LSIP)
<> 0
End_Bent_Top_ Strut
Xftype =2,3
yes
Top_Strut_Mid_ Gusset_Plate
N+1
Right_b_Gusset_ Plate
N+1
Right_t_Gusset_ Plate
no
A
Skew<90 Xftype=2,3
yes
Left_b_Gusset_ Plate
Left_t_Gusset_ Plate
End if
B

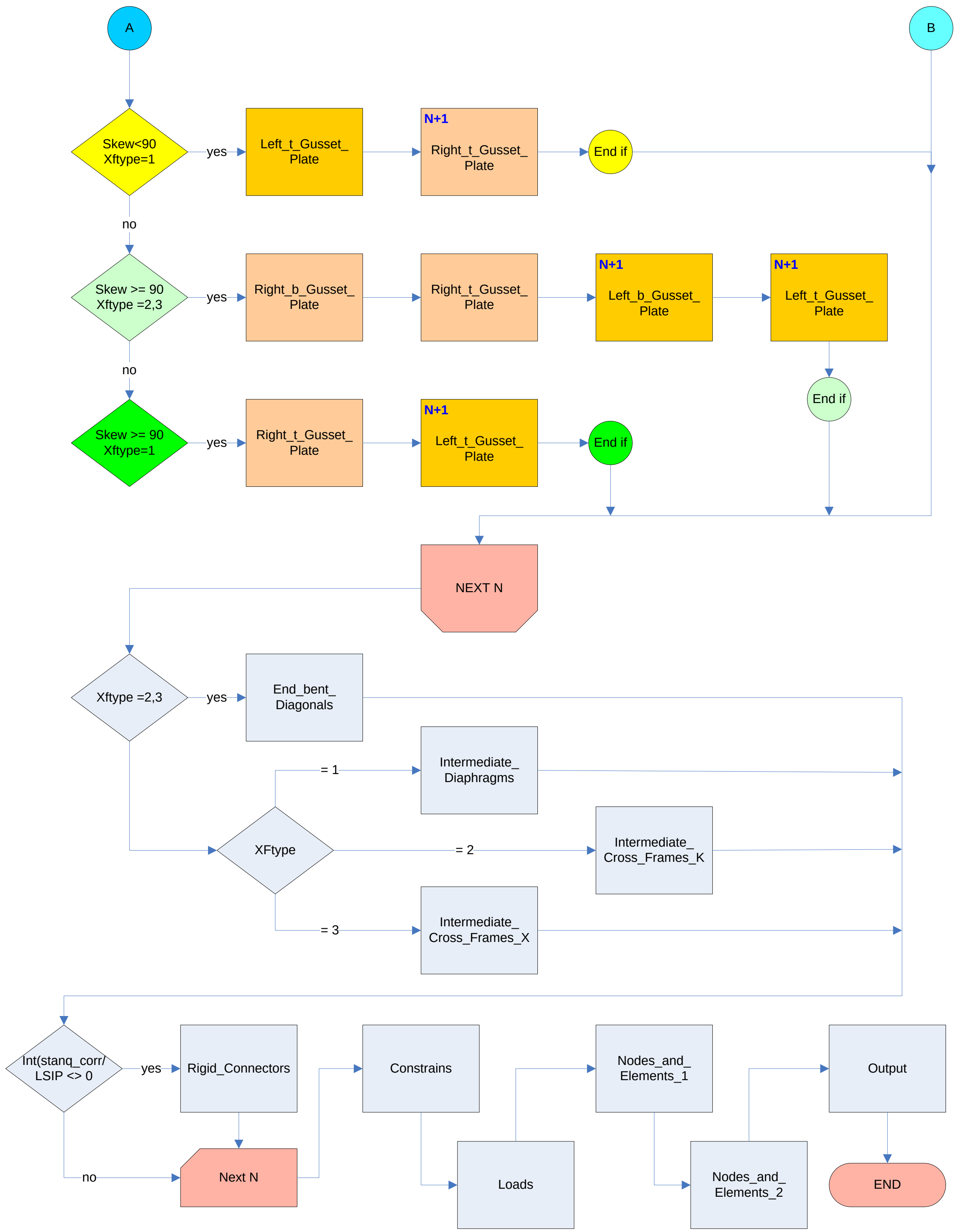
A
B
Skew<90
Xftype=1
yes
Left_t_Gusset_
Plate
N+1
Right_t_Gusset_
Plate
End if
no
Skew >= 90
Xftype =2,3
yes
Right_b_Gusset_
Plate
Right_t_Gusset_
Plate
N+1
Left_b_Gusset_
Plate
N+1
Left_t_Gusset_
Plate
End if
no
Skew >= 90
Xftype=1
yes
Right_t_Gusset_
Plate
N+1
Left_t_Gusset_
Plate
End if
NEXT N
Xftype =2,3
yes
End_bent_
Diagonals
= 1
Intermediate_
Diaphragms
XFtype
= 2
Intermediate_
Cross_Frames_K
= 3
Intermediate_
Cross_Frames_X
Int(stanq_corr/
LSIP <> 0
yes
Rigid_Connectors
Constrains
Nodes_and_
Elements_1
Output
no
Next N
Loads
Nodes_and_
Elements_2
END

Visual Basic Program used to automate model input data

- Overview

By means of Visual Basic 6.0 it was possible to create a computational program to generate the input data ANSYS uses to analyze the models. The program consists of a series of modules that logically connect with one another to generate the output text file that can be processed by ANSYS.

Initially the program needs the input data, represented by the geometrical variables of the structure, such as span, girder spacing, number of cross-frames, skew angle, girder cross-section dimensions, etc. It also requires the material properties to be inputted at the beginning of the program. In Appendix A the logical flowchart of the program is shown.

- Limitations

Some conditions must be satisfied in order to run the program and some variables are limited to certain values. To list a few:

- The structure's boundary conditions are pinned and roller connected. No vertical uplift is allowed.
- Do not include typical tapered bottom flanges at the end bents.
- All girders must have the same web height.
- All intermediate cross-frames must be the same type.

- Description

Following is a brief description of the Visual Basic 6.0 program.

1. The program requires from the user the input of a series of variables. These variables, as mentioned before, are geometric.
2. Nodes and Elements are generated for the bottom flange, top flange, web, sole plates, elastomeric pads, and end bent stiffeners (or connectors) on each girder.
3. Connectors and stay-in-place nodes and elements are then created, followed by the end bent diaphragms or cross-frames and finally the intermediate cross-frames.
4. The final step deals with the boundary conditions, constrains, loading scenarios, and output, which includes the files with deformations and forces data as well as secondary text files for verification purposes.

The aforementioned steps are just a summary of what the program does. The actual program included more than 30 different modules and procedures.

APPENDIX B

Deflections and rotations Summary for Chicken Road Bridge near Lumberton, NC.

This appendix contains a detailed description of the Chicken Road Bridge, located near Lumberton, North Carolina. It includes bridge geometry, material data, cross-frame type and size, and dead loads calculated from slab geometry. Illustrations detailing the bridge geometry and field measurement locations are included, along with tables and graphs of the field measured non-composite girder deflections and out-of-plane rotations.

A summary the ANSYS finite element model created for the Chicken Road Bridge is also included in this appendix. This summary includes a picture of the ANSYS model, details about the elements used in the model generation, the loads applied to the model, and tables and graphs of the deflections and out-of-plane rotations predicted by the model.

FIELD MEASUREMENTS SUMMARY

PROJECT NUMBER	R-513BB (Bridge on Chicken Rd. over US74)			
MEASUREMENT DATE	Tuesday, July 17, 2007			

BRIDGE DESCRIPTION

TYPE	Two Simple Spans		
AVERAGE LENGTH	131.20 ft		
NUMBER OF GIRDERS	4		
GIRDER SPACING	09.84 ft		
SKEW	137 deg		
OVERHANG	G1	G4	
	03.26 ft	03.26 ft	(average from web centerline)
BEARING TYPE	Elastomeric Bearing		

MATERIAL DATA

STRUCTURAL STEEL	Grade	Yield Strength
Girder	AASHTO M270	50 ksi

CONCRETE UNIT WEIGHT 145 pcf

SIP FORM WEIGHT 3 psf

GIRDER DATA

LENGTH	G1	G2	G3	G4
	130.62 ft	131.00 ft	131.39 ft	131.78 ft

TOP FLANGE WIDTH	14.17 in
BOTTOM FLANGE WIDTH	18.11 in
WEB THICKNESS	0.63 in
WEB DEPTH	57.09 in

FLANGES	Thickness	Begin	End
Top	0.87 in	00.00 ft	39.99 ft
Bottom	0.87 in	00.00 ft	27.53 ft
	1.57 in	27.53 ft	103.71 ft
	0.87 in	103.71 ft	131.20 ft

STIFFENERS	
Longitudinal	NONE
Bearing	PL 0.87 in x 8.74 in
Intermediate	PL 0.87 in x 8.74 in

CROSS FRAME DATA

	Type	Diagonals	Horizontals
END	K	WT 125 x 22.5	C 380 x 60 @top
			WT 125x22.5 @ bottom
INERMEDIATE	K	L 76 x 76 x 7.9	L 76 x 76 x 7.9

FIELD MEASUREMENTS SUMMARY

PROJECT NUMBER: R-513BB (Bridge on Chicken Rd. over US74)
MEASUREMENT DATE: Tuesday, July 17, 2007

DECK LOADS

Girder	Concrete		Deck Slab		Ratio
	lb/ft	N/mm	lb/ft	N/mm	
G1	858	12.54346	724	10.58446	1.19
G2	1030	15.05801	827	12.09026	1.25
G3	1030	15.05801	827	12.09026	1.25
G4	858	12.54346	724	10.58446	1.19

SLAB DATA

THICKNESS	8.66 in	
BUILD-UP	2.76 in	
REBAR	Size	Spacing
LONGITUDINAL	(metric)	(nominal)
Top	#13	16.53 in
Bottom	#16	8.66 in
TRANSVERSE		
Top	#16	5.91 in
Bottom	#16	5.91 in

GIRDER DEFLECTIONS

THEORETICAL by SIMP. PROCEDURE (in)
(design less slab*)

LOCATION	G1	G2	G3	G4
0/4	0	0	0	0
1/4	-2.76	-2.56	-2.56	-2.76
2/4	-3.74	-3.50	-3.50	-3.74
3/4	-2.76	-2.56	-2.56	-2.76
4/4	0	0	0	0

* Slab includes rebar, build-ups, sip's and girders

MEASURED CORRECTED (in)
(measured less bearing settlements)

LOCATION	G1	G2	G3	G4
0/4	0	0	0	0
1/4	-3.36	-3.18	-3.04	-3.14
2/4	-4.86	-4.55	-4.35	-4.52
3/4	-3.42	-3.24	-3.10	-3.14
4/4	0	0	0	0

GIRDER ROTATIONS

MEASURED

TOP FLANGE @ END BENT (degrees)

LOCATION	G1	G2	G3	G4
0/4	0.9	0.3	0.9	0.5

BOTTOM FLANGE (degrees)

LOCATION	G1	G2	G3	G4
0/4	-0.6	-0.3	-1.1	-0.5
1/4	0.1	0.3	0.5	0.7
2/4	-1.4	-0.3	0.1	-1
3/4	-1.6	-0.6	-0.8	-0.6
4/4	-0.4	-0.4	0.2	-0.2

WEB (degrees)

LOCATION	**G1**	**G2**	**G3**	**G4**
0/4	0.6	0.6	0.7	0.7
1/4	0.3	1.2	0.7	1.2
2/4	-0.5	0.2	0	0.2
3/4	-0.9	-0.4	-0.5	-0.2
4/4	-0.6	-0.7	-0.7	-0.5

FIELD MEASUREMENT SUMMARY

PROJECT NUMBER: R-513BB (Bridge on Chicken Rd. over US74)

MEASUREMENT DATE: 7/17/2007

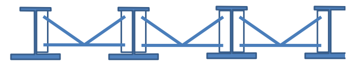

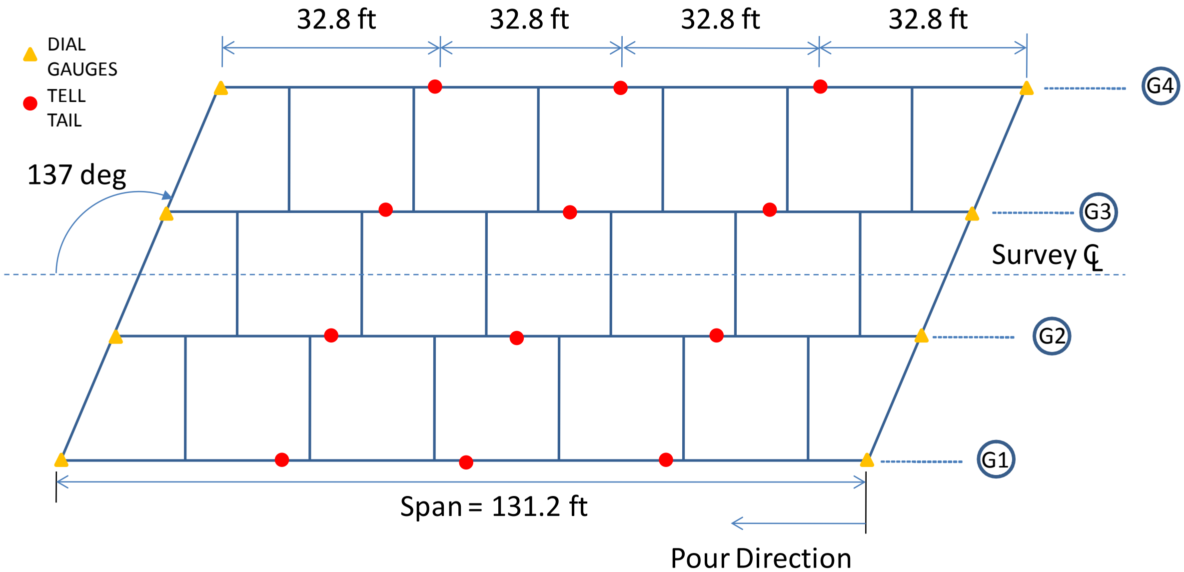

(A) Plan View (not to scale)

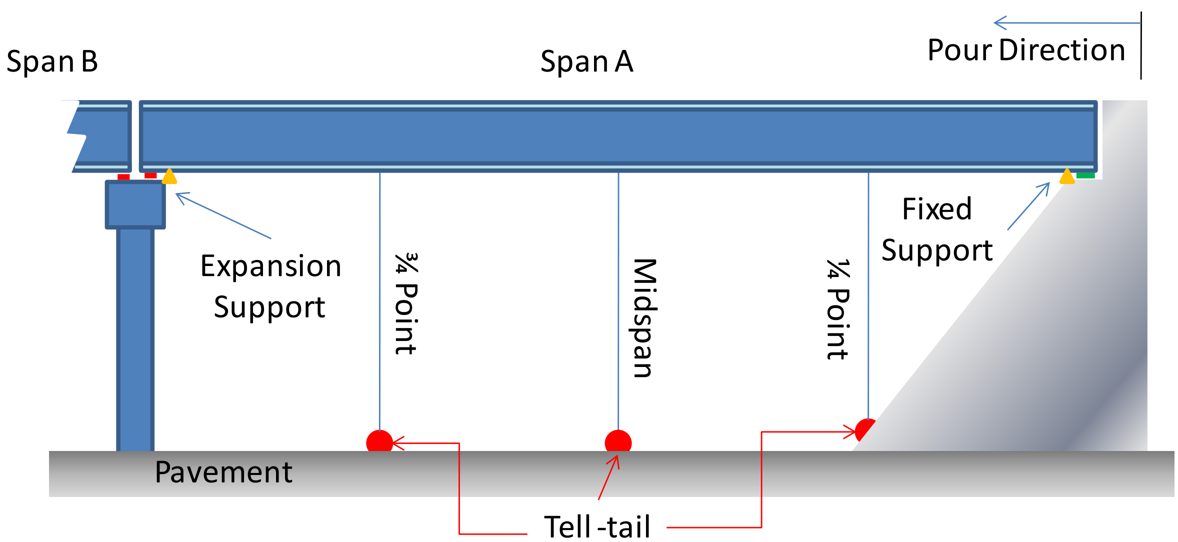

(B) Elevation View (not to scale)

Plan and Elevation View of Chicken Road Bridge

FIELD MEASUREMENT SUMMARY

PROJECT NUMBER: R-513BB (Bridge on Chicken Rd. over US74)

MEASUREMENT DATE: 7/17/2007

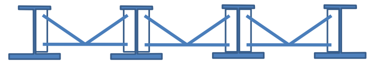

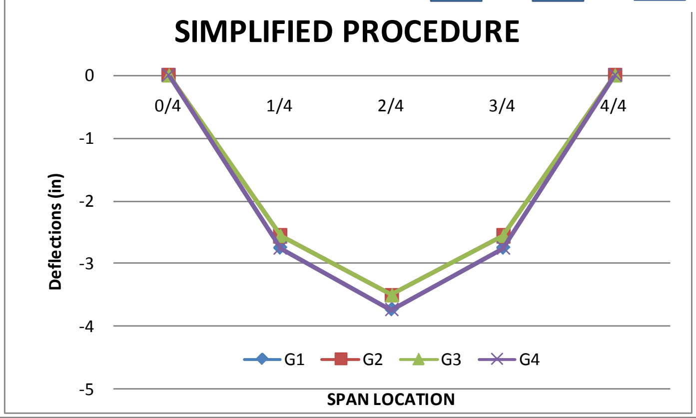

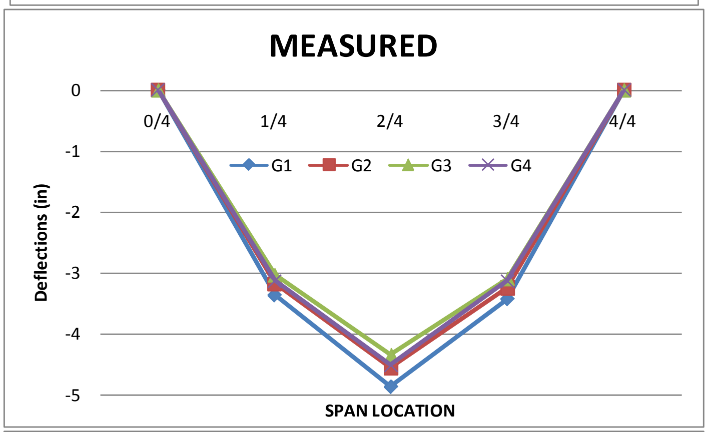

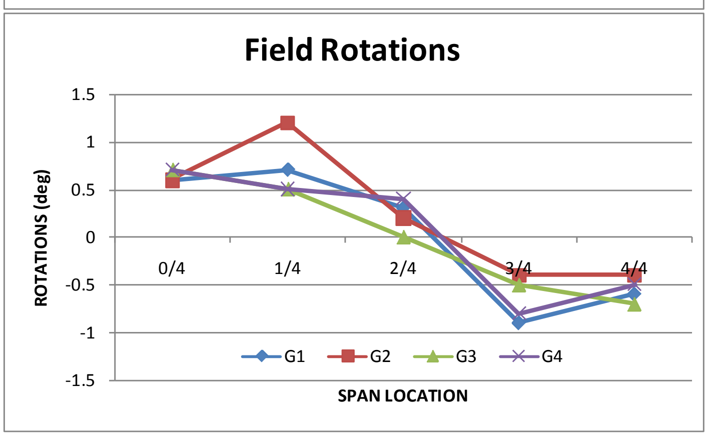

FIELD MEASUREMENT SUMMARY

PROJECT NUMBER: R-513BB (Bridge on Chicken Rd. over US74)

MEASUREMENT DATE: 7/17/2007

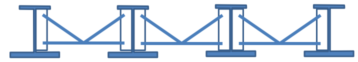

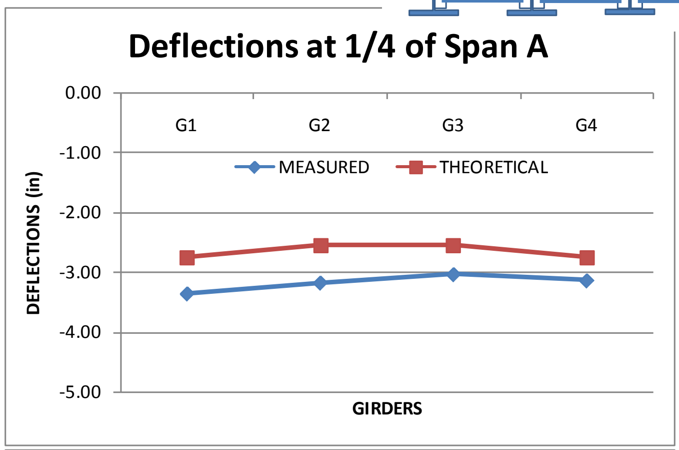

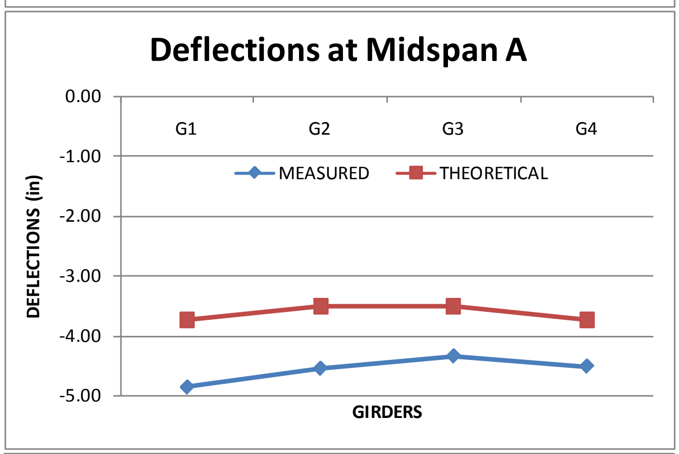

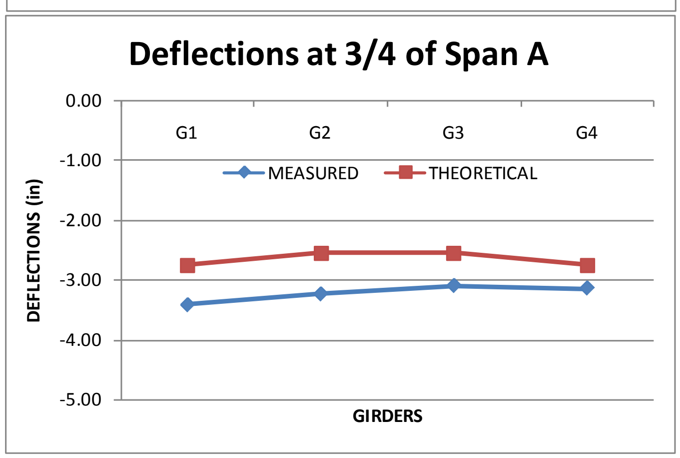

ANSYS FINITE ELEMENT MODELING SUMMARY

PROJECT NUMBER: R-513BB (Bridge on Chicken Rd. over US74)

MODEL DESCRIPTION: Steel Only, Isometric View

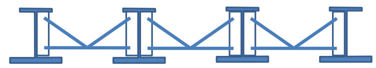

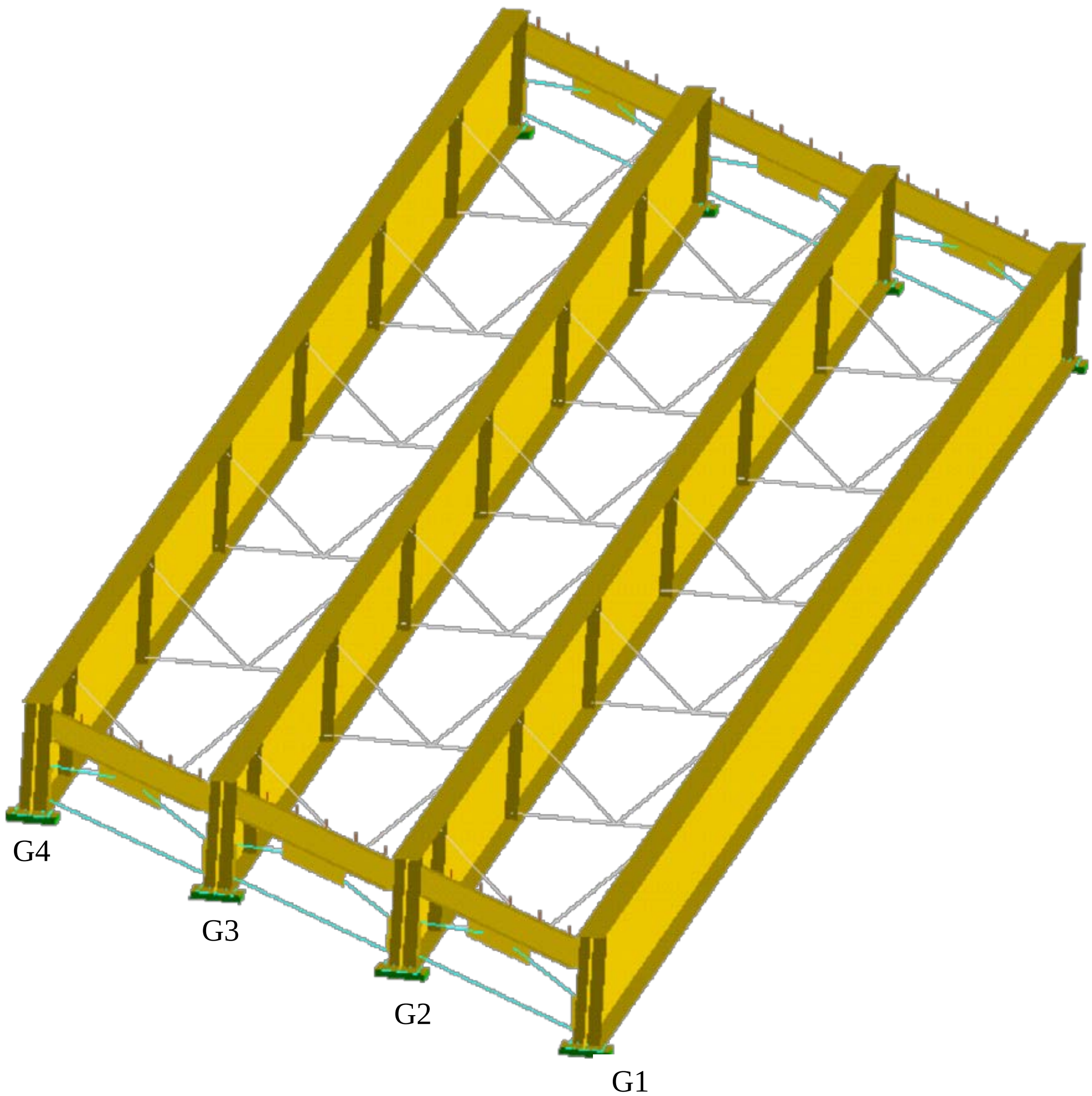

ANSYS FINITE ELEMENT MODELING SUMMARY

PROJECT NUMBER: R-513BB (Bridge on Chicken Rd. over US74)

MODEL DESCRIPTION: Steel Only, Isometric View

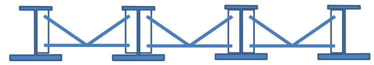

COMPONENT	ELEMENT TYPE
Girder:	SHELL 93
Connector/ Stiffener Plates:	SHELL 93
Cross Frame Members:	Link 8 (Diagonal)
	Link 8 (Horizontal)
End Diaphragm	Link 8 (Diagonal)
	Beam 4 (Horizontal)
Stay in Place Deck Forms	Link 8

Girder	lb/ft^2	N/mm^2
G1	1.34	0.064
G2	1.57	0.075
G3	1.57	0.075
G4	1.34	0.064

GIRDER DEFLECTIONS (in)
(@ COMMON NODE BETWEEN BOTTOM FLANGE AND WEB)

LOCATION	G1	G2	G3	G4
0/4	-0.00982	-0.01142	-0.01159	-0.01255
1/4	-6.30	-6.21	-6.24	-6.52
2/4	-9.02	-8.71	-8.70	-8.99
3/4	-6.55	-6.24	-6.20	-6.29
4/4	-0.00576	-0.00532	-0.0054	-0.00406

GIRDER ROTATIONS
WEB (degrees)

LOCATION	**G1**	**G2**	**G3**	**G4**
0/4	0.1	0.3	0.3	0.3
1/4	0.9	0.8	0.6	0.4
2/4	0.3	0.1	-0.1	-0.3
3/4	-0.4	-0.6	-0.8	-0.9
4/4	-0.3	-0.3	-0.3	-0.1

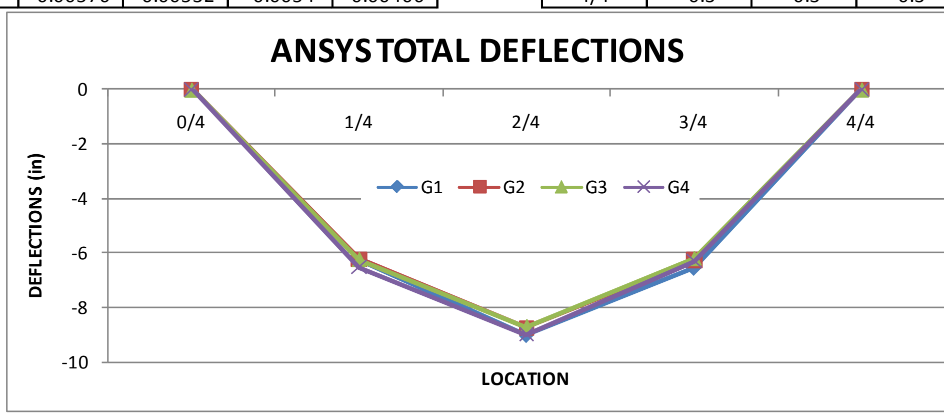

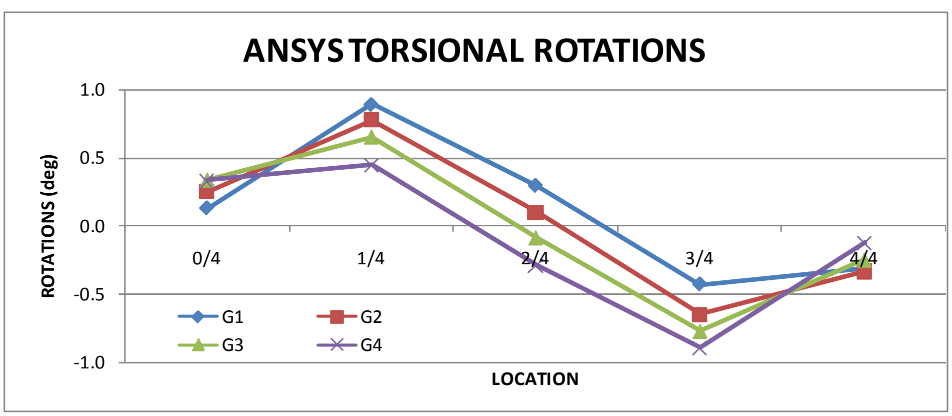

APPENDIX C

Deflections and rotations Summary for Roaring Fork Road Bridge near Jefferson, ASHE County, NC.

This appendix contains a detailed description of the Roaring Fork Road Bridge, located near Jefferson, North Carolina. It includes bridge geometry, material data, cross-frame type and size, and dead loads calculated from slab geometry. Illustrations detailing the bridge geometry and field measurement locations are included, along with tables and graphs of the field measured non-composite girder deflections and out-of-plane rotations.

A summary of the ANSYS finite element model created for the Raring Fork Road Bridge is also included in this appendix. This summary includes a picture of the ANSYS model, details about the elements used in the model generation, the loads applied to the model, and tables and graphs of the deflections and out-of-plane rotations predicted by the model.

FIELD MEASUREMENTS SUMMARY

PROJECT NUMBER	B-4013 (Bridge No. 338 over Roaring Fork Creek)
MEASUREMENT DATE	Thursday, March 06, 2008

BRIDGE DESCRIPTION

TYPE	Simple Span	
AVERAGE LENGTH	74.50 ft	
NUMBER OF GIRDERS	5	
GIRDER SPACING	6.50 ft	
SKEW	23 deg	
OVERHANG	G1	G5
	1.10 ft	1.10 ft
BEARING TYPE	Elastomeric Bearing	

MATERIAL DATA

STRUCTURAL STEEL	Grade	Yield Strength
Girder	AASHTO M270	50 ksi

CONCRETE UNIT WEIGHT	145 pcf	
SIP FORM WEIGHT	3 psf	CAT#: 30B156-20-G1BB

GIRDER DATA

LENGTH	G1	G2	G3	G4	G5
Bearing to Bearing	73.50 ft	73.50 ft	73.50 ft	73.50 ft	73.50 ft
TOTAL	74.50 ft	74.50 ft	74.50 ft	74.50 ft	74.50 ft

TOP FLANGE WIDTH	12.00 in
TOP FLANGE THICKNESS	0.75 in
BOTTOM FLANGE WIDTH	18.00 in
BOTTOM FLANGE THICKNESS	1.00 in
WEB THICKNESS	0.50 in
WEB DEPTH	32.00 in

STIFFENERS	
Longitudinal	NONE
Bearing	PL 0.75 in x 5.75 in
Intermediate	PL 0.5 in x 5.75 in

CROSS FRAME DATA

	Type	Section
END	DIAPHRAGM	MC 18 x 42.5
INERMEDIATE	DIAPHRAGM	MC 18 x 42.5

FIELD MEASUREMENTS SUMMARY

PROJECT NUMBER: B-4013 (Bridge No. 338 over Roaring Fork Creek)
MEASUREMENT DATE: Thursday, March 06, 2008

DECK LOADS

Girder	Concrete		Deck Slab		Ratio
	lb/ft	N/mm	lb/ft	N/mm	
G1	492	7.19	637	9.31	0.77
G2	731	10.69	946	13.83	0.77
G3	731	10.69	946	13.83	0.77
G4	731	10.69	946	13.83	0.77
G5	492	7.19	637	9.31	0.77

SLAB DATA

THICKNESS	8.0 in	
BUILD-UP	2.5 in	
REINFORCEMENT	Size	Spacing
LONGITUDINAL	(metric)	(nominal)
Top	#4	18.0 in
Bottom	#5	12.0 in
TRANSVERSE		
Top	#5	8.0 in
Bottom	#5	8.0 in

GIRDER DEFLECTIONS

THEORETICAL by SIMP. PROCEDURE (in)
(design less slab*)

LOCATION	G1	G2	G3	G4	G5
MIDSPAN	N/A	N/A	N/A	N/A	N/A

* Slab includes rebar, build-ups, sip's and girders

__Note__: the parameter S (Girder spacing to span ratio) on the simplified procedure was out of bounds, so it was not possible to determine the deflections

MEASURED CORRECTED (in)
(measured less bearing settlements)

LOCATION	G1	G2	G3	G4	G5
MIDSPAN	-1.22	-1.20	-1.22	-1.27	-1.42

GIRDER ROTATIONS

MEASURED

BOTTOM FLANGE (degrees)

LOCATION	G1	G2	G3	G4	G5
END BENT 1	0.6	0.1	0	0.1	-0.7
MIDSPAN	-0.3	0.4	0.3	0.1	-0.3
END BENT 2	-0.9	-0.9	-0.8	-0.3	-0.1

WEB (degrees)

LOCATION	G1	G2	G3	G4	G5
END BENT 1	-0.1	-0.2	-0.3	-0.4	0
MIDSPAN	-0.3	-0.4	0	0.2	0.2
END BENT 2	0.7	1	0.4	0.9	0.1

FIELD MEASUREMENT SUMMARY

PROJECT NUMBER: B-4013 (Bridge No. 338 over Roaring Fork Creek)

MEASUREMENT DATE: 3/6/2008

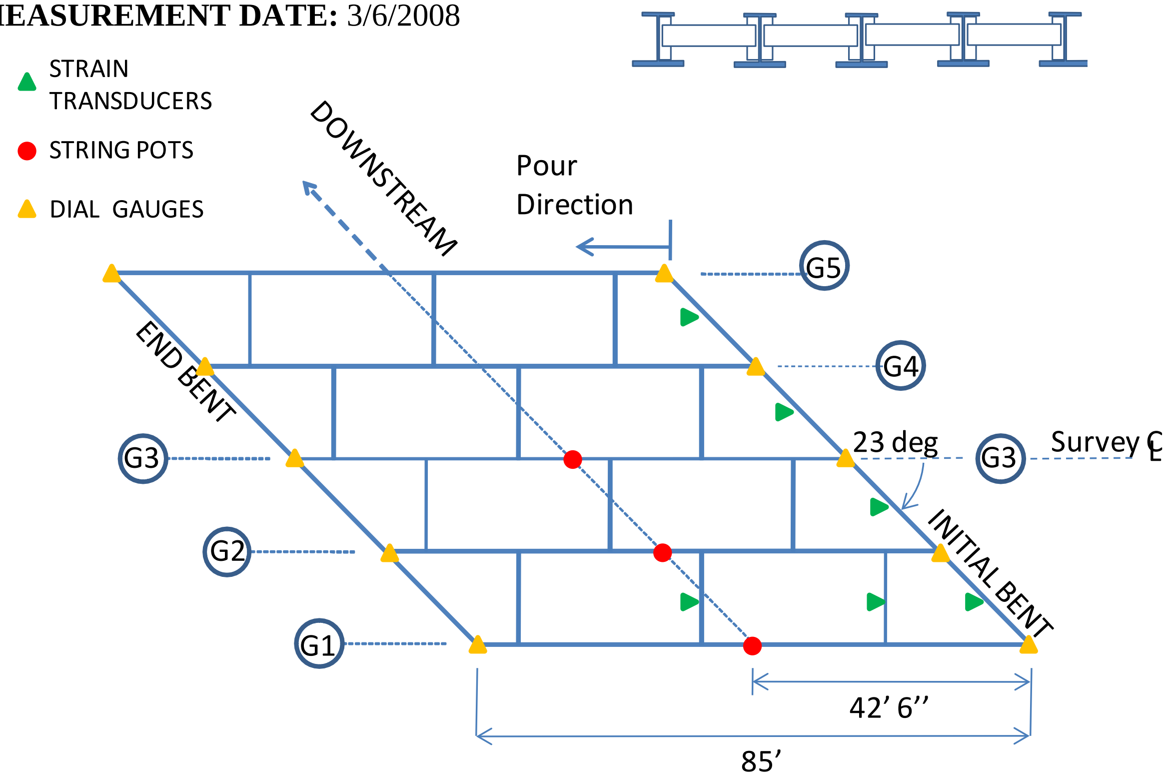

(C) Plan View (not to scale)

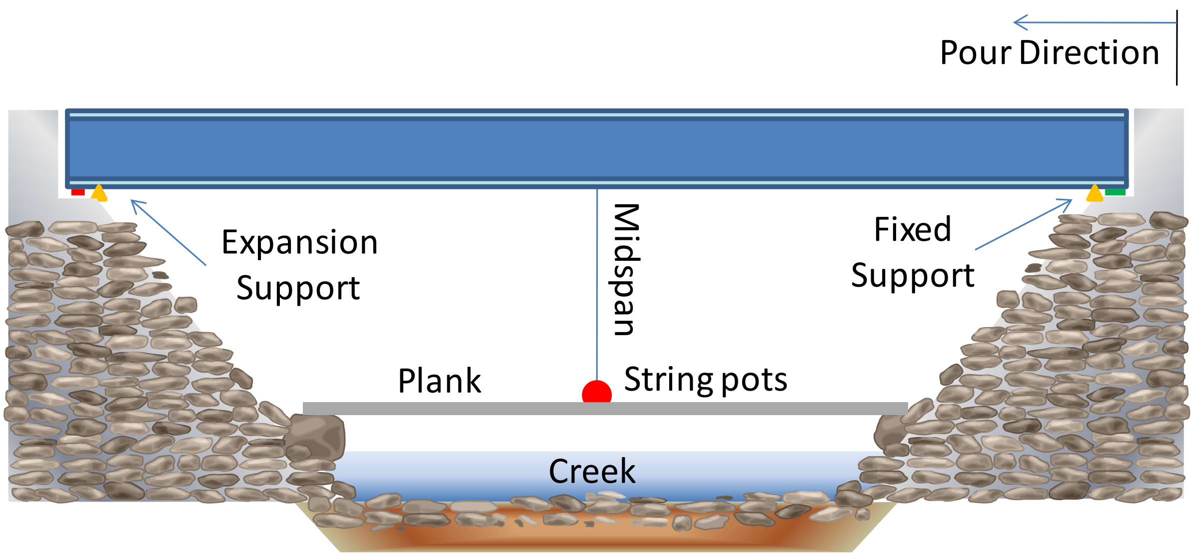

(D) Elevation View (not to scale)

FIELD MEASUREMENT SUMMARY

PROJECT NUMBER: B-4013 (Bridge No. 338 over Roaring Fork Creek)

MEASUREMENT DATE: 3/6/2008

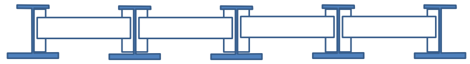

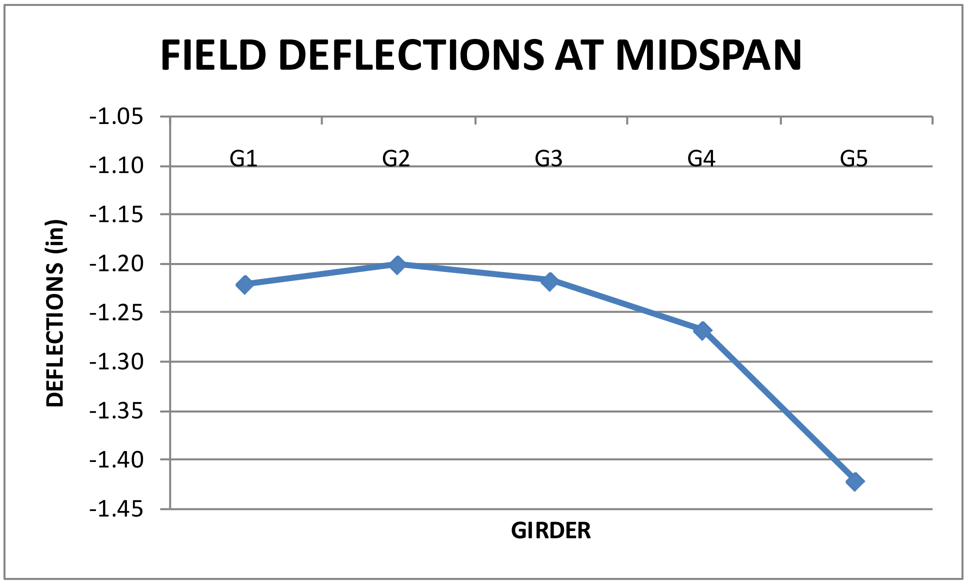

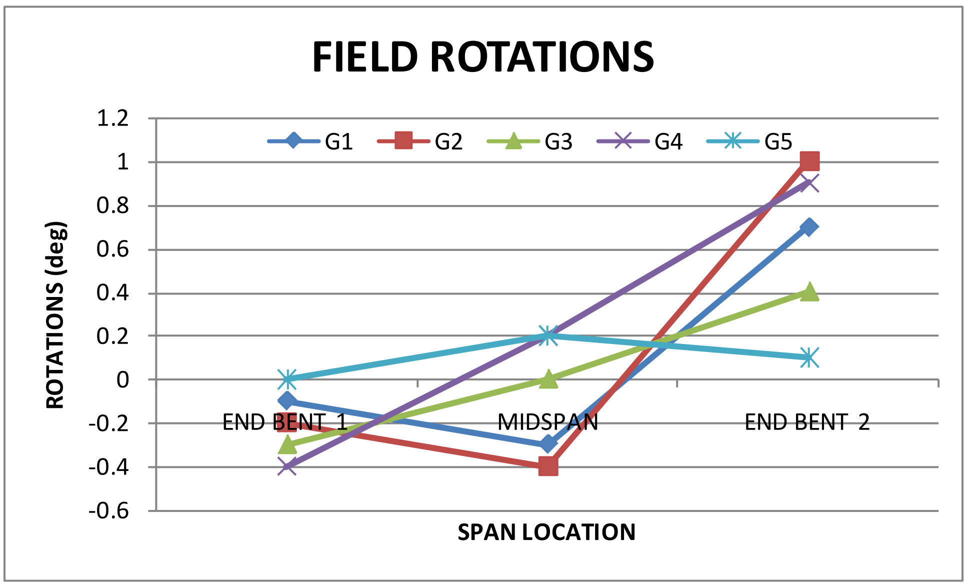

ANSYS FINITE ELEMENT MODELING SUMMARY

PROJECT NUMBER: B-4013 (Bridge No. 338 over Roaring Fork Creek)

MODEL DESCRIPTION: Steel Only, Isometric View

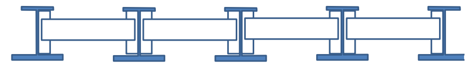

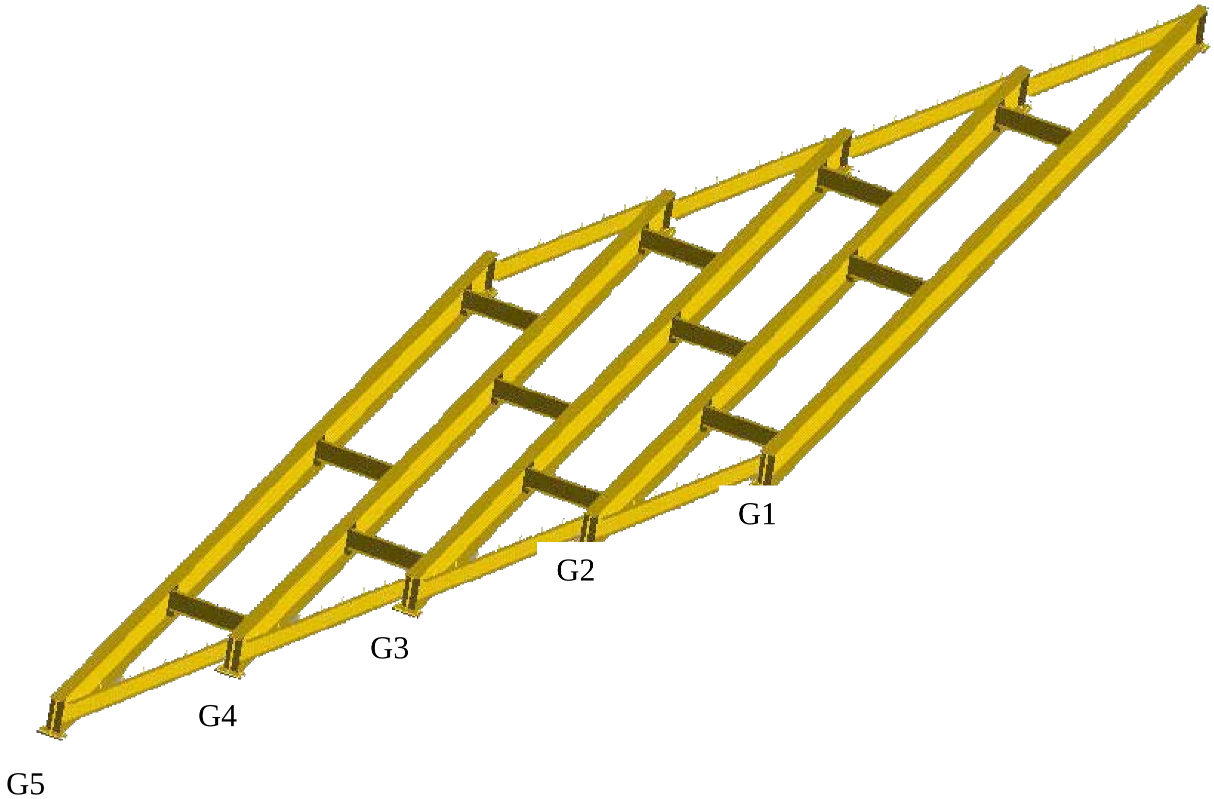

ANSYS FINITE ELEMENT MODELING SUMMARY

PROJECT NUMBER: B-4013 (Bridge No. 338 over Roaring Fork Creek)

MODEL DESCRIPTION: Steel Only, Isometric View

COMPONENT	ELEMENT TYPE
Girder:	SHELL 93
Connector/ Stiffener Plates:	SHELL 93
Cross Frame Members:	Beam 4
End Diaphragm	Beam 4
Stay in Place Deck Forms	Link 8

Girder	Load	
	lb/ft2	N/mm2
G1	492.0	0.023
G2	731.0	0.035
G3	731.0	0.035
G4	731.0	0.035
G5	492.0	0.023

GIRDER DEFLECTIONS (in)

(@ COMMON NODE BETWEEN BOTTOM FLANGE AND WEB)

LOCATION	G1	G2	G3	G4	G5
0/4	0.00	0.00	0.00	0.00	0.00
1/4	-1.02	-1.06	-1.05	-1.05	-1.13
2/4	-1.54	-1.51	-1.50	-1.50	-1.53
3/4	-1.15	-1.07	-1.06	-1.07	-1.03
4/4	0.00	0.00	0.00	0.00	0.00

GIRDER ROTATIONS

WEB (degrees)

LOCATION	G1	G2	G3	G4	G5
0/4	0.0	-0.1	-0.1	-0.1	-0.1
1/4	-0.50	-0.55	-0.53	-0.50	-0.19
2/4	-0.34	-0.08	0.00	0.08	0.31
3/4	0.26	0.51	0.53	0.55	0.51
4/4	0.05	0.08	0.09	0.07	0.01